



**March 2022**  
**Report No. 21-028**

**Charles D. Baker**  
Governor

**Karyn E. Polito**  
Lieutenant Governor

**Jamey Tesler**  
MassDOT Secretary & CEO

# Development of Comprehensive Inspection Protocols for Deteriorated Steel Beam Ends

**Principal Investigator (s)**  
**Georgios Tzortzinis, Graduate Researcher**  
**Dr. Sergio F. Brena**  
**Dr. Simos Gerasimidis**



**Research and Technology Transfer Section**  
**MassDOT Office of Transportation Planning**



**U.S. Department of Transportation**  
**Federal Highway Administration**

[This blank, unnumbered page will be the back of your front cover]

# Technical Report Document Page

1. Report No. 22-028	2. Government Accession No.	3. Recipient's Catalog No.	
4. Title and Subtitle Development of Comprehensive Inspection Protocols for Deteriorated Steel Beam Ends		5. Report Date March 31, 2022	
		6. Performing Organization Code	
7. Author(s) Georgios Tzortzinis, Gabrielle Pryor, Kshitij Yadav, Simos Gerasimidis, and Sergio F. Breña		8. Performing Organization Report No. 22-028	
9. Performing Organization Name and Address University of Massachusetts Amherst UMass Transportation Center 130 Natural Resources Way Amherst, MA 01003		10. Work Unit No. (TRAIS)	
		11. Contract or Grant No.	
12. Sponsoring Agency Name and Address Massachusetts Department of Transportation Office of Transportation Planning Ten Park Plaza, Suite 4150, Boston, MA 02116		13. Type of Report and Period Covered Final Report – March 31, 2022 [February 1, 2020–March 31, 2022]	
		14. Sponsoring Agency Code n/a	
15. Supplementary Notes Project Champion -			
16. Abstract Recent research has developed new improved procedures that accurately describe the remaining load-carrying capacity of these deteriorated members. These new procedures are based on computational simulations and experimental testing of real deteriorated beams. The outcome of a recently completed research project (“Development of Load Rating Procedures for Deteriorated Steel Beam Ends,” completed July 2019) has found new parameters that are extremely important when assessing the residual capacity of the bridge and the load rating procedure. Examples of these parameters include the out-of-plane imperfection of the beam web, the surface area of corrosion, and others. Currently, inspectors are not aware of the new findings and these important parameters, and they have no clear guidance on what and how to measure when inspecting a deteriorated beam end. Drawing on the recent findings made while developing new load rating procedures, the project at hand first documents the current state of practice of beam end inspections, then explores new technological solutions for improvement of these inspection techniques using LiDAR and unmanned aircraft systems (drones), and finally performs preliminary analysis of a bridge system.			
17. Key Word load-carrying capacity, inspection protocols, deteriorated steel beam ends, corrosion, LiDAR, unmanned aircraft systems		18. Distribution Statement	
19. Security Classif. (of this report) unclassified	20. Security Classif. (of this page) unclassified	21. No. of Pages 126	22. Price n/a

This page left blank intentionally.

# **Development of Comprehensive Inspection Protocols for Deteriorated Steel Beam Ends**

## **Final Report**

Prepared By:

**Georgios Tzortzinis**

Graduate Researcher

**Gabrielle Pryor**

Graduate Researcher

**Kshitij Kumar Yadav**

Graduate Researcher

**Sergio Breña, Ph.D.**

Co-Principal Investigator

**Simos Gerasimidis, Ph.D.**

Principal Investigator

University of Massachusetts Amherst  
130 Natural Resources Way, Amherst, MA 01003

Prepared For:

Massachusetts Department of Transportation  
Office of Transportation Planning, Ten Park Plaza, Suite 4150  
Boston, MA 02116

March 2022

This page left blank intentionally.

# **Acknowledgments**

Prepared in cooperation with the Massachusetts Department of Transportation, Office of Transportation Planning, and the United States Department of Transportation, Federal Highway Administration.

## **Disclaimer**

The contents of this report reflect the views of the author(s), who is responsible for the facts and the accuracy of the data presented herein. The contents do not necessarily reflect the official view or policies of the Massachusetts Department of Transportation or the Federal Highway Administration. This report does not constitute a standard, specification, or regulation.

This page left blank intentionally.



# Executive Summary

This study of “Development of Comprehensive Inspection Protocols for Deteriorated Steel Beam Ends” was undertaken as part of the Massachusetts Department of Transportation (MassDOT) Research Program. This program is funded with Federal Highway Administration (FHWA) State Planning and Research (SPR) funds. Through this program, applied research is conducted on topics of importance to the Commonwealth of Massachusetts transportation agencies.

As New England’s bridge population ages, MassDOT inspection engineers are increasingly witnessing instances of extensive corrosion at steel beam ends. Due to the increased use of deicing techniques, the increased incidence of this condition can be primarily attributed to leaking through deck joints. The leaking water contains high concentrations of chemical substances used seasonally to winterize the road above. Deterioration of the steel is most often initiated by the buildup of this runoff on the top face of the bottom flange. When this process is sustained, the buildup of runoff triggers a corrosive process in the bottom flange, the structural components above it, and the web. The resulting section loss leads to a significant reduction in the girder’s load-carrying capacity. Several cases exist wherein the extreme effects of this phenomenon have caused closure of the bridge to ensure life safety. The nonuniformity of the corroded shape and the variable thickness reduction along the corroded area provide substantial challenges in calculating realistic estimates of the remaining capacity of the girder’s end.

Recent research has developed new improved procedures that accurately describe the remaining load-carrying capacity of these deteriorated members. These new procedures are based on computational simulations and experimental testing of real deteriorated beams. The outcome of a recently completed research project (“Development of Load Rating Procedures for Deteriorated Steel Beam Ends,” completed July 2019) has found new parameters that are extremely important when assessing the residual capacity of the bridge and the load rating procedure. Examples of these parameters include the out-of-plane imperfection of the beam web, the surface area of corrosion, and others. Currently, inspectors are not aware of the new findings and these important parameters, and they have no clear guidance on what and how to measure when inspecting a deteriorated beam end.

It is important for MassDOT to strongly consider the new load rating procedures in drawing realistic conclusions. Two areas of need are

- i. the measurement and classification of important parameters that have not been typically measured in the past by inspectors, and
- ii. enhancement of the inspection protocols so that important deterioration information needed for the new improved procedures is documented during inspections.

Drawing on the recent findings made while developing new load rating procedures, the project at hand first documents the current state of practice of beam end inspections, then explores

new technological solutions for improvement of these inspection techniques, and finally performs preliminary analysis of a bridge system. The research work has four distinct aspects:

Research effort 1. Evaluation of current inspection procedures.

Research effort 2. New technological solutions for more efficient data collection (LiDAR).

Research effort 3. New technological solutions for more efficient data collection (Unmanned aircraft systems [drones]).

Research effort 4. Bridge system behavior.

In detail, Section 2 presents the study on a questionnaire that was handed out to inspectors in the state of Massachusetts. It explores what is and what is not working with the current inspection procedures. The first half of this section presents a questionnaire that was distributed to MassDOT inspectors and consultants. The second half summarizes and processes the responses that were collected and provides areas of improvement for potential procedures based on the data collected.

Section 3 discusses the implementation of LiDAR technology to the substructure's condition assessment for steel bridges as well as the results documentation within the inspection report. In this framework, a field corroded beam obtained from a decommissioned bridge is scanned, and a methodology for estimating the remaining web thickness is developed and evaluated based on measurements taken with a thickness gauge.

Section 4 presents the results of a literature review focused on different corrosion technologies and how they are or can be used with drones to estimate corrosion. The reports for this chapter were broken into two sections: contact nondestructive testing methods and noncontact nondestructive testing methods. Some methods had reports where researchers attached the technology to a drone, whereas others only detailed technology that could be used to measure steel thickness for corrosion estimation. The reports dealing only with corrosion measurement technology were included because the research had promising results and could potentially be used on drones as technology advances.

Finally, Section 5 provides an exploration to understand the behavior of bridge systems having deteriorated beam ends and is based on computation analysis of a bridge with a deteriorated beam whose one end is corroded with a common corrosion pattern.

Conclusions are discussed in Section 6, and references are added at the end of the report.

# Table of Contents

Technical Report Document Page.....	i
Acknowledgments.....	v
Disclaimer.....	v
Executive Summary.....	vii
Table of Contents.....	ix
List of Tables.....	xi
List of Figures.....	xiii
1.0 Introduction.....	1
1.1 Background Information.....	1
1.2 Research Goals.....	2
2.0 Evaluation of Current Inspection Procedures and the Impact of the Important Parameters.....	3
2.1 Introduction.....	3
2.1.1 Background Information.....	3
2.1.2 Questionnaire Goals and Methodology.....	3
2.2 Data Collection.....	4
2.2.1 General Bridge Inspection Practices.....	4
2.2.2 Corrosion Assessment.....	5
2.2.3 Equipment.....	8
2.3 Questionnaire Responses from MassDOT Inspectors and Consultants.....	10
2.3.1 General Bridge Inspection Practices Section Responses.....	10
2.3.2 Corrosion Assessment Section Responses.....	19
2.3.3 Equipment Section Responses.....	38
2.4 Conclusions.....	52
3.0 LiDAR-Based Inspection Methods for Efficient Data Collection for Beam End Inspections.....	54
3.1 Developed Tools.....	54
3.1.1 Specimen Collection.....	54
3.1.2 Corrosion Topology.....	55
3.1.3 Methodologies for Thickness Estimation.....	56
3.1.3.1 Thickness Estimation with Gauge.....	57
3.1.3.2 Thickness Estimation with LiDAR.....	58
3.1.3.3 Scan and Post-Processing.....	59
3.2 Methodology Application.....	61
3.2.1 Experimental Work.....	61
3.2.1.1 Specimen Selection.....	61
3.2.1.2 Remaining Thickness.....	62
3.2.1.3 Experimental Configuration.....	62
3.2.1.4 Instrumentation Configuration.....	63
3.2.2 Computational Capacity Evaluation.....	64
3.2.2.1 Section Loss Simulation.....	64
3.2.3 Material Properties.....	65
3.2.4 Boundary and Loading Conditions.....	65
3.2.5 Geometric Imperfection.....	65
3.2.6 Finite-Element Model.....	66
3.2.7 Analytical Capacity Evaluation.....	67
3.3 Results.....	68

3.3.1 Thickness Gauge.....	68
3.3.2 LiDAR .....	69
3.3.3 Comparison.....	71
3.3.4 Implementation .....	72
3.4 Application Results.....	73
3.4.1 Experimental Results .....	73
3.4.2 Computational Results.....	74
3.4.3 Analytical Results .....	75
3.4.4 Implementation .....	76
3.5 Conclusions.....	77
4.0 Technological Solutions for Efficient Data Collection for Beam End Inspections: Unmanned Aircraft Systems (Drones).....	78
4.1.1 UAV Usage for Transportation Purposes .....	78
4.1.2 UAV Usage for Bridge Inspections .....	84
4.1.3 UAV Usage for Corrosion Estimation.....	97
4.1.3.1 Contact Nondestructive Testing Methods.....	98
4.1.3.2 Noncontact Nondestructive Testing Methods.....	101
4.2 Conclusions.....	106
5.0 Bridge System Behavior.....	108
5.1 Research Goals.....	108
5.2 Methodology for Computational Work.....	108
5.2.1 Geometry of the Representative Bridge.....	109
5.2.2 Corrosion Pattern .....	109
5.2.3 Material Properties.....	110
5.3 Geometric Imperfections.....	110
5.4 Finite-Element Modeling .....	111
5.5 Results.....	112
5.5.1 Capacity of the Bridge .....	112
5.5.2 Reaction Forces.....	113
5.6 Conclusions.....	114
5.7 Limitations and Future Work.....	115
6.0 Conclusions .....	116
6.1 Phase I: Evaluation of Current Inspection Procedures.....	116
6.2 Phase II: New LiDAR-Based Inspection Methods for More Efficient Data Collection for Beam End Inspections .....	117
6.3 Phase III: New Technological Solutions for More Efficient Data Collection for Beam End Inspections—Unmanned Aircraft Systems (Drones).....	118
6.4 Phase IV: Bridge System Behavior.....	118
7.0 Limitations and Future Work .....	120
8.0 References .....	122

# List of Tables

Table 2.1: Other technologies used by inspectors .....	21
Table 2.2: Accuracy of D-meters used .....	25
Table 2.3: Measurement points on unstiffened beam.....	28
Table 2.4: Measurement points on stiffened beam.....	30
Table 2.5: Advantages and disadvantages of bridge inspection equipment .....	40
Table 2.6: Is a new load rating needed? .....	48
Table 3.1: Comparison between thickness gauge and LiDAR estimations.....	71
Table 4.1: Transportation activities for UAVs .....	83
Table 4.2: Possible UAV outputs and uses .....	95
Table 4.3: Detection possibilities of UAVs and how they are detected .....	95
Table 4.4: Summary of UAV features.....	96
Table 4.5: Other technology used with the UAVs.....	97
Table 4.6: Methods for corrosion assessment .....	105

This page left blank intentionally.

# List of Figures

Figure 2.1: Upper edge of a web hole bearing on the flange.....	6
Figure 2.2: Corrosion on an unstiffened bridge beam.....	7
Figure 2.3: Corrosion on a stiffened bridge beam.....	7
Figure 2.4: Web deviating from straightness.....	8
Figure 2.5: A portable LiDAR.....	9
Figure 2.6: Current positions of MassDOT respondents.....	11
Figure 2.7: Current positions of consultant respondents.....	11
Figure 2.8: District breakdown for MassDOT employees.....	12
Figure 2.9: Engineering firms for responding consultants.....	12
Figure 2.10: Number of bridges MassDOT employees are responsible for.....	13
Figure 2.11: Number of bridges consultants are responsible for.....	14
Figure 2.12: Bridges inspected by MassDOT respondents.....	15
Figure 2.13: Bridges inspected by consultant respondents.....	15
Figure 2.14: Training procedures for bridge inspectors.....	16
Figure 2.15: Materials before performing bridge inspections.....	17
Figure 2.16: Aspects that slow bridge inspectors down.....	18
Figure 2.17: Difficult parts of the 2015 MassDOT inspection handbook.....	19
Figure 2.18: Challenges faced when assessing corrosion.....	20
Figure 2.19: Bridge inspection technologies used by inspectors.....	21
Figure 2.20: Advanced technologies used by bridge inspectors.....	22
Figure 2.21: Upper edge of a web hole bearing on the flange.....	23
Figure 2.22: D-meters to measure web thickness.....	23
Figure 2.23: D-meter models used by inspectors.....	24
Figure 2.24: Accuracy of the D-meters.....	25
Figure 2.25: Other technology to measure web thickness.....	26
Figure 2.26: Technology able to measure web thickness.....	27
Figure 2.27: Thickness measurement points for unstiffened beam.....	28
Figure 2.28: Additional measurement points for unstiffened beam.....	29
Figure 2.29: Possible measurement points for stiffened beam.....	30
Figure 2.30: Additional measurement points for stiffened beam.....	31
Figure 2.31: Thickness point measurements taken during inspections.....	32
Figure 2.32: How Thickness Measurement Point are Chosen.....	33
Figure 2.33: Thickness measurements taken of the stiffener.....	34
Figure 2.34: Witnessing web deviation from straightness.....	35
Figure 2.35: Measured web deviation from straightness.....	35
Figure 2.36: Equipment to measure web deviation.....	36
Figure 2.37: Accuracy of equipment to measure web deviation.....	37
Figure 2.38: Other equipment to measure web deviation.....	37
Figure 2.39: Equipment inspectors have to inspect bridges.....	39
Figure 2.40: Gauge calibration frequency by MassDOT inspectors.....	42
Figure 2.41: Gauge calibration frequency by consultants.....	43
Figure 2.42: Equipment changes desired by MassDOT inspectors.....	44
Figure 2.43: Equipment changes desired by consultants.....	44
Figure 2.44: Carrying a portable scanner and tablet/cell phone.....	45
Figure 2.45: Removing delamination above the bridge support.....	46
Figure 2.46: Reasons delamination cannot be removed by inspectors.....	46
Figure 2.47: Time spent documenting the data.....	47

Figure 2.48: Do inspectors believe a new load rating is needed?.....	48
Figure 2.49: Using drones for MassDOT activities.....	50
Figure 2.50: Activities of the drones .....	50
Figure 2.51: Bridge inspectors who considered using drones .....	51
Figure 3.1: Field corroded girder used for the study .....	55
Figure 3.2: (a) In-service configuration, (b) construction details for the support, and (c) web condition at midspan.....	56
Figure 3.3: Scanned beam and the area of interest.....	57
Figure 3.4: Condition of the web before and after coating and rust were removed .....	58
Figure 3.5: Flat steel plate and the corresponding point distribution with removed noise.....	59
Figure 3.6: Developed method for capacity estimation.....	60
Figure 3.7: a) Hole through the deck, and b) map cracking with heavy efflorescence at the O-03-009 bridge.....	61
Figure 3.8: The tested specimen.....	62
Figure 3.9: Remaining thickness contours for the tested end.....	63
Figure 3.10: Experimental and instrumentation configuration.....	63
Figure 3.11: Section loss simulation at the finite-element model .....	64
Figure 3.12: Material properties.....	65
Figure 3.13: The developed finite-element model.....	66
Figure 3.14: Area of interest for residual capacity estimation.....	68
Figure 3.15: Web domain and remaining thickness estimation (in.).....	69
Figure 3.16: Representation of web right and left faces (in.).....	70
Figure 3.17: Representation of web thickness.....	71
Figure 3.18: Typical sketch and photograph in MassDOT inspection reports .....	72
Figure 3.19: Applied load–vertical displacement plot and reaction force developed at the cross-beam area.....	73
Figure 3.20: Side and profile views of the specimen .....	74
Figure 3.21: Load-displacement curves.....	75
Figure 4.1: Drone built by the University of California at Davis research team.....	79
Figure 4.2: How IDOT used drone collected images and data.....	80
Figure 4.3: Iowa DOT’s DJI Phantom 4 .....	80
Figure 4.4: Highway survey photo taken with DJI Phantom 4 .....	81
Figure 4.5: Contour map using data collected by a UAV .....	82
Figure 4.6: Flood monitoring conducted using UAVs in Vermont.....	83
Figure 4.7: DJI Mavic inspecting the Fall River Bridge in Idaho .....	85
Figure 4.8: MDOT’s Bergen Hexacopter with dual FLIR cameras .....	86
Figure 4.9: FLIR Vue Pro onboard the Bergen Hexacopter.....	86
Figure 4.10: Velodyne LP-16 LiDAR attached to the Bergen Quad-8 UAV.....	87
Figure 4.11: Mariner 2 Splash with GoPro cameras .....	87
Figure 4.12: SenseFly Albris UAV .....	89
Figure 4.13: Flyability Elios UAV .....	89
Figure 4.14: DJI Inspire UAV used by NCDOT.....	90
Figure 4.15: DJI Phantom 3 Pro with a pilot.....	91
Figure 4.16: ARIA MAV and a bridge model produced using the MAV collected data.....	92
Figure 4.17: MAV-F8 built by the Florida Tech research team.....	93
Figure 4.18: UAVs used by Union Pacific to conduct railroad bridge inspections.....	94
Figure 4.19: Typical condition of aged bridges.....	98
Figure 4.20: Different eddy current probes that can be used on a drone.....	99
Figure 4.21: How impedance-based nondestructive testing works and the equipment needed .....	100
Figure 4.22: Amerapex drone with UT equipment.....	101
Figure 4.23: Amerapex drone measuring wall thickness .....	101



Figure 4.24: Experimental setup for the microwave 3D imaging .....	102
Figure 4.25: Experimental setup for the terahertz radiation and imagery .....	102
Figure 4.26: Experimental setup for the infrared pulsed (active) thermography.....	103
Figure 5.1: Representative bridge system used in this study.....	109
Figure 5.2: Type 1 corrosion pattern used in this study .....	110
Figure 5.3: First eigenmode of the bridge solved using an eigenvalue buckling analysis algorithm and when the load is only on the top of the deteriorated end .....	111
Figure 5.4: Applied loads on the bridges.....	112
Figure 5.5: Applied load against the time .....	113
Figure 5.6: Reaction forces at the beam ends .....	114
Figure 5.7: Failure of deteriorated beam ends and the middle adjacent beam end .....	114

This page left blank intentionally.

# 1.0 Introduction

## 1.1 Background Information

---

As New England's bridge population ages, MassDOT inspection engineers are increasingly witnessing instances of extensive corrosion at steel beam ends. Due to the increased use of deicing techniques, the increased incidence of this condition can be primarily attributed to leaking through deck joints. The leaking water contains high concentrations of chemical substances used seasonally to winterize the road above. Deterioration of the steel is most often initiated by the buildup of this runoff on the top face of the bottom flange. When this process is sustained, the buildup of runoff triggers a corrosive process in the bottom flange, the structural components above it, and the web. The resulting section loss leads to a significant reduction in the girder's load-carrying capacity. Several cases exist wherein the extreme effects of this phenomenon have caused closure of the bridge to ensure life safety. The nonuniformity of the corroded shape and the variable thickness reduction along the corroded area provide substantial challenges in calculating realistic estimates of the remaining capacity of the girder's end.

Ongoing research is developing new improved procedures that accurately describe the remaining load-carrying capacity of these deteriorated members. These new procedures are based on computational simulations and experimental testing of real deteriorated beams. The outcome of a recently completed research project ("Development of Load Rating Procedures for Deteriorated Steel Beam Ends," completed July 2019) has found new parameters that are extremely important when assessing the residual capacity of the bridge and the load rating procedure. Examples of these parameters include the out-of-plane imperfection of the beam web, the surface area of corrosion, and others. Currently, inspectors are not aware of the new findings and these important parameters, and they have no clear guidance on what and how to measure when inspecting a deteriorated beam end.

It is important for MassDOT to strongly consider the new load rating procedures in drawing realistic conclusions. Two areas of need are the measurement and classification of important parameters that have not been typically measured in the past by inspectors, and enhancement of the inspection protocols so that important deterioration information needed for the new improved procedures is documented during inspections. Drawing on the recent findings made while developing new load rating procedures, the project at hand aims at procedures to collect important real-world data from deteriorated bridges and then explore enhanced data gathering technologies such as LiDAR scanning. The second part of the project involves processing and classifying this data and ultimately developing a comprehensive inspection protocol for deteriorated steel beam ends.

## 1.2 Research Goals

---

The completed research project (July 2019) on the development of load rating procedures for deteriorated steel beam ends has highlighted the need for additional measurements that are essential for the accurate estimation of the capacity of beam ends. One main finding from the experimental testing and the computational work conducted demonstrates that out-of-plane displacement of the web at the beam end is a major factor in the calculation of the deteriorated beam end capacity. Another finding is that the area of interest for which thickness loss measurements are needed is different than the one described currently in the bridge manual procedures. Based on these conclusions, MassDOT is considering incorporating a new inspection protocol for deteriorated beam ends that is focused on systematically measuring the most important parameters needed for the estimation of the remaining capacity. Capitalizing on these recent findings, the current research report provides the following:

1. Effective and efficient procedures for collecting important data from deteriorated steel beam ends using new procedures such as LiDAR scanning techniques.
2. Exploration of new practical inspection techniques and inspection solutions using new technology such as LiDAR scanning or drone technology to obtain the critical measurements.
3. Comprehensive inspection and documentation protocol that will be used along with the new load rating procedures for more accurate and effective load rating of steel bridge beam ends. This protocol will be developed accounting for the trade-off between accuracy and quantity of in-field measurements and refined assessment of residual capacity.
4. Identification and classification of unique cases that would require future research or advanced modeling that cannot be described by the new load rating procedures.
5. Computational evaluation of steel girders with end corrosion as part of a bridge system.

## **2.0 Evaluation of Current Inspection Procedures and the Impact of the Important Parameters**

An unavoidable result of the aging of bridges [1] in the United States is the deterioration of their assets. Malfunctioning joints fail to prevent water and deicing chemicals from penetrating into the superstructure, especially at load-carrying components. For bridges made of steel girders, the buildup of this runoff triggers a corrosive process afflicting the as-designed dimensions of the elements at the support area. Topologically nonuniform and highly uncertain, the appearance of corrosion makes the residual bearing capacity quite challenging to assess. Recent research is developing new and improved procedures that accurately describe the remaining load-carrying capacity of stiffened beam ends. Before these procedures are developed it is important to get an accurate assessment of the existing bridge inspection procedures.

This section explores what is and what is not working with the current inspection procedures. The first half of this section presents a questionnaire that was distributed to MassDOT inspectors and consultants. The second half summarizes and processes the responses that were collected and provides areas of improvement for potential procedures based on the data collected.

### **2.1 Introduction**

---

#### **2.1.1 Background Information**

Approximately 40% of the roughly 600,000 bridges included in the National Bridge Inventory have been in service for more than five decades [1]. Ongoing research is developing new and improved procedures that accurately describe the remaining load-carrying capacity of stiffened beam ends. These new procedures are based on computational simulations and experimental testing of real deteriorated beams. Previous research work [2] conducted by the researchers has found new parameters that are extremely important when assessing the residual capacity of unstiffened girder ends. Examples of these parameters include the out-of-plane imperfection of the beam web, the surface area of corrosion, and others. Currently, inspectors are not aware of the new findings and these important parameters, and they have no clear guidance on what and how to measure when inspecting a deteriorated beam end.

#### **2.1.2 Questionnaire Goals and Methodology**

Within this section the researchers review the existing inspection procedures in terms of the general procedures, corrosion assessment, utilized equipment, data collection, and documentation. In this framework, and in coordination with MassDOT, a questionnaire was prepared and distributed to inspectors across the state.

The following goals were kept in mind while gathering information and creating the questionnaire:

1. The people who inspect bridges,
2. The general bridge inspection procedures,
3. How corrosion and corrosion of beam ends is currently being estimated and assessed,
4. The equipment that inspectors have, and
5. Drone use or possible drone use for transportation related activities.

This questionnaire had three sections and a total of 42 questions regarding general bridge inspections practice, bridge corrosion assessment, and bridge inspection equipment. The questionnaire was made using Google Forms and was distributed to those involved in MassDOT bridge inspections. The responses obtained from 34 bridge inspection personnel are presented and analyzed in Section 2.3 of this report, and they will aid in the creation of new inspection procedures, particularly concerning corrosion assessment.

## **2.2 Data Collection**

---

This section includes the creation of a questionnaire to review the current inspection procedures across the different MassDOT districts. The approach will allow the researchers to correlate findings from a previously completed research project [2] with the established data acquisition techniques and corrosion documentation.

Regarding the inspection methods, the thorough examination of inspection reports revealed that the quality of measurements taken in the field is highly susceptible to accessibility, weather conditions, and available equipment. A common finding among all districts is that rarely more than two points are measured along a deteriorated end. Consequently, part of the developed questionnaire is oriented to interpret the point selection process by the inspectors.

Both the experimental and the computational part highlighted the importance of web deviation from straightness to the remaining bearing capacity of unstiffened girders. In detail, the failure mechanism of a specimen was strongly affected by the initial lateral web imperfection: Numerical analyses revealed cases where the capacity was reduced by 40%. Although this finding is consistent with basic plates or shells theory, it was not part of the existing procedures or the current inspection protocol. Based on this result, inspection reports were reviewed for one more time, and it was found that this type of imperfection is more common than previously thought; therefore, it is a highly important parameter to be measured. In this framework, questions that explore techniques to assess the extent of web deviation with the current or potential equipment were also included.

### **2.2.1 General Bridge Inspection Practices**

The purpose of this section was to help the researchers gain an overall understanding of the current bridge inspections practices and identify aspects that may be problematic. These

questions will highlight what aspects of the current MassDOT procedures are and are not working, so that we may develop an improved inspection procedure.

Keeping their overall experience in mind, the inspectors were asked the following questions:

1. What is your name and email address?
2. What is your current position?
3. What district do you work for?
4. How many bridges are you responsible for?
5. How many bridges do you inspect per week?
6. What training procedure did you follow to become a bridge inspector?
7. Prior to performing a bridge inspection, do you have any of the following materials?  
(You may choose more than 1.)
  - a. Drawing
  - b. Plans
  - c. Previous Reports
  - d. Other: \_\_\_\_\_
8. What aspect(s) of inspections slow you down the most?
9. Is there any part of the 2015 MassDOT inspection handbook that is hard to implement?

### **2.2.2 Corrosion Assessment**

The purpose of this section was to help the researchers gain an overall understanding of how corrosion of steel bridge beam ends is being assessed during bridge inspections. These questions will highlight what aspects of the current MassDOT procedures are and are not working, and how to best develop new procedures for the assessment of corroded steel beam ends.

Referring to only their knowledge and experience with steel bridge corrosion, the inspectors were asked the following questions:

1. What challenges do you face with assessing corrosion?
2. What technologies have you used for bridge inspections? (You may choose more than 1.)
  - a. Visual
  - b. D-Meter
  - c. Advanced Technologies
  - d. Other: \_\_\_\_\_
3. If you selected Advanced Technologies, list those technologies.
4. Have you ever witnessed the upper edge of a web hole bearing on the flange (Figure 2.1)?

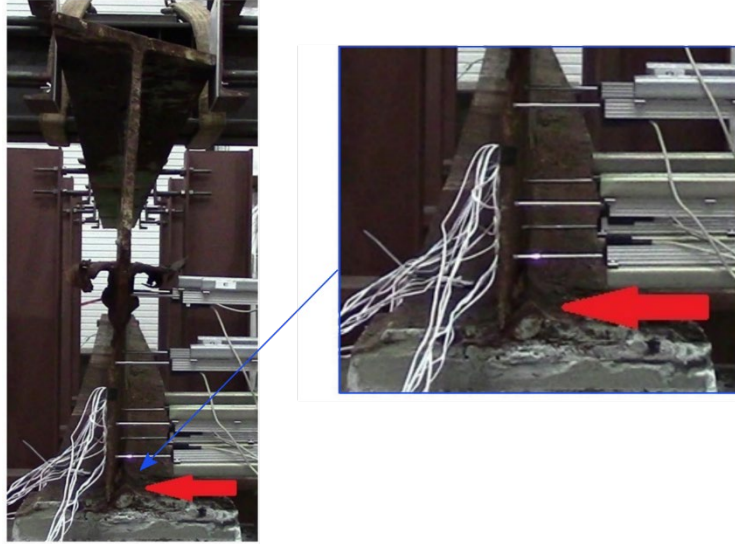


**Figure 2.1: Upper edge of a web hole bearing on the flange**

- a. Yes for a stiffened beam
  - b. Yes for an unstiffened beam
  - c. Yes for both a stiffened and unstiffened beam
  - d. No
  - e. Other: \_\_\_\_\_
5. Do you measure web thickness using a D-Meter?
    - a. Yes
    - b. No
  6. If you answered yes, what D-Meter model(s) do you use?
  7. If you answered yes, how accurate are the measurements of the D-Meter you use?
    - a. Very accurate
    - b. Moderately accurate
    - c. Not at all accurate
    - d. Other: \_\_\_\_\_
  8. If you answered no, what technology do you use to measure web thickness?
  9. What other technology could be used to measure web thickness?
  10. At which points would you take thickness measurements for an unstiffened bridge beam (Figure 2.2)?



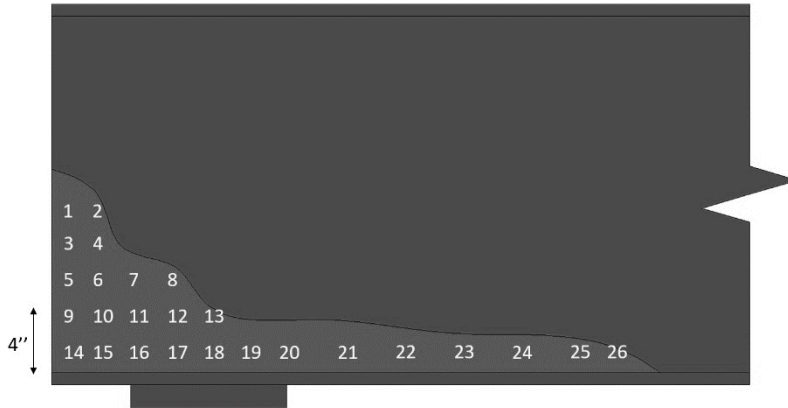


**Figure 2.2: Corrosion on an unstiffened bridge beam**

\*The numbers shown correspond to points at which inspectors could take measurements.

11. Are there any additional places where you would take measurements from that are not shown in the sketch?
12. At which points would you take thickness measurements for a stiffened bridge beam (Figure 2.3)?

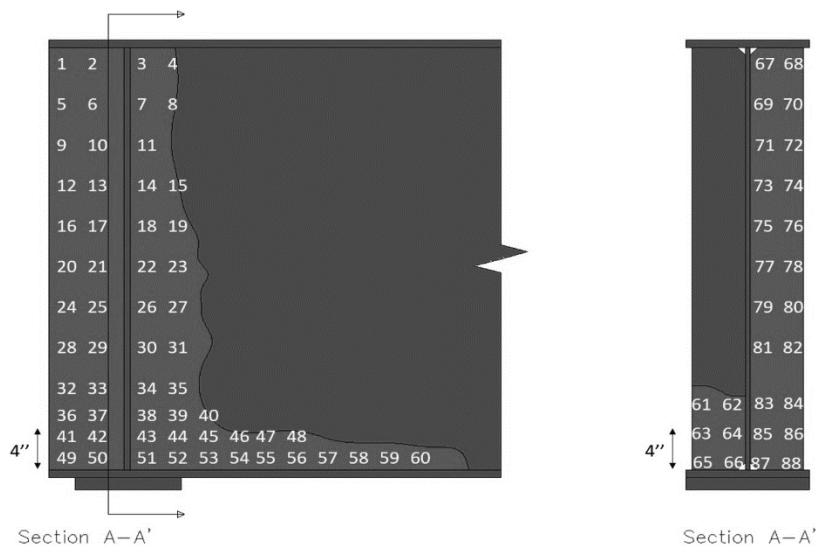


**Figure 2.3: Corrosion on a stiffened bridge beam**

\*The numbers shown correspond to points at which inspectors could take measurements on both a web and stiffeners.

13. Are there any additional places where you would take measurements from that are not shown in the sketch?
14. How many points do you typically measure?
15. How do you choose where to take thickness measurements?
16. Do you normally take thickness measurements of corroded stiffeners?
  - a. Yes
  - b. No

17. Have you ever witnessed beam webs that deviate from straightness (Figure 2.4)?

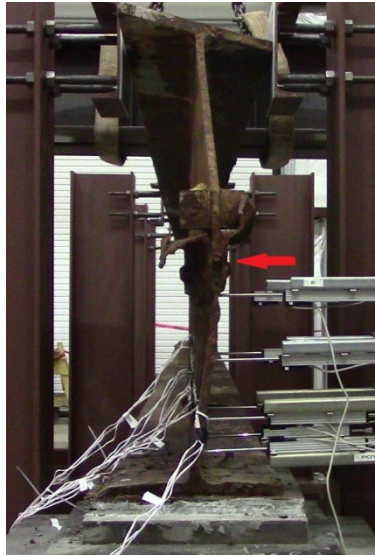


**Figure 2.4: Web deviating from straightness**

- c. Yes for a stiffened beam
  - d. Yes for an unstiffened beam
  - e. Yes for both a stiffened and unstiffened beam
  - f. No
  - g. Other: \_\_\_\_\_
18. Do you measure web deviation from straightness?
- h. Yes
  - i. No
19. If you answered yes, what do you use to measure web deviation from straightness?
20. If you answered yes, how accurate are the measurements you take for web deviation from straightness?
- j. Very accurate
  - k. Moderately accurate
  - l. Not at all accurate
  - m. Other: \_\_\_\_\_
21. What other technology can be used to measure web deviation from straightness?

### **2.2.3 Equipment**

The purpose of this section was to help the researchers gain an understanding of the equipment being used for bridge inspections. These questions will highlight what is available for inspections to better inform our decisions regarding inspection protocol.

Referring to only their knowledge and experience of the technology utilized for bridge inspections, the inspectors were asked the following questions:

1. What equipment do you typically have on hand during an inspection? (Please provide the advantages and disadvantages for each.)
2. Are gauges calibrated periodically? If so, how often?
3. What would you change about the equipment you use?
4. Would you be able to carry a portable laser scanner like the one below (Figure 2.5), and potentially a tablet or a cell phone?



**Figure 2.5: A portable LiDAR**

- a. Yes
- b. No
- c. Maybe
5. Is it possible to remove delamination along the domain above the support?
  - a. Yes
  - b. No
  - c. Maybe
6. If not, why?
7. How much time do you currently spend on documenting the collected data into a routine inspection report?
  - a. None
  - b. 1–2 hours
  - c. 3–4 hours
  - d. 5–6 hours
  - e. Other: \_\_\_\_\_
8. Do you spend additional time for measurements and documentation for a bridge that a new load rating may be required?
9. Have you ever used a drone or witnessed a drone being used for any MassDOT-related activities?

- a. Yes
  - b. No
10. If so, what was that activity?
11. Have you ever considered using drones for bridge inspections?
- a. Yes
  - b. No, but I think they could be useful to implement in the future
  - c. No, and I do not think they would be useful to implement in the future
12. Any additional comments and/or suggestions that we should know?

## 2.3 Questionnaire Responses from MassDOT Inspectors and Consultants

---

After sending out the questionnaire, a total of 34 responses—11 MassDOT employees and 23 consultants—were recorded, and the data has been processed.

### 2.3.1 General Bridge Inspection Practices Section Responses

For privacy reasons the responses for the first question that asked for names and email addresses has been omitted from this report. To organize the four questions that followed the first, it was decided that the answers would be split into two categories: responses from MassDOT employees and responses from consultants.

Figures 2.6 and 2.7 were made using the current position(s) data collected from the respondents. It is important to note that some respondents listed multiple positions in their response. Overall, the consultants listed more positions, and the positions that are listed are more diverse than just “bridge inspector.” This was an expected result because the consultants may have other responsibilities besides bridge inspections, and therefore they may not have the same experience as the MassDOT employees when it comes to inspecting bridges.

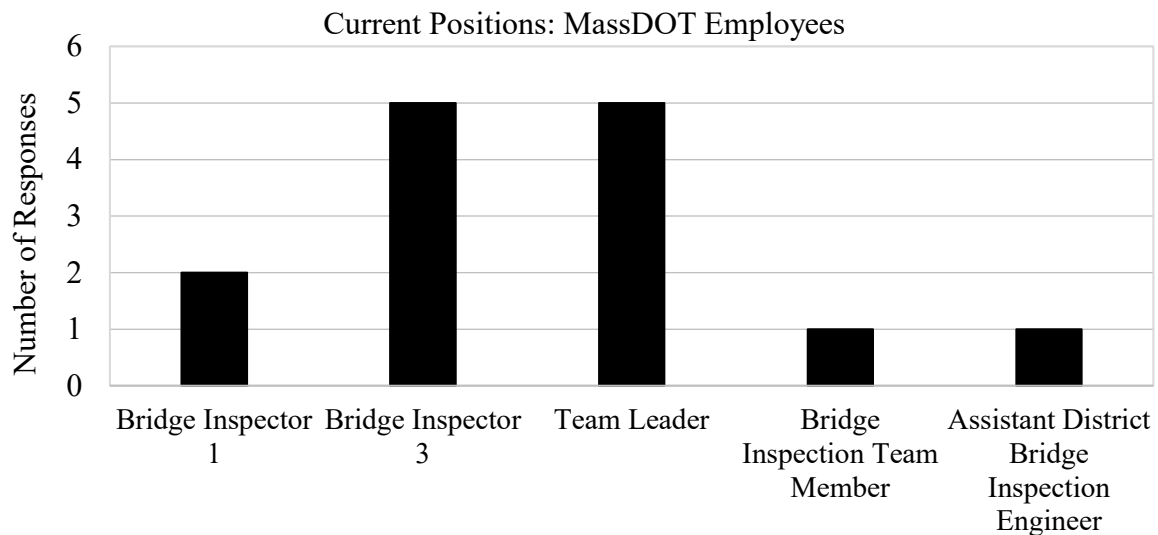


**Figure 2.6: Current positions of MassDOT respondents**

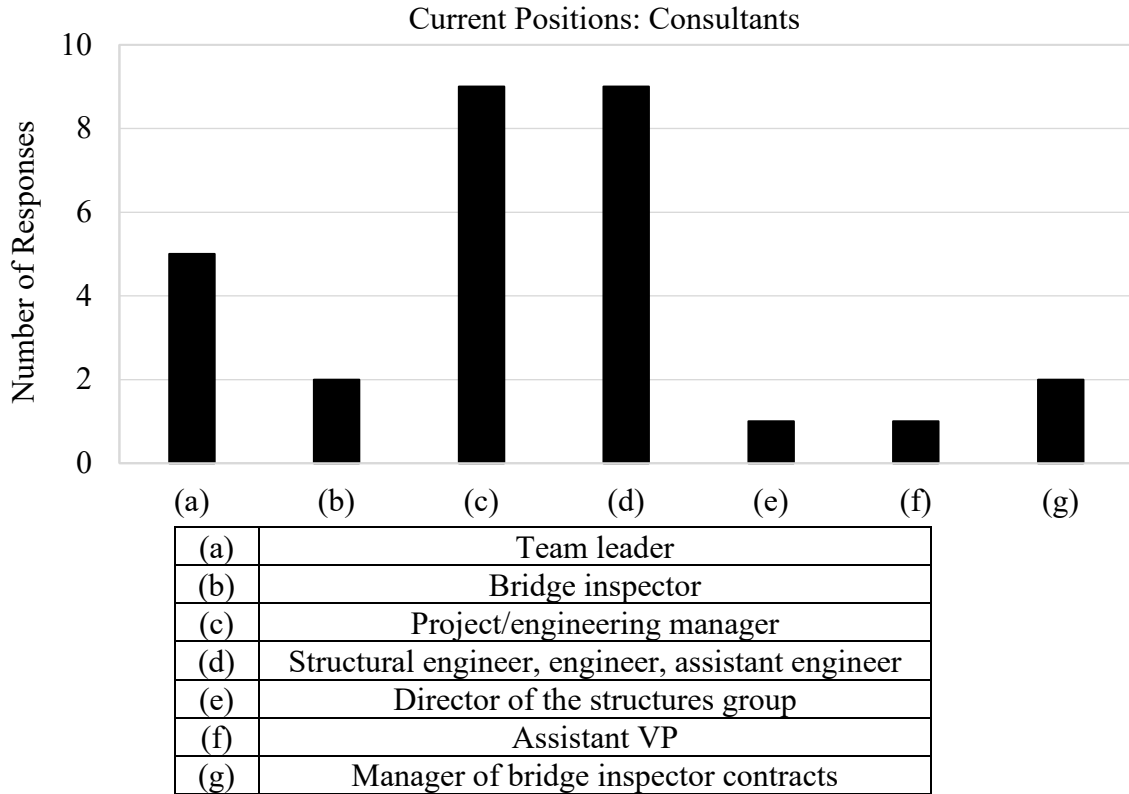


**Figure 2.7: Current positions of consultant respondents**

Regarding the districts that the respondents work for, the more definitive answers for this question came from the MassDOT employees because they are hired to work in one particular district. At least one person responded from each district, except for Districts 3 and 6 (Figure 2.8). In terms of scale, the MassDOT inspectors stated that Districts 2 and 5 have about 2,000 bridges, District 1 has about 1,200 bridges, and District 4 has about 1,630 bridges. Since consultants are not tied to one district, Figure 2.9 instead shows consulting engineering firms and how many consultants from each firm answered the questionnaire.

It is important to note that all the consultants stated that they work for all the districts. However, two consultants deal mostly with bridges from District 6, one consultant deals mostly with Districts 3 and 4, one consultant deals mostly with Districts 4 and 5, one consultant deals mostly with Districts 4, 5, and 6, and one consultant deals with all the districts except District 3. This is important because, although no MassDOT inspectors from Districts 3 and 6 responded, these districts are still being represented by the consultants that frequently carry out inspections within them.

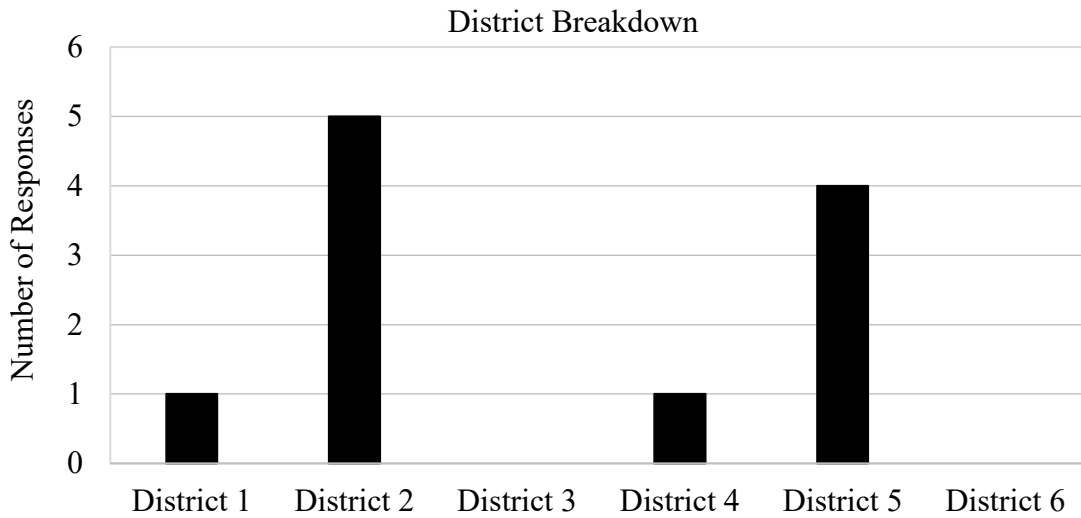
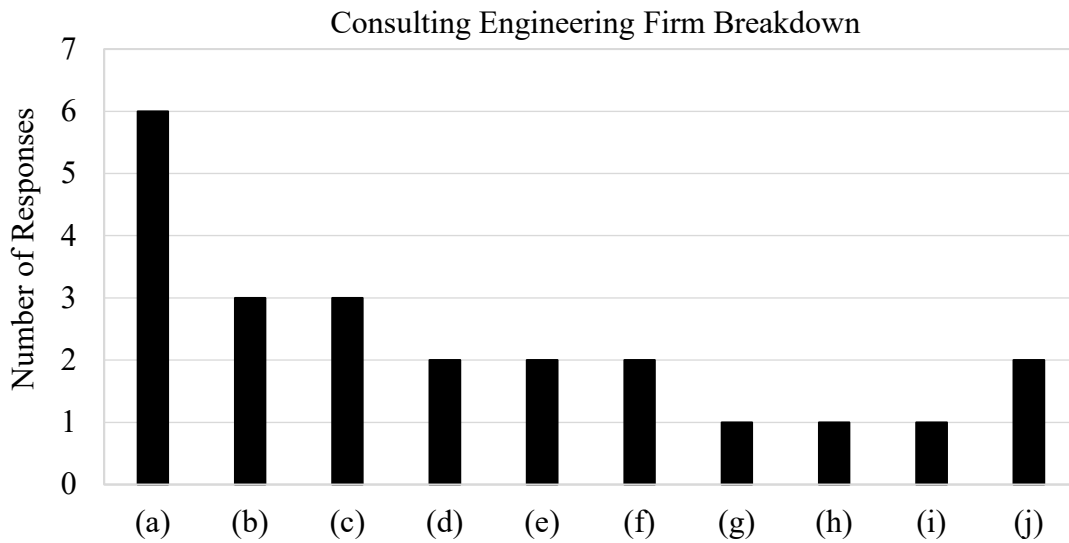


**Figure 2.8: District breakdown for MassDOT employees**



(a)	TranSystems
(b)	Collins Engineering
(c)	Gill Engineering
(d)	AI Engineering
(e)	Benesch
(f)	HNTB
(g)	Engin Group
(h)	AE Com
(i)	Green International
(j)	Unknown

**Figure 2.9: Engineering firms for responding consultants**

To gauge the workload of each inspector, the next two figures show how many bridges inspectors are responsible for. The responses for the MassDOT employees are presented in Figure 2.10 and the responses for the consultants are presented in Figure 2.11. Overall, MassDOT employees appear to be responsible for about 8 to 12 bridges per month, whereas the consultants are only responsible for those they are assigned, which varies by inspection contract and/or task order.

The responses for this question show that MassDOT inspectors may typically be responsible for more bridges, which means they may not have as much time to carry out each inspection per month. Therefore, a new corrosion estimation method utilizing LiDAR should not take too much time to carry out given the typical workload of the bridge inspectors.

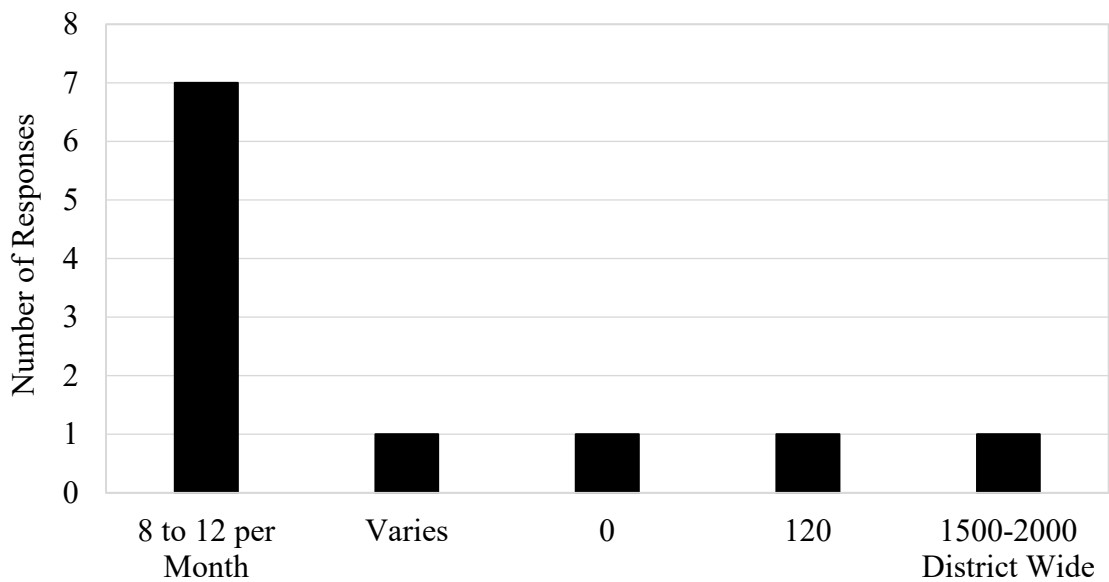


**Figure 2.10: Number of bridges MassDOT employees are responsible for**

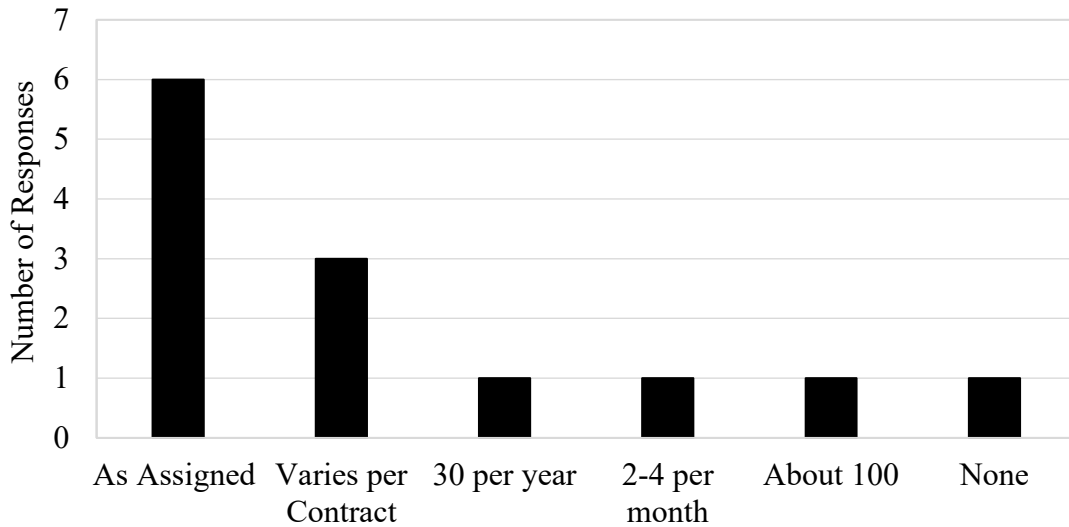


**Figure 2.11: Number of bridges consultants are responsible for**

Looking at a much shorter time frame to gauge workload, Figures 2.12 and 2.13 records how many bridges are inspected per week for MassDOT employees and consultants, respectively. There is a lot of variation in answers for this question, but overall it seems that MassDOT employees inspect more bridges per week, which is to be expected since they are hired to mainly do inspections. These responses again suggest that inspectors may not have as much time to carry out and document each inspection per week, which highlights the need for a new data acquisition method.

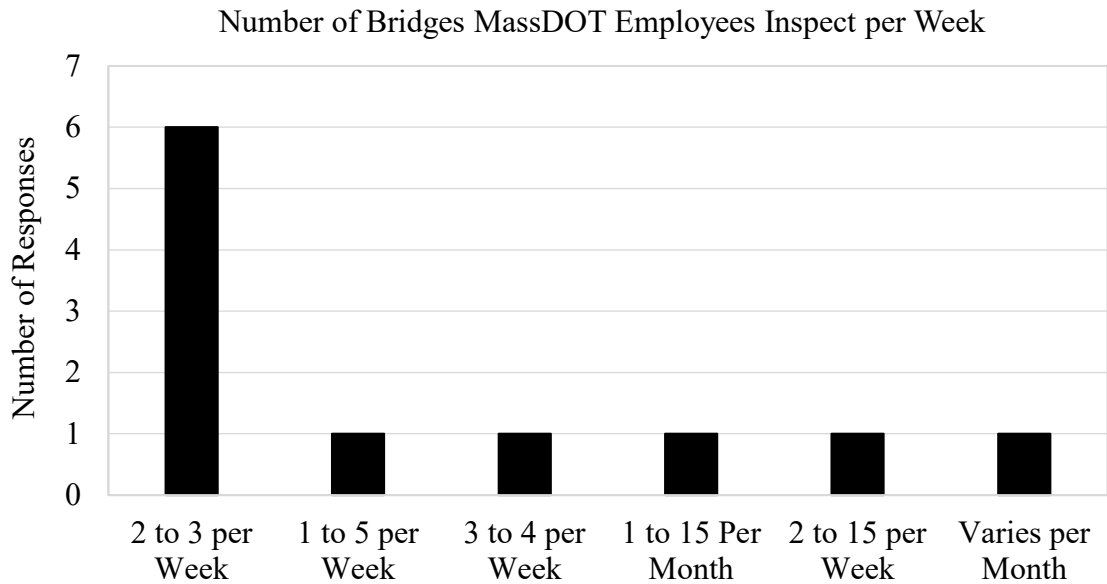




**Figure 2.12: Bridges inspected by MassDOT respondents**

The remaining figures and tables contain the responses of both MassDOT employees and consultants. Regarding inspectors' training, Figure 2.14 shows that most inspectors took National Highway Institute (NHI) or Federal Highway Association (FHWA) Courses to become a bridge inspector. Many of the respondents named the specific NHI/FHWA that they took.

Those specific courses included a 2-week course on inspection of in-service bridges, an 80-hour bridge course, a course on fracture critical inspections, a course on tunnel inspection, a course on ancillary inspection, and the refresher courses that are offered for each course. This indicates that each inspector starts out with the same basic knowledge from the required NHI course, but their experience and on-the-job training will differ and ultimately influence how they perform bridge inspections. This should be kept in mind when considering how the bridge inspectors will be trained on the new corrosion estimation that will be made.

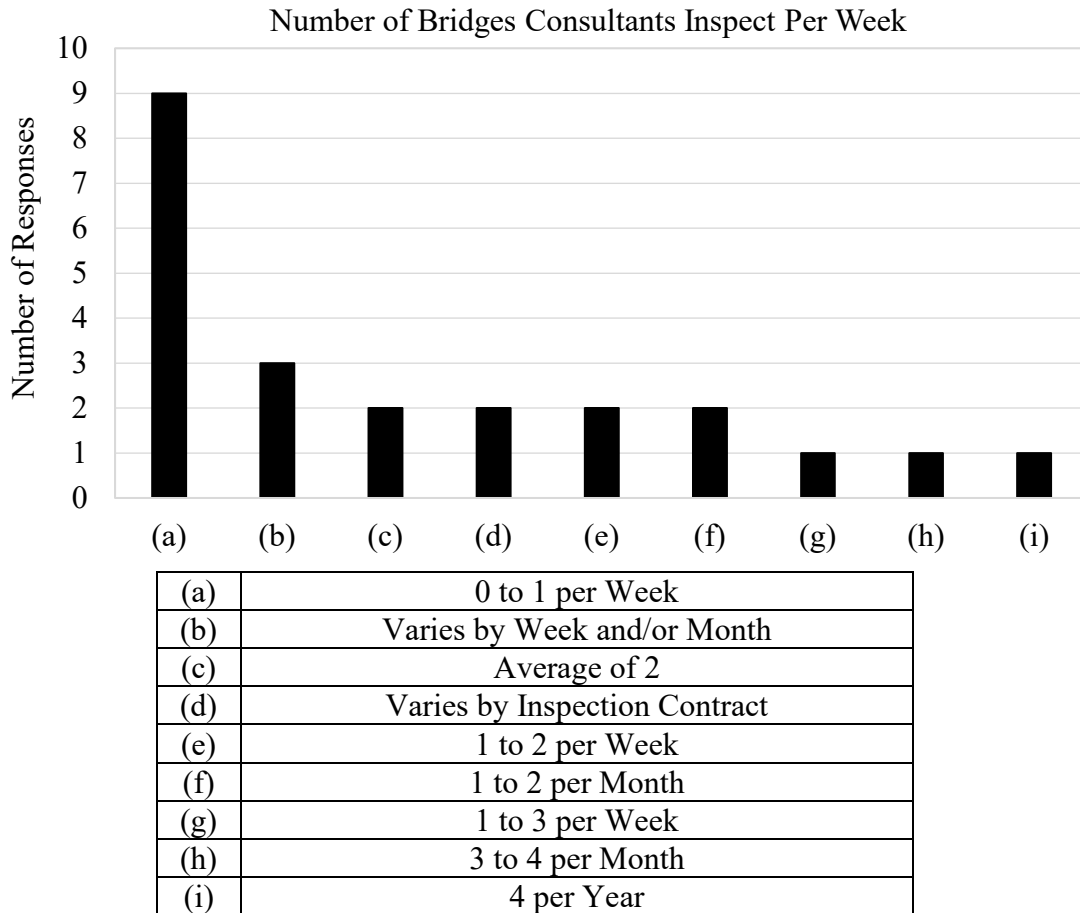
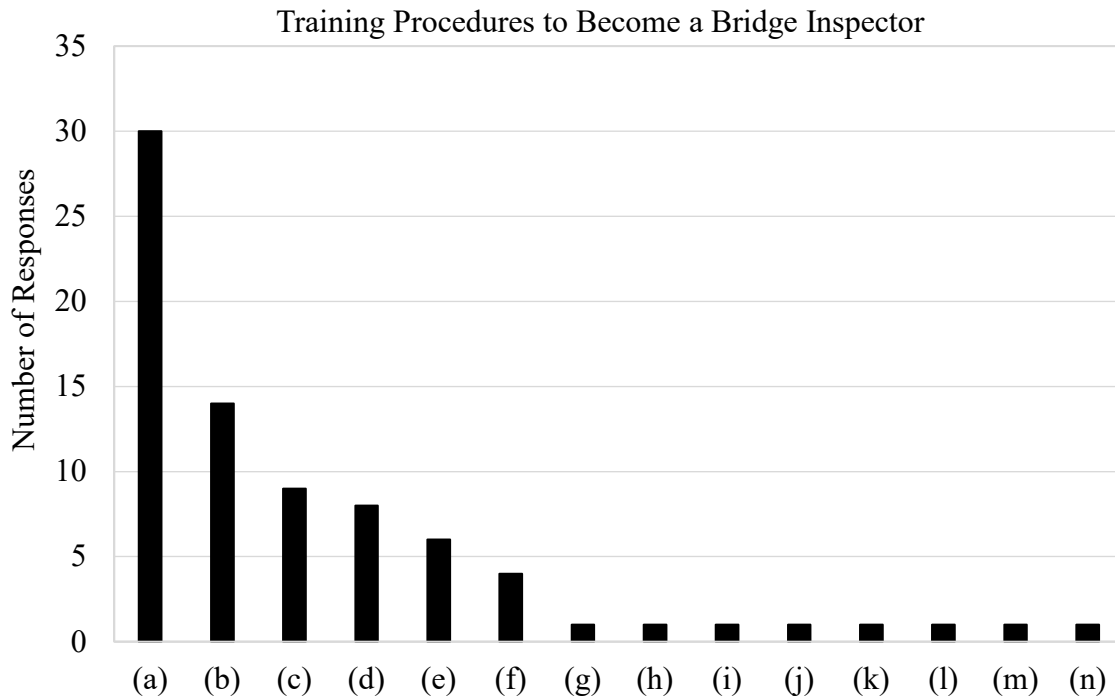


**Figure 2.13: Bridges inspected by consultant respondents**



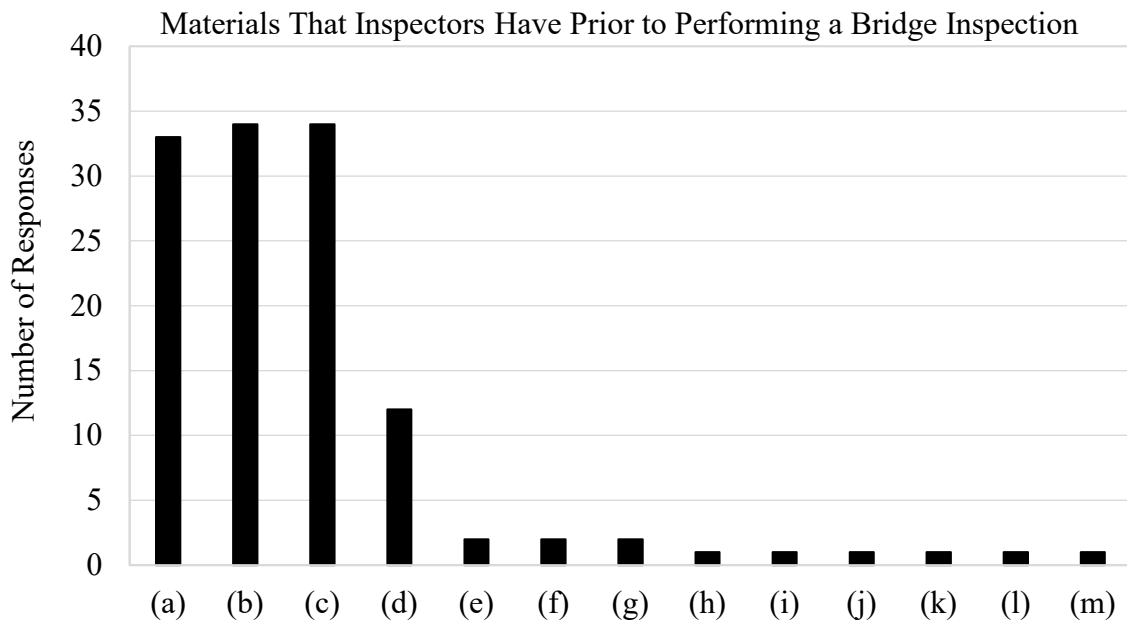
(a)	NHI/Federal Highway course	(h)	NICET
(b)	College degree (B.S. and/or M.S.)	(i)	Basic civil engineer 1
(c)	Year of experience	(j)	OSHA 10-hour course
(d)	On the job training/hands on learning	(k)	Snooper truck training
(e)	EIT exam	(l)	Bucket truck training
(f)	PE exam	(m)	Aerial lift training
(g)	In-house training	(n)	Destructive and nondestructive procedures

**Figure 2.14: Training procedures for bridge inspectors**

The materials both MassDOT inspectors and the consultants have prior to performing a bridge inspection are recorded in Figure 2.15, which highlights that almost all the respondents chose the three given options:

- drawings,
- plans, and
- previous reports.

Many also provided an “other” answer, a majority of which wrote load rating reports as their other material that they typically have before a bridge inspection. Overall, inspectors have a lot of information prior to inspecting a bridge, and these materials can help in the development and execution of potential corrosion assessment procedures.

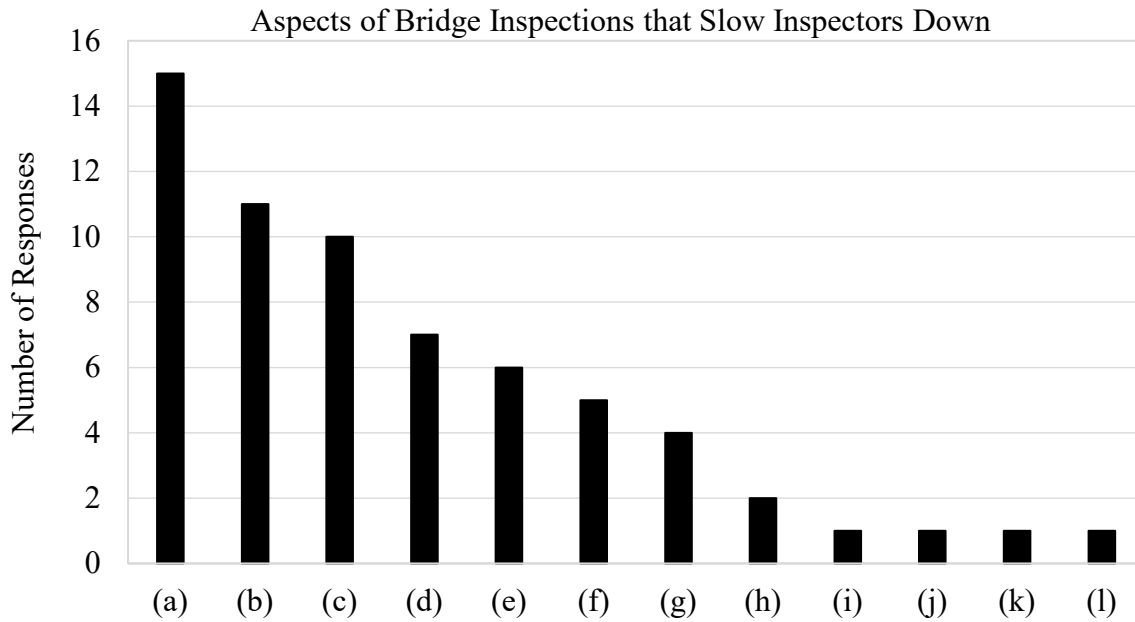


(a)	Drawings	(h)	MassDOT bridge inspection handbook
(b)	Plans	(i)	Bridge inspection reference manual
(c)	Previous reports	(j)	Blank diagram/sketches
(d)	Load rating reports	(k)	Oral history
(e)	Talk to previous inspection team	(l)	Forms prepared based on received information
(f)	Inventory photos	(m)	Safety equipment and tools
(g)	Fracture critical procedures		

**Figure 2.15: Materials before performing bridge inspections**

When analyzing the data on different aspects of bridge inspection, the ability to access, view, and be hands-on with the bridge, as well as measuring and documenting for inspection reports and traffic control for bridge inspections, are the aspects of bridge inspections that slow inspectors down the most (Figure 2.16). For this question many inspectors made a list of several aspects and did not give only one aspect.

The responses given for this question indicate that any new procedure and technology that is proposed should be able to easily access and measure corrosion without taking too much post-processing time so that the inspectors are not additionally slowed down using the new procedure and technology.



(a)	Access, visibility, hands-on inspection	(g)	Tool limitations (D-meters, trucks, ladders)
(b)	Measuring, documenting, reporting, and/or sketching	(h)	Timber, mesh, protective shielding, shearing
(c)	Traffic control issues	(i)	Scheduling in general
(d)	Railroad issues	(j)	Previous inspection reports are unclear
(e)	Large amount of deterioration	(k)	Deterioration not previously noted
(f)	Removing rust and debris	(l)	Sand accumulation

**Figure 2.16: Aspects that slow bridge inspectors down**

Figure 2.17 records the parts of the 2015 MassDOT inspection handbook that inspectors find difficult to implement. The overall consensus was that no part of the handbook is hard to implement, but there were still six other responses recorded in Figure 2.17. Some respondents gave additional comments besides just no.

One such response that was found to be important to remember was that the state puts their requirements in the handbook and the inspectors find time to meet those requirements based on budget. Another respondent wrote that policy directives have been helpful in clarifying certain procedures or implementing new procedures, which highlights a promising way that a new corrosion estimation procedure could be introduced and explained to inspectors.

Overall, the current handbook is written in a way that is not hard for inspectors to implement, therefore any new procedures should follow a similar format so that they too are not hard to implement. However, there were concerns brought up by some of the inspectors, but those concerns can and should be fixed for corrosion estimation in particular.

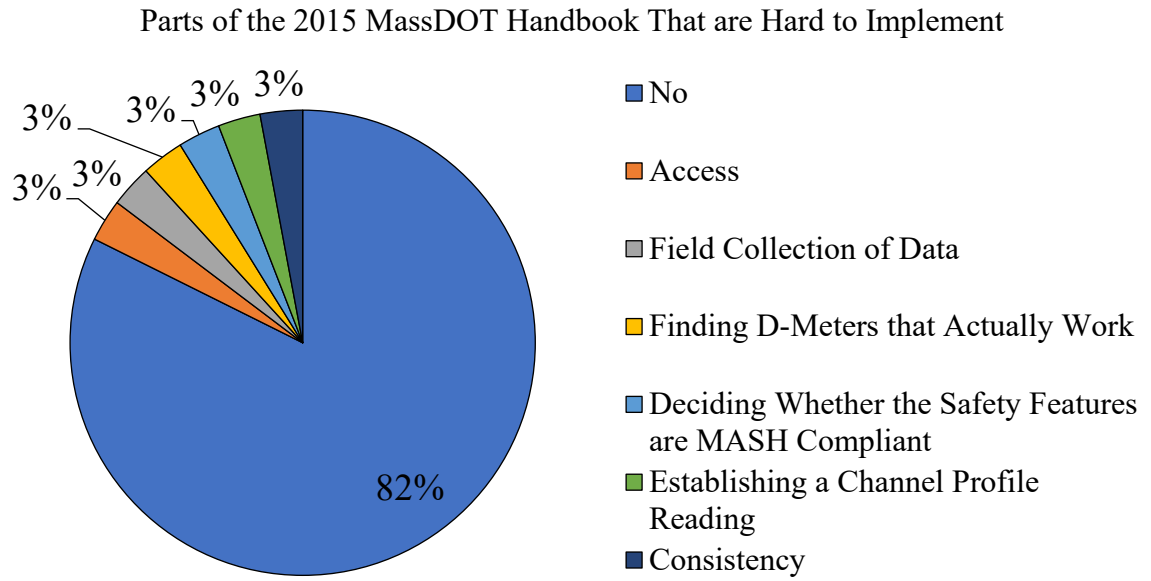
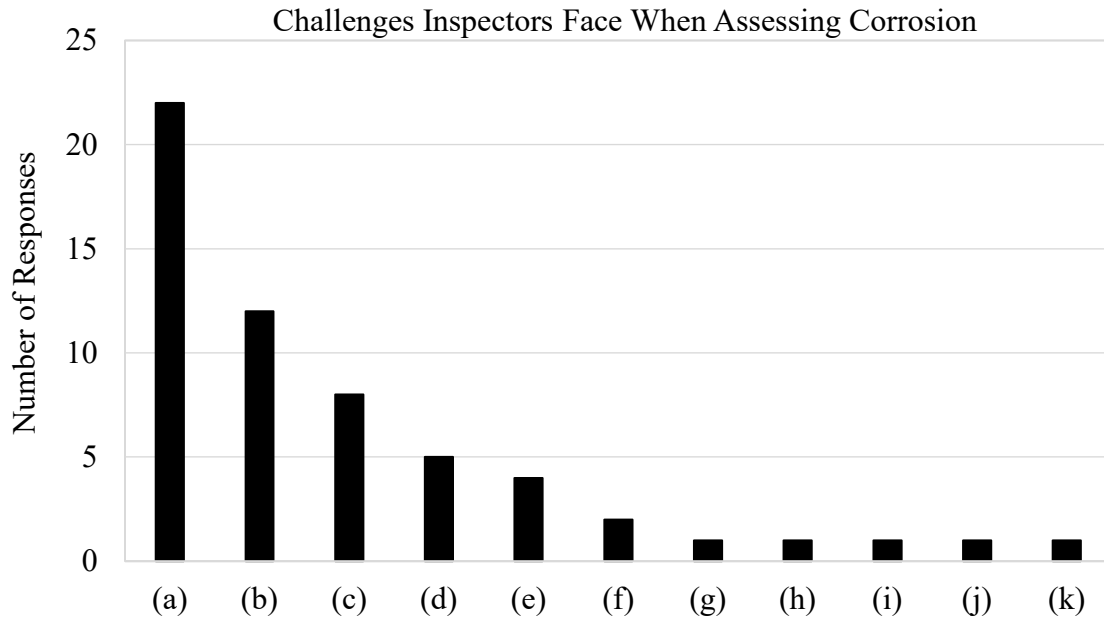


**Figure 2.17: Difficult parts of the 2015 MassDOT inspection handbook**

### 2.3.2 Corrosion Assessment Section Responses

Moving into the corrosion assessment section of the questionnaire, Figure 2.18 summarizes the challenges inspectors face when assessing corrosion. Most respondents listed many challenges, and cleaning off the rust from corroded areas, viewing the corroded area, and accessing the corroded areas are the biggest challenges with assessing corrosion.

The challenges listed suggest that any new corrosion assessment technology and procedure should allow for the estimation of corrosion with little to no need for the cleaning and removing of rust and should be able to access and view areas that are typically corroded.



(a)	Cleaning steel/removing rust	(g)	Irregularities
(b)	Access/visibility	(h)	Measuring consistently over time
(c)	Measuring and getting accurate measurements	(i)	Previously documented incorrectly
(d)	Tool limitations (especially on uneven surfaces)	(j)	Finding when previous inspectors didn't recheck
(e)	D-meter problems	(k)	Cleaning when there is lead paint
(f)	Assessing extent of corrosion		

**Figure 2.18: Challenges faced when assessing corrosion**

When asked about the technologies used for bridge inspections, all the respondents chose more than one of the provided options, and many gave an additional technology. Of the three given choices, most of the respondents checked off that they use visual technology, D-meters, and other technology (Figure 2.19). The other technologies noted by 27 of 34 respondents are provided in Table 2.1, which shows that most use calipers or a straight edge or ruler as their “other” technology.

This indicates that many inspectors may not be as familiar with the more advanced technologies, so it may be harder to implement a corrosion technology if it is more advanced. Therefore, it is best to consider a corrosion estimation procedure that can be done just as well with technology they currently use as a more advanced technology.

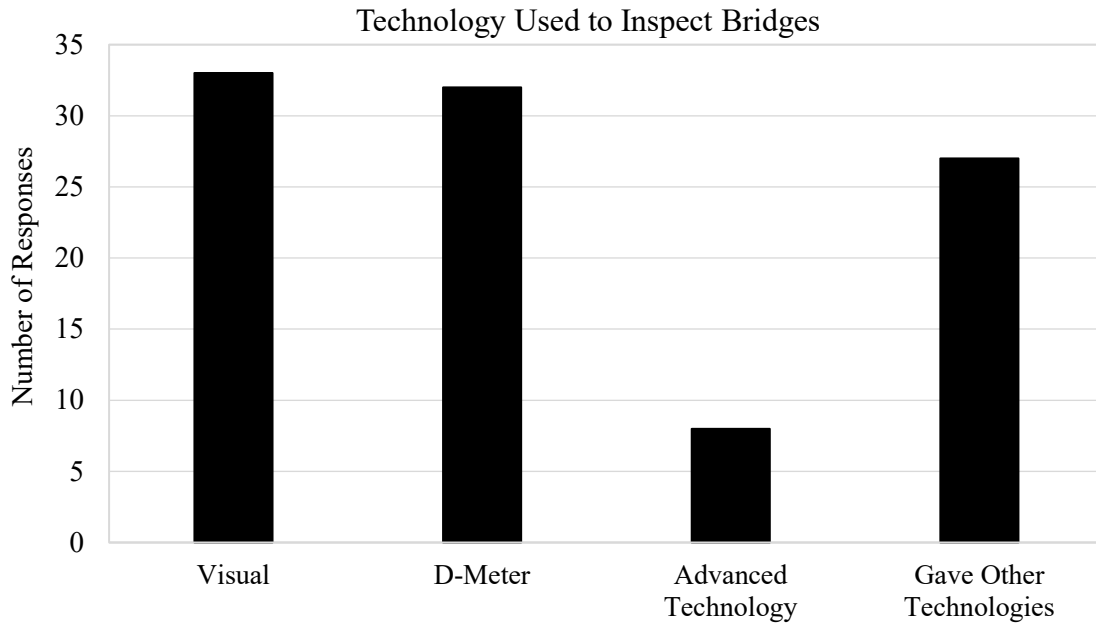


**Figure 2.19: Bridge inspection technologies used by inspectors**

**Table 2.1: Other technologies used by inspectors**

<b>Other technologies</b>	<b>Number of responses for each</b>
Calipers	9
Straight edge/ruler	5
Plumb bob	2
Level	2
Pneumatic drill/needle gun scaler	1
Hammer/hammer sounding	1
NDT	1

Those that chose advanced technology were asked to list the technologies they were referring to. Most respondents count their dye penetrant testing kits as their “advanced technology” (Figure 2.20). The responses recorded in the Figure 2.20 were very informative and guided our research toward seeing if any of the technology listed could be used for corrosion assessment and estimation.

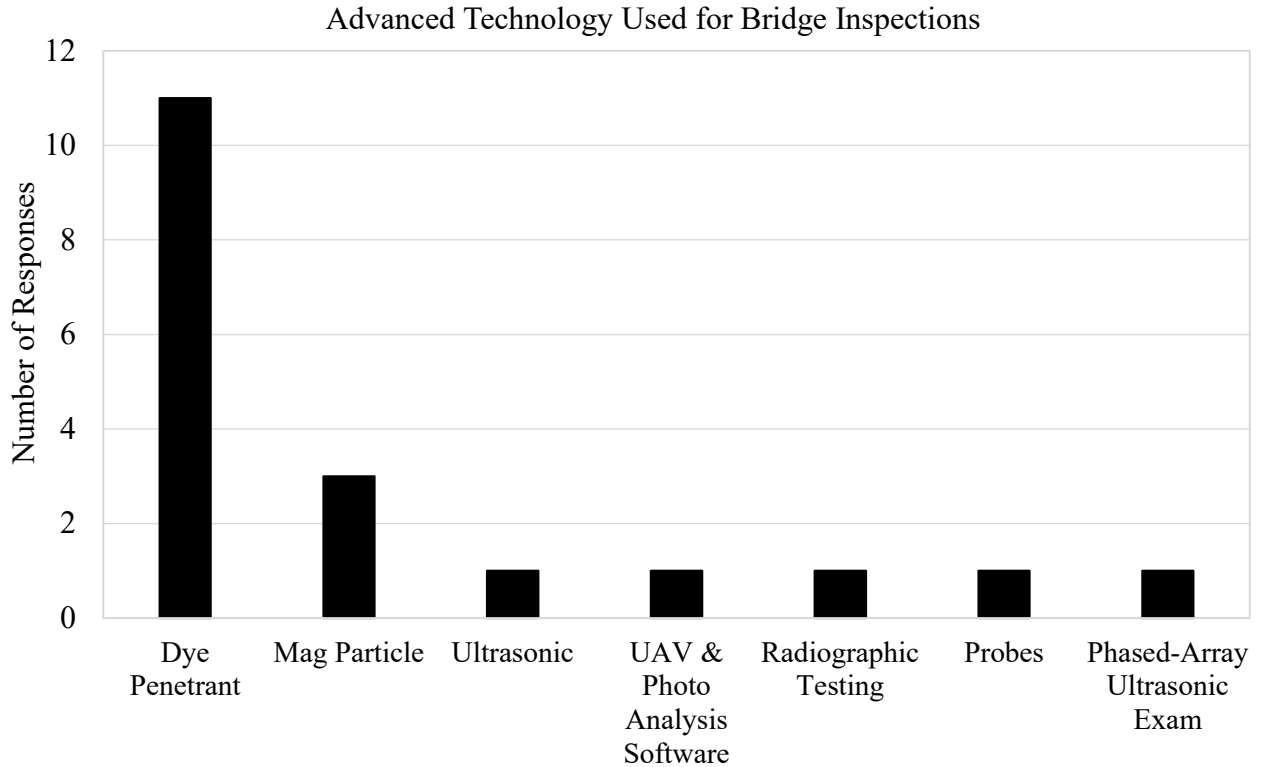


**Figure 2.20: Advanced technologies used by bridge inspectors**

Given an example photo (Figure 2.1), inspectors were asked if they had ever witnessed the upper edge of a web hole bearing on the flange for a stiffened and/or unstiffened bridge beam. Many respondents (38.2%) claimed that they have seen this scenario for both a stiffened and unstiffened beam, while the second most frequent answer was that they had not seen this situation at all (Figure 2.21). Since there was an “other” option included in this question, three people commented that they did not understand the question. It is concerning that more than 60% have seen this situation, because it can greatly affect the structural integrity of the bridge beam. Because this situation is being seen by most inspectors it would be good to consider addressing it in any future handbook, particularly in the corrosion section since corrosion is typically the cause of holes in beam webs.



Have You Ever Witnessed the Upper Edge of a Web Hole Bearing on the Flange?

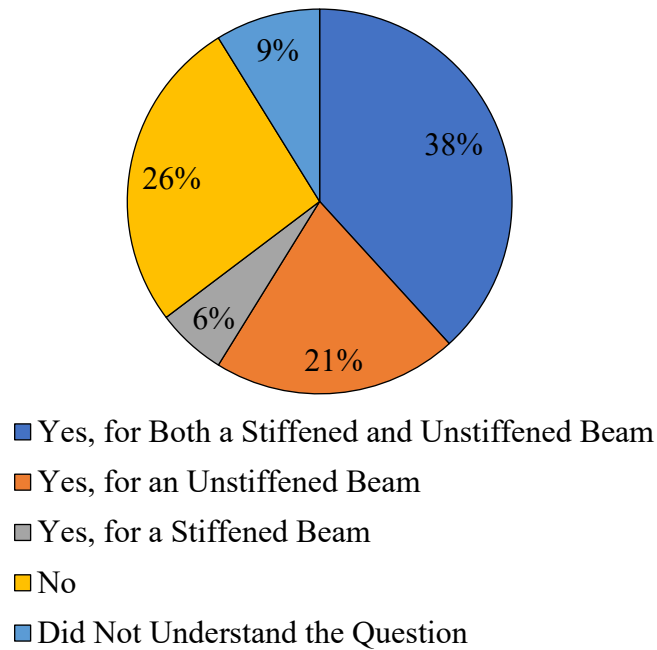


**Figure 2.21: Upper edge of a web hole bearing on the flange**

When asked about their D-meter use, 91.2% of the MassDOT personnel and consultants that took this questionnaire said that they use a D-meter to measure web thickness (Figure 2.22). This shows that as of now the primary way inspectors measure corrosion is by using a D-meter.

Do You Measure Web Thickness Using a D-Meter?

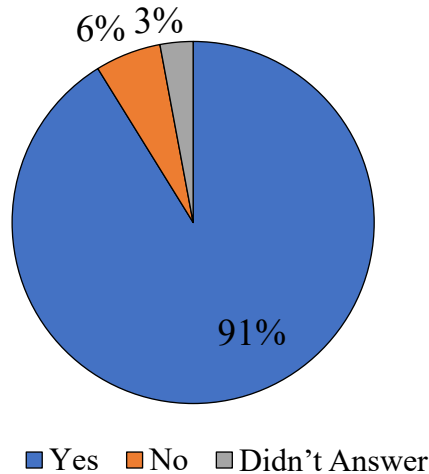


**Figure 2.22: D-meters to measure web thickness**

To get a sense of the most popular D-Meter models, Figure 2.23 was created to show the responses from those who use D-meters for inspecting bridges. The most popular model seems

to be the Olympus brand. It is good to know the models that are being used in order to assess their accuracy, reliability, and shortcomings.

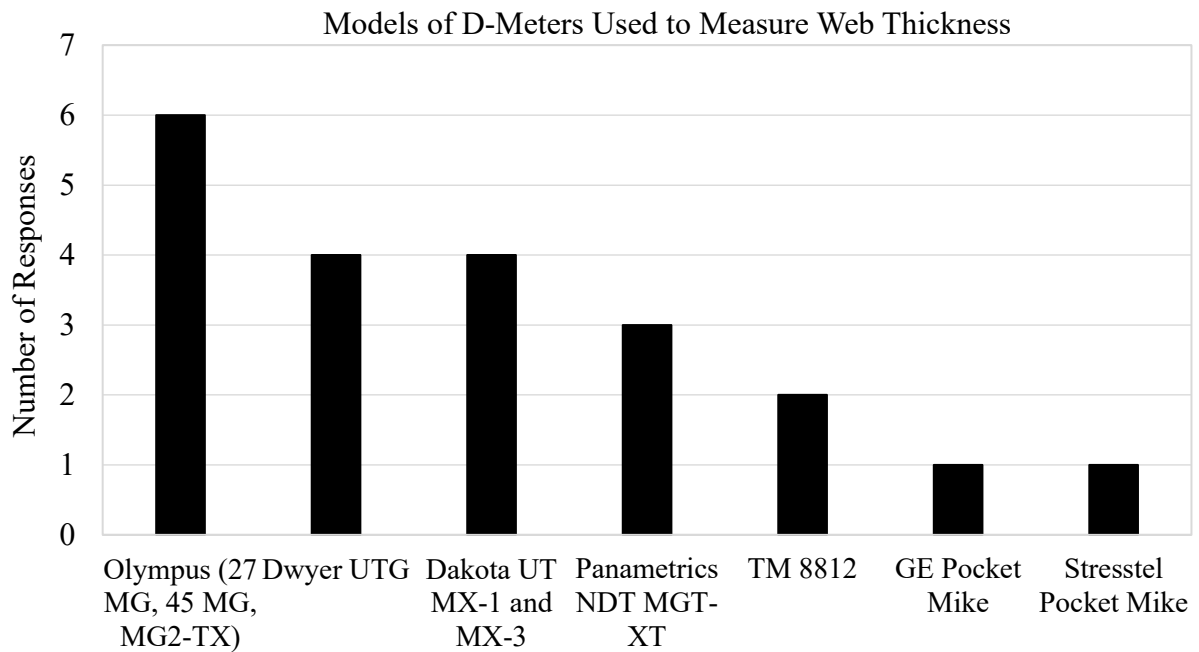


**Figure 2.23: D-meter models used by inspectors**

To gain a sense of what a new corrosion assessment method should encompass, it is critical to know the limitations of the equipment available to inspectors, especially the accuracy of that equipment. This is why inspectors were asked about their D-meter’s accuracy, and the results for this question are summarized in Figure 2.24.

Most inspectors agreed that the D-meter they used was only moderately accurate. It also shows that 11 respondents provided additional comments for this question. A summary of these comments is presented in Table 2.2. The comments revolve around how it is hard to judge the accuracy of the D-meters and how some have found a way to try and verify the D-meter measurements. However, because most felt that the D-meter readings are moderately accurate, that means there is room for improvement.

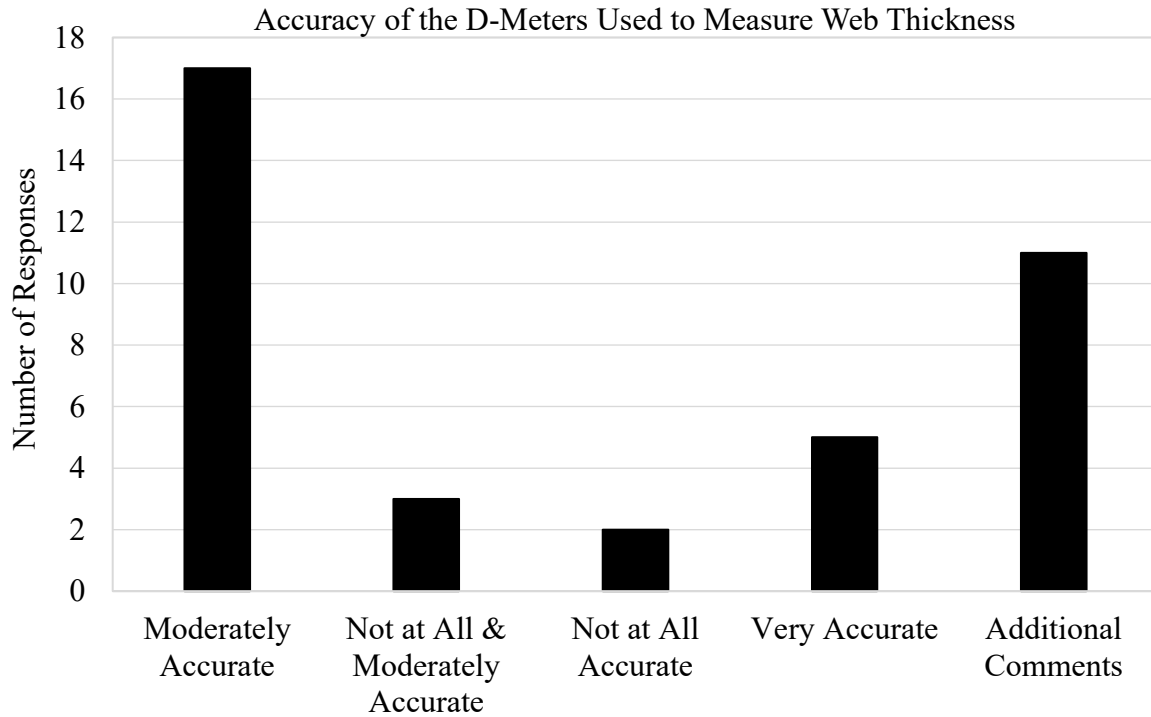


**Figure 2.24: Accuracy of the D-meters**

**Table 2.2: Accuracy of D-meters used**

<b>Comments</b>	<b>Number of responses</b>
Works well in fair weather and on clean surfaces	4
Hard to estimate the accuracy	2
Check against straight edge measurement	2
Repeat readings/average the reading you get	2
Results vary widely and are often unrepeatable	1
Hard to measure on uneven and heavily rusted surfaces	1

For those who do not use D-meters, it was clear that calipers and straight edge/rulers were the more popular tools to use instead (Figure 2.25).

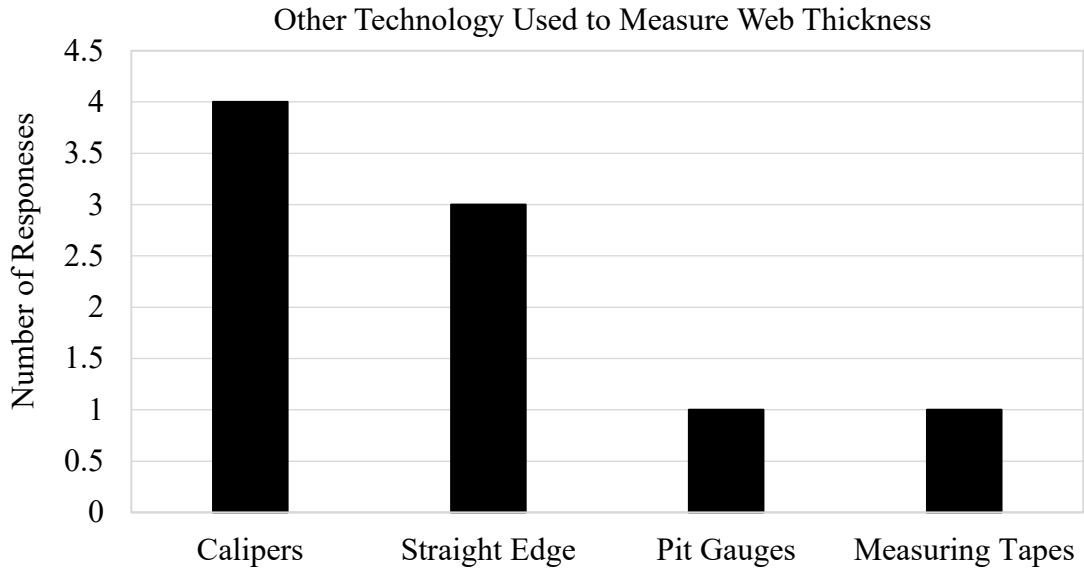


**Figure 2.25: Other technology to measure web thickness**

To account for any other possible tool used to measure web thickness, inspectors were asked what technology could potentially be used to measure web thickness. Similar to the previous responses, calipers and straight edges/rulers were the most common possible technologies (Figure 2.26). Although all responses are important to consider, the responses that were most interesting for this study were the ultrasonic technology, or via drone or camera, and laser scanning. These technologies were investigated further to see if they could be used for corrosion estimation.

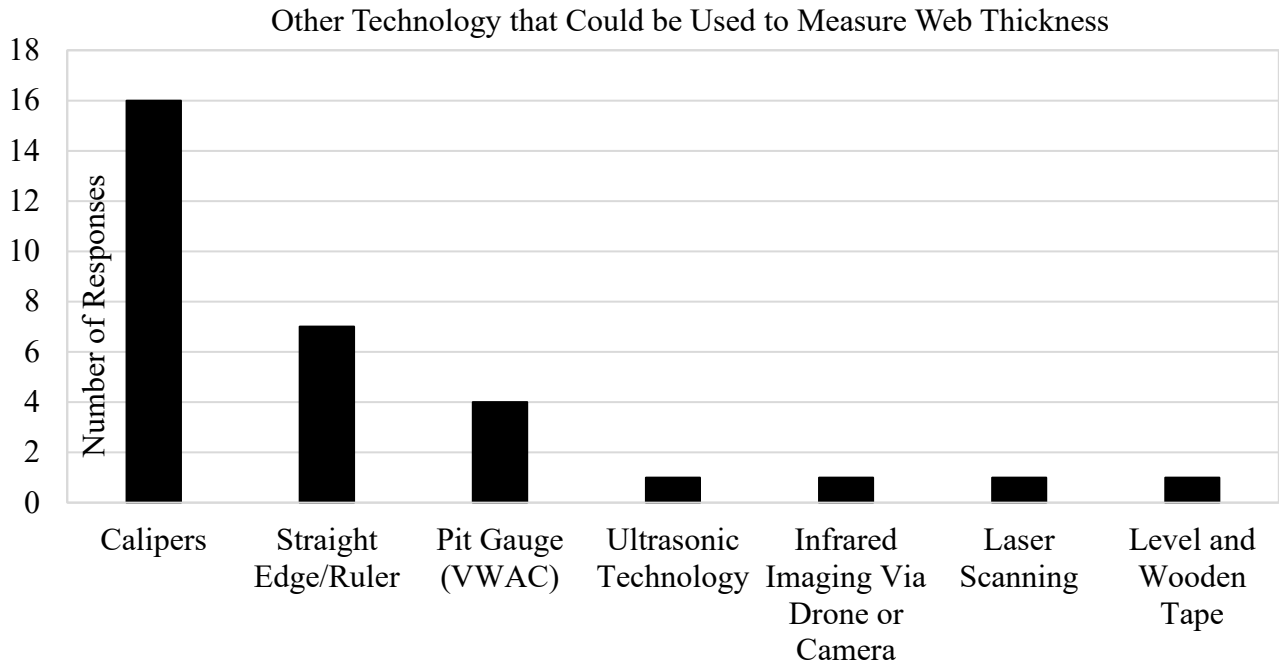


**Figure 2.26: Technology able to measure web thickness**

Moving on to the sketch of an unstiffened beam, respondents were asked to pick numbers that better represent the points at which they would take thickness measurements. Figure 2.27 shows the same image, but this time with certain points boxed. The numbers that are boxed represent the points that were chosen by 10 or more respondents. Several inspectors added additional comments to their responses, which are recorded in Table 2.3. Many of the points that were frequently measured fall within, or slightly above, 4 in. from the bottom of the web. It is good to know these points so that the accessibility issue can be addressed by any future corrosion procedures and technology.

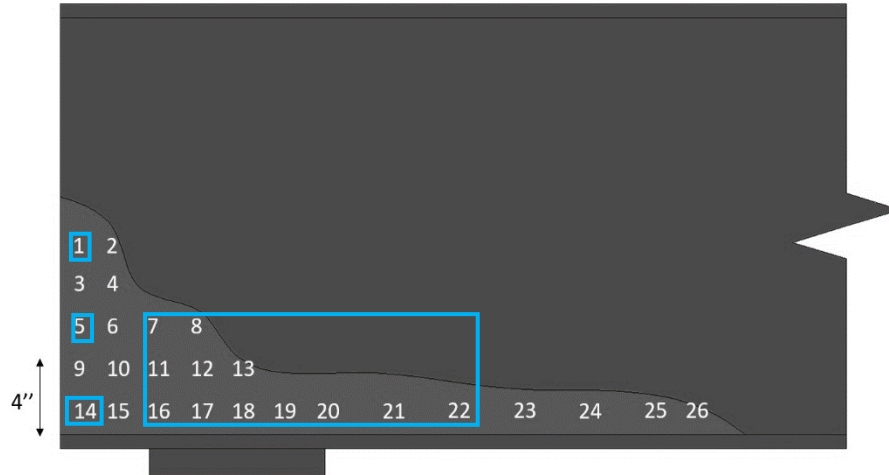


**Figure 2.27: Thickness measurement points for unstiffened beam**

\*The most frequently picked points are in the boxes.

**Table 2.3: Measurement points on unstiffened beam**

<b>Additional comments</b>
Points should be taken on either side of the bearing
Whether to continue measuring or stop measuring depends on readings acquired and the inspector's judgment
Emphasis should be placed on the numbers over and in front of the bearing
Sudden dips and holes would change the chosen points
What is actually recorded may be different than what is measured

Knowing that there are many other places that could be measured on Figure 2.27, Figure 2.28 details the additional points respondents would measure. Many stated they would measure points without any corrosion to compare with the corroded measurements, verify the accuracy of the D-meter readings, and confirm the dimensions on the bridge plans. Those who said they would measure the top flange losses are doing so because that is typically the location of negative bending. Additionally, those who said they would measure the bottom flange losses are doing so because that is usually necked down. It is good to know that some inspectors are both checking the accuracy of their measurements against uncorroded areas and checking structurally critical areas.

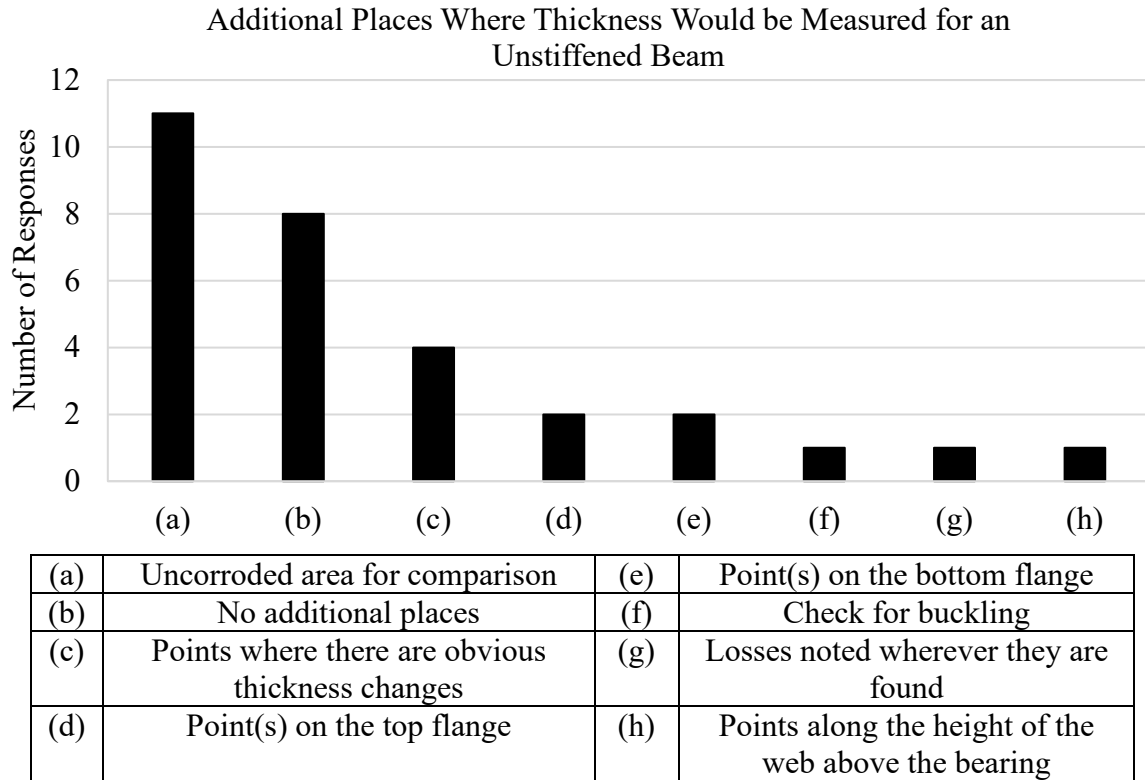


**Figure 2.28: Additional measurement points for unstiffened beam**

The same questions were asked for stiffened beams, and the points that are boxed in Figure 2.29 are points that were picked by 10 or more inspectors. Table 2.4 lists the additional comments included with the points selected for the stiffened beam, and Figure 2.30 presents the additional points that inspectors would take measurements of. The additional points are similar to those stated for the unstiffened beam, but it is important to point out that the person who wrote “heavily laminated areas” chose that as an additional point because steel section loss will begin to accelerate in that area. Also, the person that said they would additionally measure “previously identified loss points” would do so because they will get worse with time once rust has begun.

For stiffened beams, more than half of the points most frequently mentioned are above 4 in. from the bottom of the web on the beam itself. This is different from the stiffener measurements, where it appears that most of the highlighted points fall within 4 in. from the bottom of the web. Much like the unstiffened beam, knowing the points that are highlighted here will help address accessibility issues and make proper measurement recommendations within future procedures and technology.

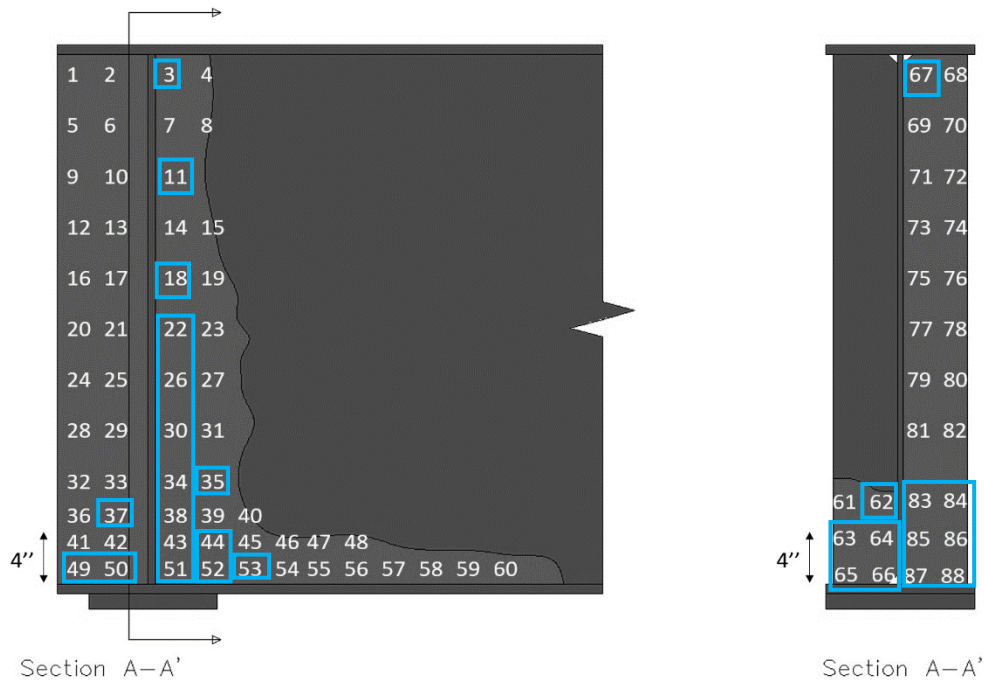


**Figure 2.29: Possible measurement points for stiffened beam**

\*The most frequently picked points are in boxes.

**Table 2.4: Measurement points on stiffened beam**

<b>Additional comments</b>
Important to measure points until you find full thickness above the 4 in., then find the minimum below the 4 in.
Use the minimum stiffener dimensions
Whether to continue measuring or stop measuring depends on readings acquired and the inspector's judgment
Sudden dips and holes would change the chosen points
Emphasis should be placed on the numbers over and in front of the bearing
Very critical to measure the bearing stiffener and web on the side of the bearing stiffener extending toward midspan
Web holes are common in end portion of the web behind the bearing stiffener due to leaking deck joints
What is actually recorded may be different than what is measured



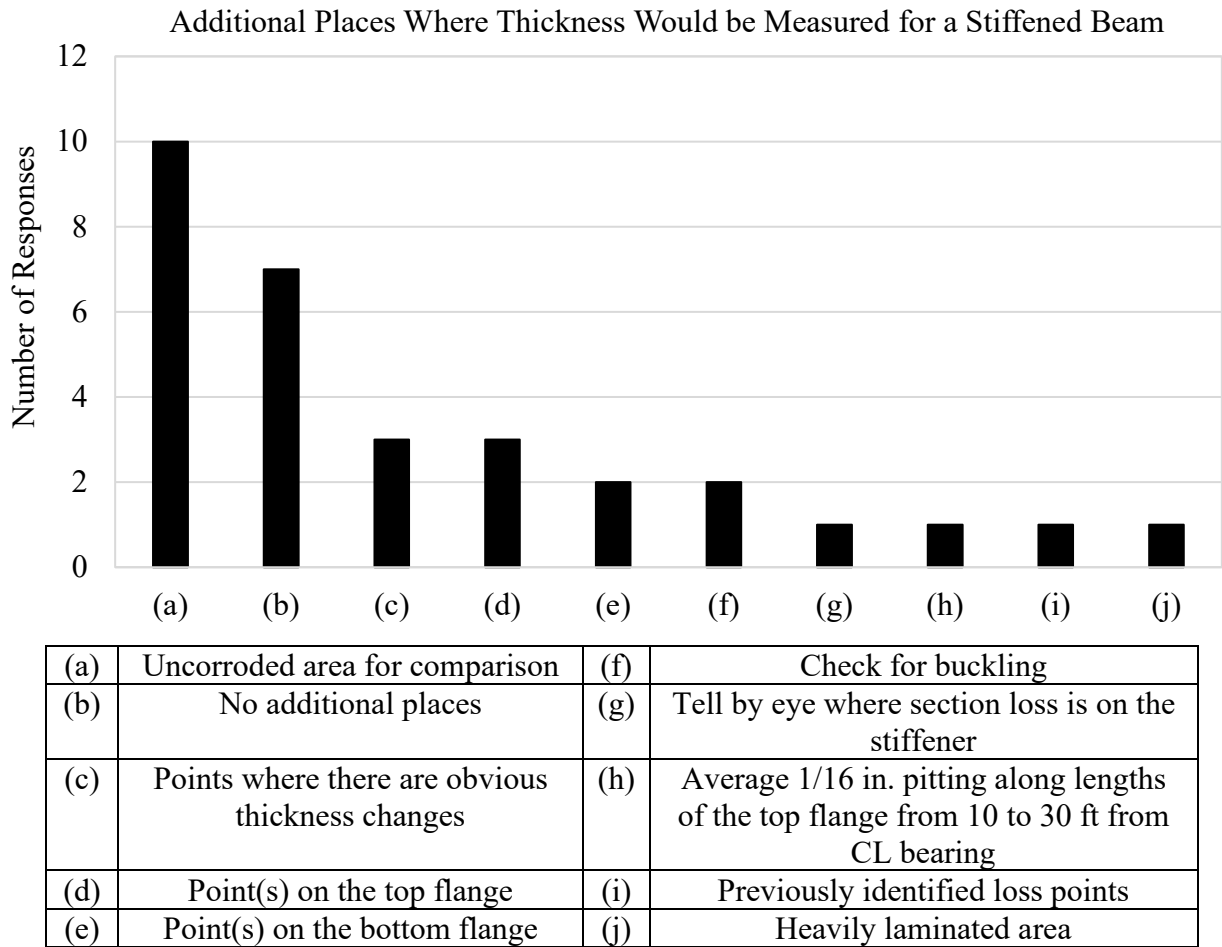
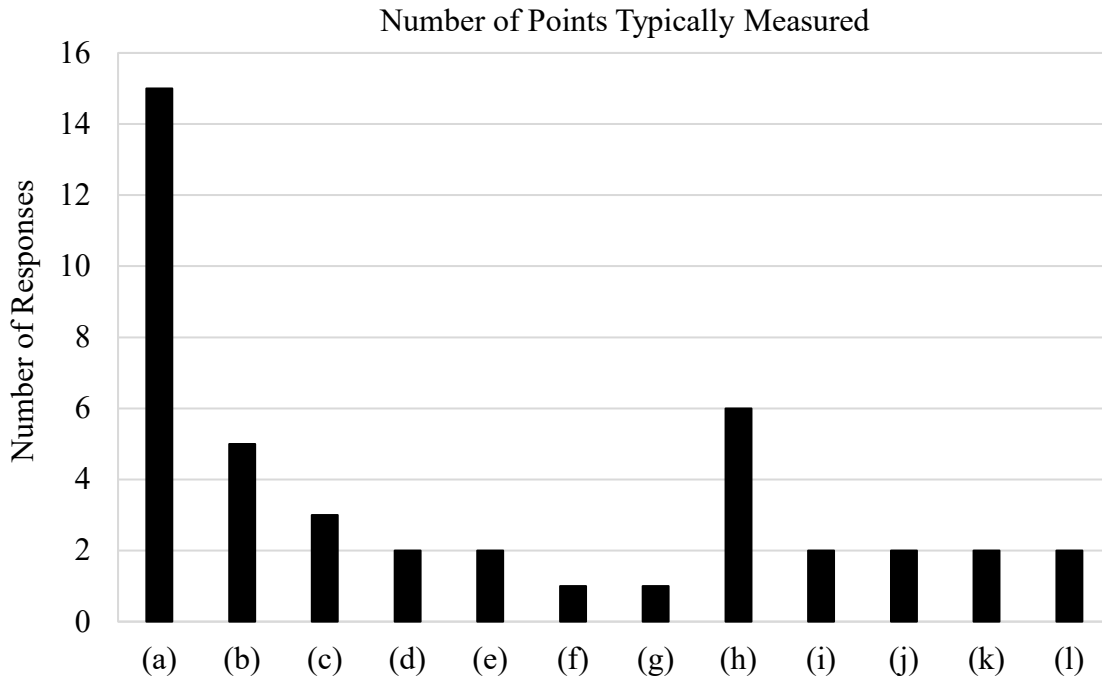


**Figure 2.30: Additional measurement points for stiffened beam**

As to how many points would actually be measured for a bridge inspection, those who responded to the questionnaire offered many different responses. Among those recorded in Figure 2.31, the most frequent response was that the number of points measured depends on the amount, distribution, and variability of the corrosion. The more corrosion and corrosion variability, the more points that are taken to capture the in situ condition of the beam. Along with that, the more consistent a corroded area is, the fewer points need to be measured. Although some inspectors gave a more qualitative response, some offered a quantitative response, the most frequent response being that they would take between two and five web thickness measurements.

Based on these results, it may be beneficial to make recommendations on how many measurement points to take to ensure that there is more consistency with measurements. It may also be helpful to provide a recommendation on technology that can measure more points or scan the entire area to estimate the amount of section loss.



(a)	Depends on amount, distribution, and variability of corrosion	(g)	DBIE wants several points for load ratings
(b)	Depends on beam size and depth	(h)	2 to 5 points
(c)	Depends on how many measurements to accurately show the section	(i)	5 to 10 points
(d)	Depends on how the critical location is	(j)	At least 5 points
(e)	Work in a grid pattern	(k)	4 to 6 points
(f)	Record mapped loss and not singular points	(l)	10 points

**Figure 2.31: Thickness point measurements taken during inspections**

Similar to how many points are taken, the responses for how the thickness measurement points are chosen also varied substantially. However, although there is a variety of choices, it is very apparent that most of the inspectors' measurement points typically fall within areas that are the most corroded (worst area) and/or they choose points they believe will accurately represent the corroded area. Many of them also stated that they would choose points in areas that would affect the structural strength of the system. The "\*" symbol in Figure 2.32 is there to highlight that the points that affect the structural strength of the system are usually in areas that experience high amounts of stresses, shear, compression/buckling, and/or moment/bending, which is noted below Figure 2.32. An interesting thing to note for this question is that four inspectors said they would use a caliper to measure the thickness of the stiffener, and they would use a D-meter or straight edge with a ruler to measure the rest.

Overall, most points that are measured represent the worst of the corroded area and some also account for structurally important areas, which means inspectors have the potential to make a good assessment of the safety of a bridge with that information. This information could direct

recommendations for how to choose measurement points, which could be included within the corrosion estimation procedure to promote more consistency among inspection reports.

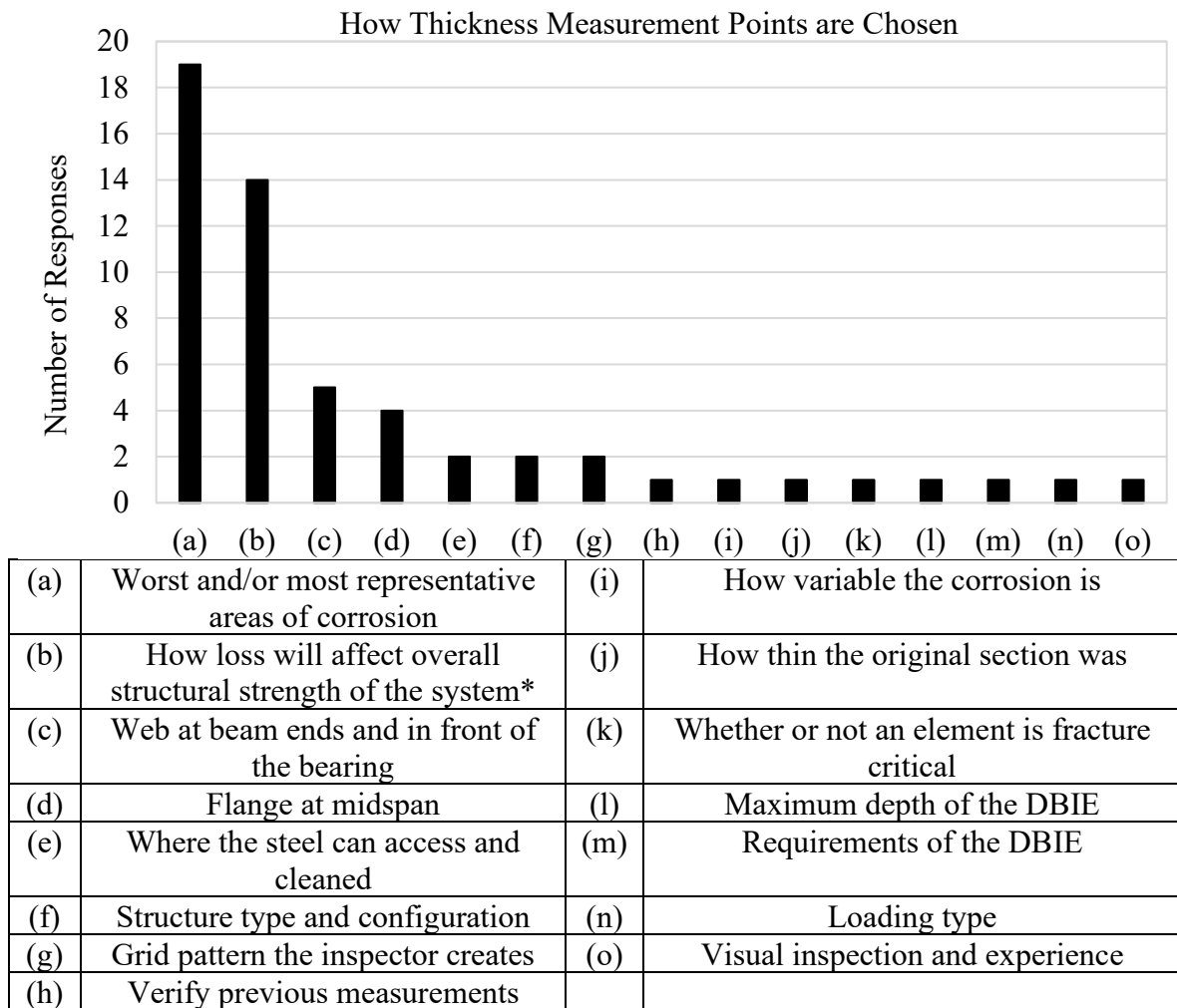


**Figure 2.32: How Thickness Measurement Point are Chosen**

\*Those points are usually within areas that will experience high amounts of stresses, shear, compression/buckling, and/or moment/bending.

Knowing that a corroded stiffener can also affect the capacity of a stiffened beam, it was important to know whether or not inspectors take thickness measurements of the stiffeners. A majority (79.4%) of the inspectors picked yes to indicate that they do in fact measure the thickness of the stiffeners (Figure 2.33).

Although a majority of inspectors do measure corroded stiffeners, it would be important to include a statement within the new estimation methods that specifically says that inspectors must measure the thickness of corroded stiffeners to thoroughly assess the corroded bridge girder and promote consistency.

Do You Normally Take Thickness Measurements  
of Corroded Stiffeners?

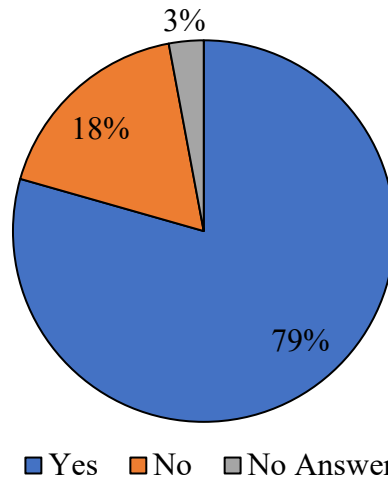


**Figure 2.33: Thickness measurements taken of the stiffener**

Moving on to data pertaining to web deviation from straightness, or out-of-plane displacement, inspectors were asked if they had witnessed beam webs that deviated from straightness for stiffened and/or unstiffened beams similar to Figure 2.4. A majority chose “Yes for an unstiffened beam” (53%) and “Yes for both a stiffened and unstiffened beam” (38.2%; Figure 2.34). No one answered that they had seen this for only a stiffened beam. Two inspectors added additional comments: one stated that they had only seen this occur due to collision, usually at midspan, and the other stated that they had seen it for a stiffened beam, an unstiffened beam, and a compression member of a truss. It is concerning that most of the inspectors who responded to the questionnaire had seen webs that deviated from straightness, because this can cause significant loss in beam capacity and can be very unsafe. Any new procedure should address how to estimate the condition and safety of the bridge based on how much web deviation there is.

Have You Ever Witnessed Beam Webs that Deviate from Straightness?

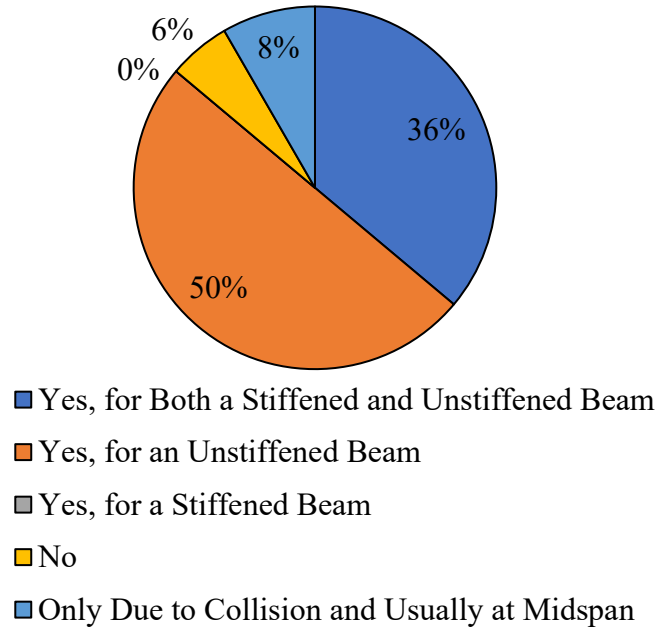


**Figure 2.34: Witnessing web deviation from straightness**

When asked whether they measure web deviation from straightness, all but one inspector said that they do in fact measure out of place displacement. This means that 97% of inspectors that answered this questionnaire measure web deviation from straightness (Figure 2.35). Because inspectors are consistently measuring how much the bridge beam web deviates from straightness, there may be no need to reinforce this in any future standard.

Do You Measure Web Deviation from Straightness?

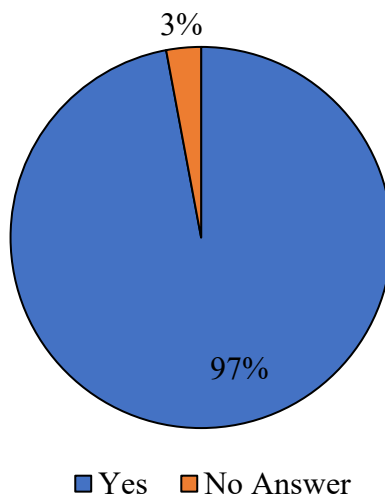


**Figure 2.35: Measured web deviation from straightness**

To measure the out-of-plane displacement of a beam web, many inspectors said that they would use a straight edge and a ruler, a level, a plumb bob or plumb line, a tape measure, and/or magnetic angle gravity tools. The first three tools proved to be the most common among inspectors (Figure 2.36).

Much like the web thickness measurement, when asked about accuracy, many respondents felt that their measurements were moderately accurate using the tools they have (Figure 2.37). It is promising to see that even without advanced technology inspectors can still get a moderately accurate measurement of the web deviation to assess the bridges condition, but it is still important to consider improving the equipment so that inspectors can improve the accuracy of their measurements.

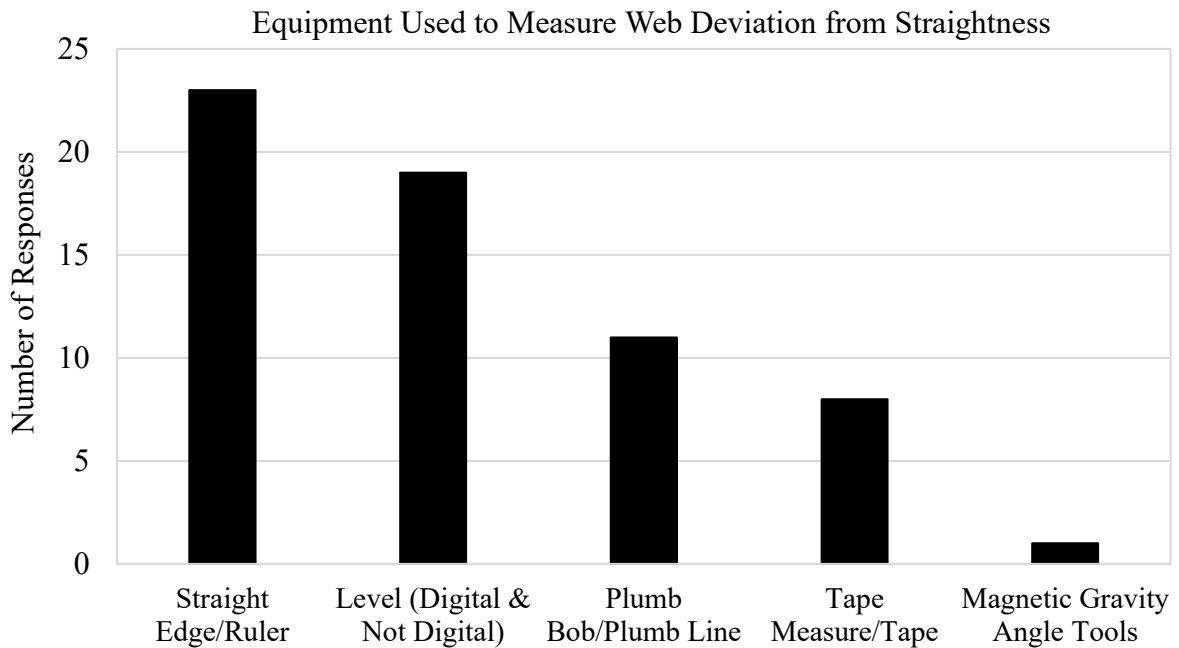


**Figure 2.36: Equipment to measure web deviation**

There was the possibility other equipment could be used to measure web deviation from straightness, and that other equipment is presented in Figure 2.38. Most of this other equipment was also mentioned in Figure 2.36, except for the laser scanning, which is a more advanced technology that should be kept in mind when coming up with a new corrosion assessment methodology.

How Accurate are the Measurements Taken for Web Deviation from Straightness?

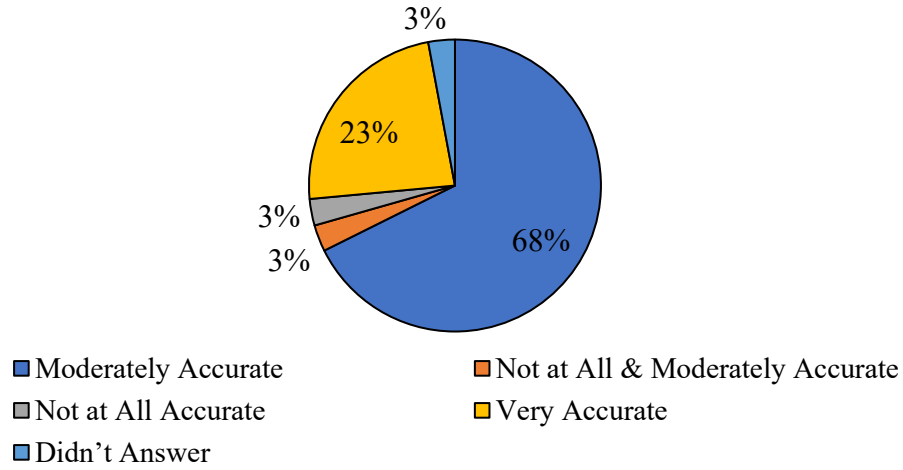


Figure 2.37: Accuracy of equipment to measure web deviation

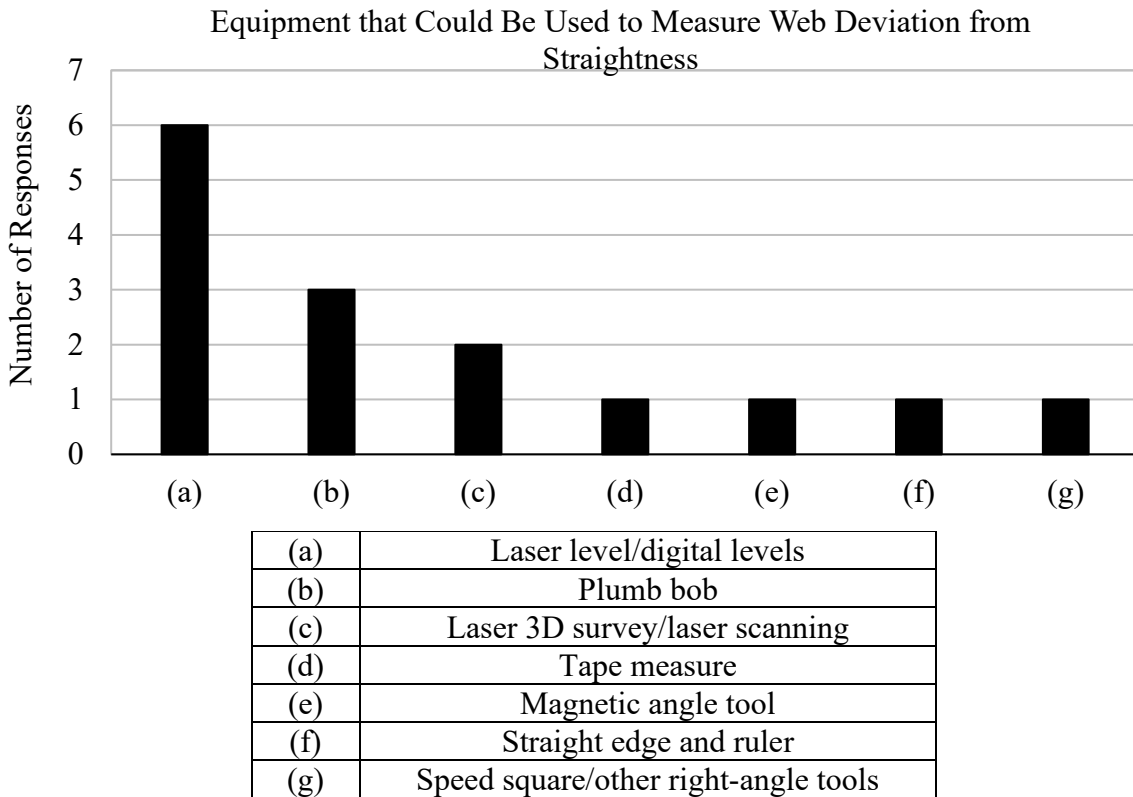
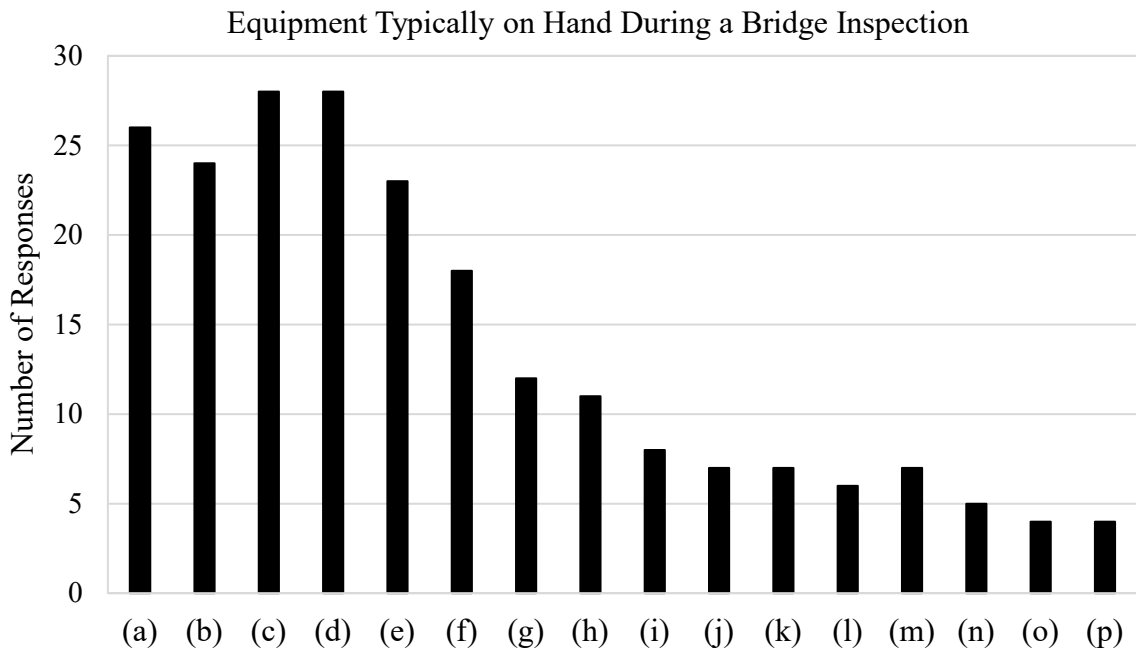


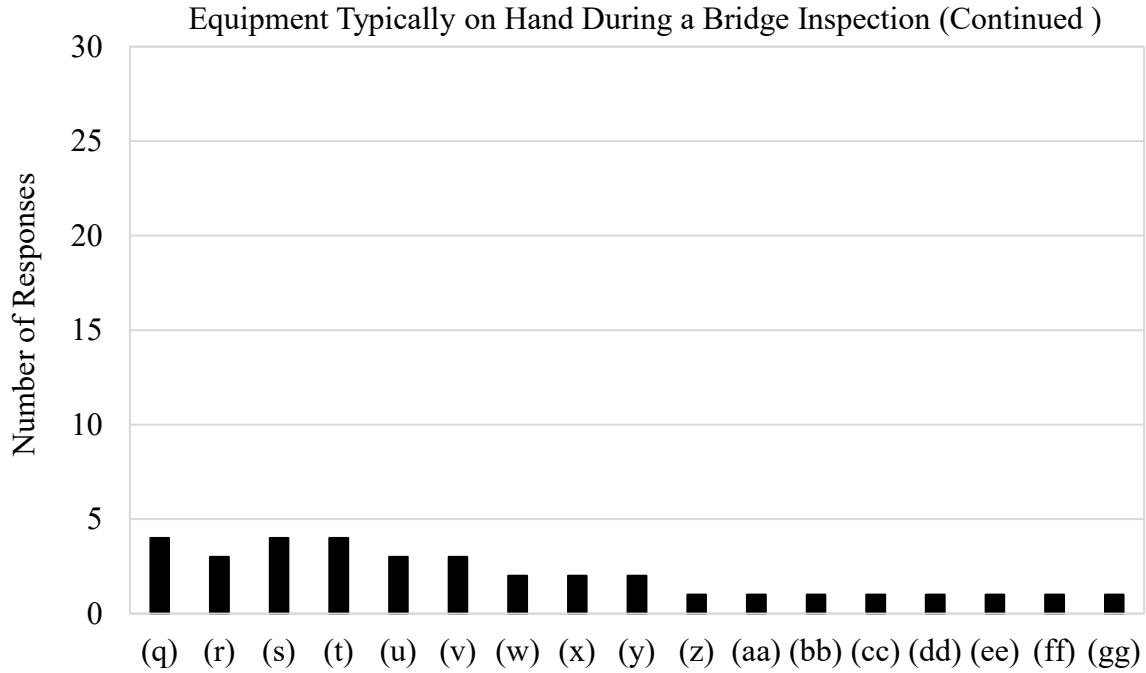
Figure 2.38: Other equipment to measure web deviation

### 2.3.3 Equipment Section Responses

Moving on to the equipment section of the questionnaire, inspectors were first asked to list the equipment that they have on hand to perform a bridge inspection. The most popular answers included D-meters, calipers, straight edge/ruler, hammer(s), and tape measures, among many others (Figure 2.39). Along with listing the equipment, respondents were also asked to state the advantages and disadvantages of the equipment they listed. Unfortunately, only 14 out of 34 people actually gave advantages and disadvantages for their equipment, so advantages and disadvantages were not supplied for all the tools, but the information gathered was still very informative. Most of the advantages and disadvantages focused on ease of use, accuracy, and reliability, among many others (Table 2.5). Knowing this information will help guide research toward a technology that has ease of use, accuracy, and reliability as advantages instead of disadvantages.







	First graph		Second graph
(a)	D-meter	(q)	Keel/kiel
(b)	Calipers	(r)	Other hand tools
(c)	Straight edge/ruler	(s)	Plum bob/plumb line
(d)	Hammer(s)	(t)	Grinder
(e)	Tape measures	(u)	Lumber crayons/marketing utensils
(f)	Wire/steel brush	(v)	Paint pen, paint crayons, tape paint
(g)	Ladders, accessing equipment, PPE	(w)	Crack gauge
(h)	Level	(x)	Thickness gauges/filler gauges
(i)	Camera	(y)	Apple laptop or tablet with AC/DC converter
(j)	Laser distance measurer	(z)	Gravity angle measurement tool
(k)	Pitting gauge (VWAC)	(aa)	Wood tape
(l)	Flashlight/headlamp	(bb)	Pneumatic drill
(m)	Dye penetrant	(cc)	Wheel
(n)	Chalk	(dd)	Awl
(o)	Pen, pencil, paper	(ee)	Mirror
(p)	Chisel/scrapper	(ff)	NDT tools used for previous inspections
		(gg)	Steel square

**Figure 2.39: Equipment inspectors have to inspect bridges**

**Table 2.5: Advantages and disadvantages of bridge inspection equipment**

<b>Equipment</b>	<b>Advantages</b>	<b>Disadvantages</b>
Field papers	<ul style="list-style-type: none"> <li>• Quickest way to verify and note deterioration</li> </ul>	<ul style="list-style-type: none"> <li>• Cleanliness</li> <li>• Legibility</li> </ul>
Tablet	<ul style="list-style-type: none"> <li>• Cleaner notes</li> <li>• Less time in office cleaning up field notes</li> </ul>	<ul style="list-style-type: none"> <li>• Takes more time to use</li> <li>• Limited battery life</li> <li>• Data could be lost</li> </ul>
D-meter	<ul style="list-style-type: none"> <li>• Small and easy to transport</li> <li>• Easy to read</li> <li>• Potentially accurate and precise</li> <li>• Best to use for web losses</li> <li>• Best to use when one side is not accessible (example given)</li> <li>• Good to use when losses are too widespread, and a straight edge cannot be projects to an area of no loss</li> <li>• Provides section remaining instead of section loss</li> </ul>	<ul style="list-style-type: none"> <li>• Questionable reliability of the D-meter</li> <li>• Readings may be inaccurate on uneven surfaces</li> <li>• Hard to clean and flatten the surface enough to get an accurate reading</li> <li>• Hard to get consistent readings</li> <li>• Easy to get inaccurate readings</li> <li>• Requires more time to use because of the surface preparation that is required</li> <li>• Can be large in size, and cords can be in the way</li> <li>• Requires batteries</li> <li>• Requires training</li> <li>• With the right setup, it can survey large areas</li> <li>• Only gives a point measurement</li> </ul>
Hand tools	<ul style="list-style-type: none"> <li>• Gives an overall assessment of losses, not just a point measurement</li> <li>• Relatively simple tools that everyone has for easy reproduction</li> </ul>	<ul style="list-style-type: none"> <li>• N/a</li> </ul>
Calipers	<ul style="list-style-type: none"> <li>• Easy to use</li> <li>• Easy to read</li> <li>• Easy to transport</li> <li>• Accurate and precise</li> <li>• Durable</li> <li>• No batteries</li> <li>• Can get flange and beam end web measurements</li> <li>• Effective and economical to use for flange and</li> </ul>	<ul style="list-style-type: none"> <li>• Limited access if measuring too far into web</li> <li>• Can only measure where it can reach</li> <li>• Not feasible in all situations</li> <li>• May require more space than what's available</li> <li>• Training required for proper use</li> <li>• Steel must be clean to use for measuring</li> <li>• Can't measure large areas of section loss</li> </ul>

	bearing stiffener measurements	
Hammer	<ul style="list-style-type: none"> <li>• Can clean/remove delamination and rust from beam ends</li> <li>• Can be effective</li> <li>• Good for sounding</li> </ul>	<ul style="list-style-type: none"> <li>• Can be a lot of work to use</li> <li>• Tiring</li> <li>• Weight/can be heavy</li> <li>• May not have room to swing it</li> <li>• Destructive and sets a path for more losses</li> </ul>
Wire brush	<ul style="list-style-type: none"> <li>• Good for cleaning surfaces</li> </ul>	<ul style="list-style-type: none"> <li>• Destructive and sets a path for more losses</li> <li>• Sharp bristles</li> </ul>
Ladders	<ul style="list-style-type: none"> <li>• Can be effective</li> </ul>	<ul style="list-style-type: none"> <li>• Can be a lot of work to use</li> </ul>
Tape measure	<ul style="list-style-type: none"> <li>• Good for measuring large objects</li> <li>• Accurate</li> <li>• Cheap</li> <li>• No batteries</li> </ul>	<ul style="list-style-type: none"> <li>• Bad for measuring depth and distance</li> <li>• Can be inaccurate</li> <li>• Fails in dirty environments</li> </ul>
Ruler	<ul style="list-style-type: none"> <li>• Cheap</li> <li>• No batteries</li> <li>• Good for measuring small objects</li> <li>• Simple to use</li> <li>• Easy to transport</li> <li>• Easy to read</li> <li>• Accurate enough for most purposes</li> </ul>	<ul style="list-style-type: none"> <li>• Limited precision</li> <li>• Bad for large objects</li> <li>• Can be inaccurate</li> </ul>
Straight edge and ruler/tape measure combo	<ul style="list-style-type: none"> <li>• Can get accurate web loss measurements</li> <li>• Good for one sided web loss measurements</li> <li>• Faster than using a D-meter</li> </ul>	<ul style="list-style-type: none"> <li>• Decrease in measurement accuracy as the surface becomes more uneven</li> </ul>
Level	<ul style="list-style-type: none"> <li>• Small and easy to carry</li> </ul>	<ul style="list-style-type: none"> <li>• Works only on small areas</li> </ul>
Pitting gauges	<ul style="list-style-type: none"> <li>• N/A</li> </ul>	<ul style="list-style-type: none"> <li>• Limited to a small area</li> </ul>
Dye penetrant	<ul style="list-style-type: none"> <li>• N/A</li> </ul>	<ul style="list-style-type: none"> <li>• Messy</li> <li>• Only allows you to spot things, doesn't actually measure anything</li> </ul>
Laser measure	<ul style="list-style-type: none"> <li>• N/A</li> </ul>	<ul style="list-style-type: none"> <li>• Only to get longer lengths</li> <li>• Not to measure losses</li> </ul>
Camera	<ul style="list-style-type: none"> <li>• N/A</li> </ul>	<ul style="list-style-type: none"> <li>• Sometimes it breaks</li> </ul>
NDT used in previous inspections	<ul style="list-style-type: none"> <li>• N/A</li> </ul>	<ul style="list-style-type: none"> <li>• Can get bulky</li> <li>• Unable to use in some areas</li> </ul>

To gain a sense of equipment upkeep, the MassDOT employees and consultants were asked how often gauges were calibrated. The responses were split into the two categories of MassDOT inspectors and consultants to compare the difference between the two sets of inspectors. Those directly from MassDOT claimed that they calibrated gauges before every use to ensure accurate measurements. Most of the consultants also stated that their gauges were calibrated before each use, but others said that they were calibrated based on the manufacturer’s guidelines or that there is a built-in calibration, among other answers (Figures 2.40 and 2.41).

Because the gauges are typically calibrated often or as recommended, it makes sense that the readings they get should be moderate to very accurate. Although it was not a frequent answer, it may be good to check why some inspectors responded with “yearly,” “every few years,” or “no” to see if that has a substantial effect on their measurements.

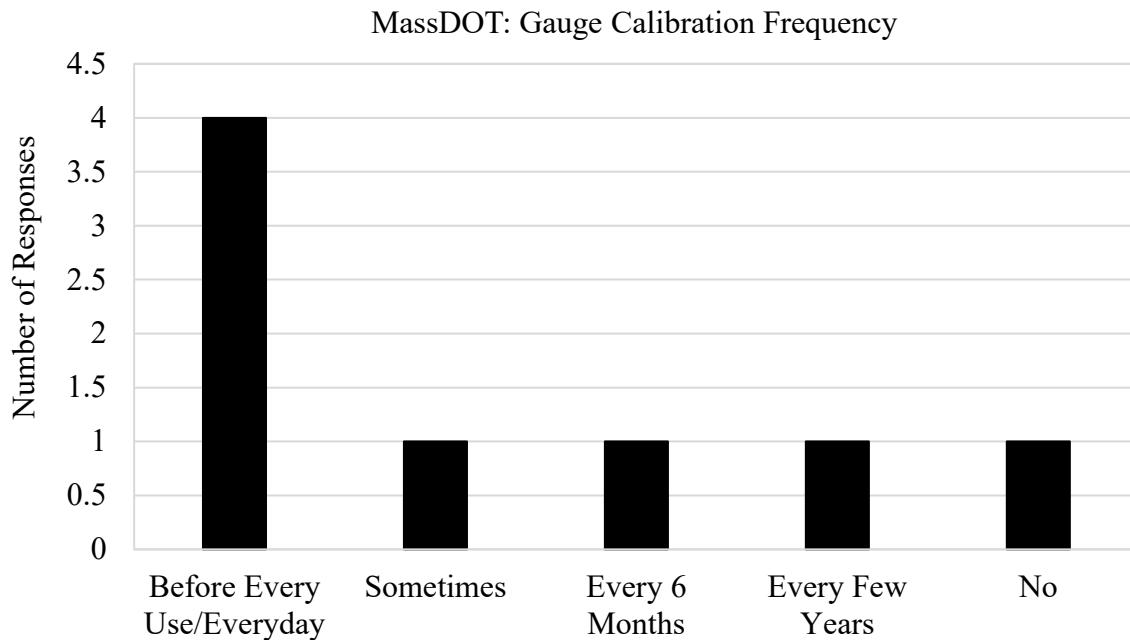


**Figure 2.40: Gauge calibration frequency by MassDOT inspectors**

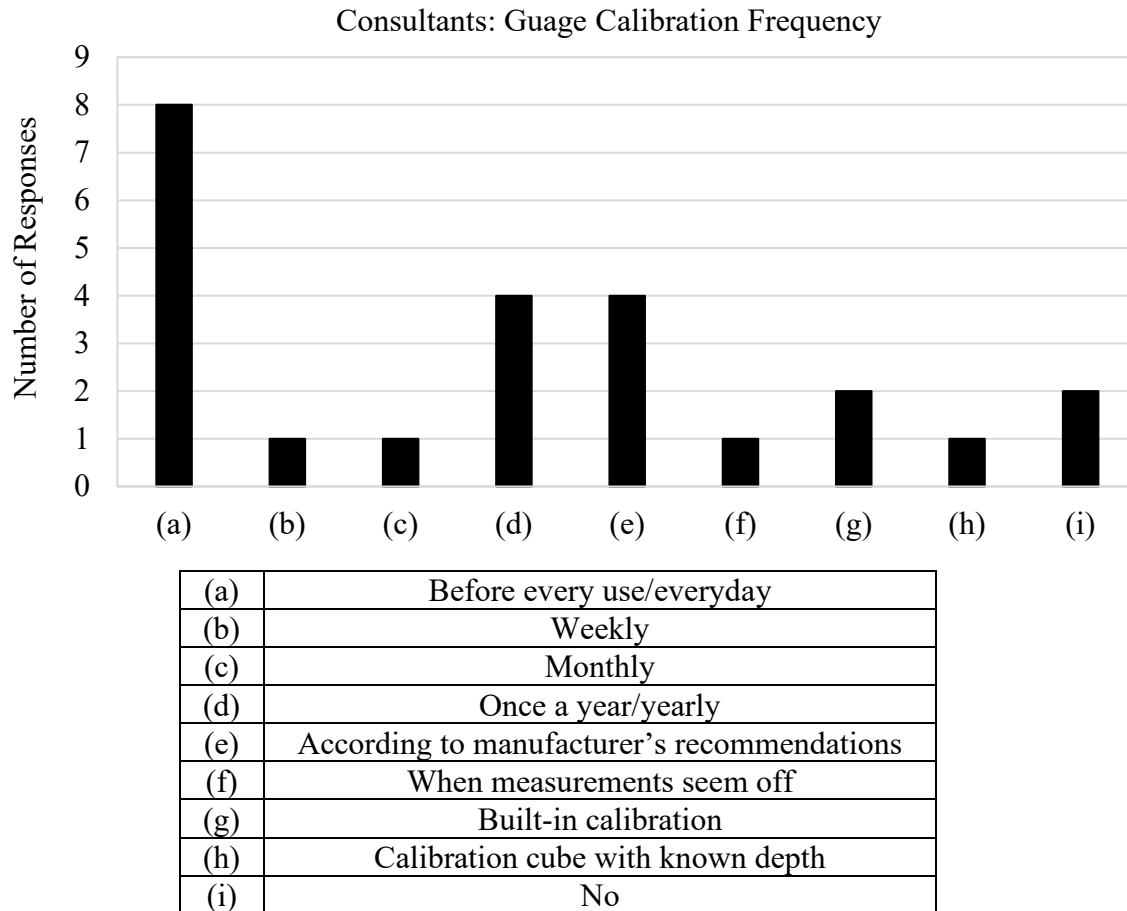
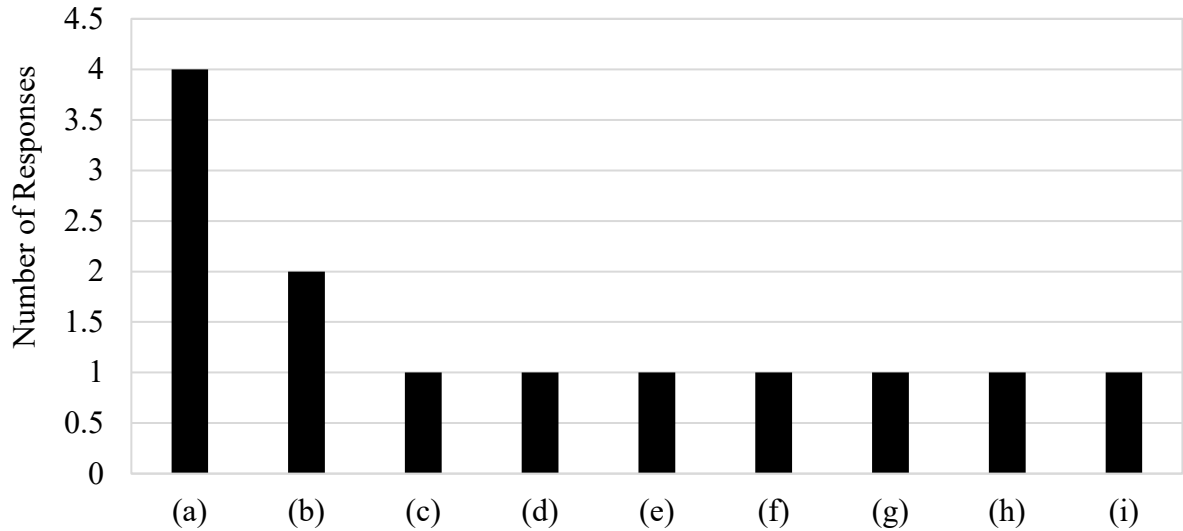


**Figure 2.41: Gauge calibration frequency by consultants**

To understand what inspectors want and need their equipment to do, they were asked to provide what changes they would make to the equipment they currently used. As before, the responses were split into the two categories to clearly view how these groups differ. Figures 2.42 and 2.43 show that the MassDOT inspectors believed their equipment is in need of more changes compared to the equipment of the consultants. Overall, the key changes that were mentioned were more accurate and more reliable equipment that is durable in the field. This question provided really good criteria that should be considered before selecting any new corrosion technology or bridge inspection technology in general.

What Would MassDOT Inspectors Change About the Equipment They Use



(a)	More accurate/more reliable D-meter	(f)	Functioning speech text software
(b)	Battery powered angle grinder/wire wheel	(g)	PocketMike in place of another D-meter
(c)	Better methods for cleaning steel	(h)	Newer equipment
(d)	Bucket truck with more lateral reach	(i)	Truck that they can stand up in
(e)	Tripod for laser level		

Figure 2.42: Equipment changes desired by MassDOT inspectors

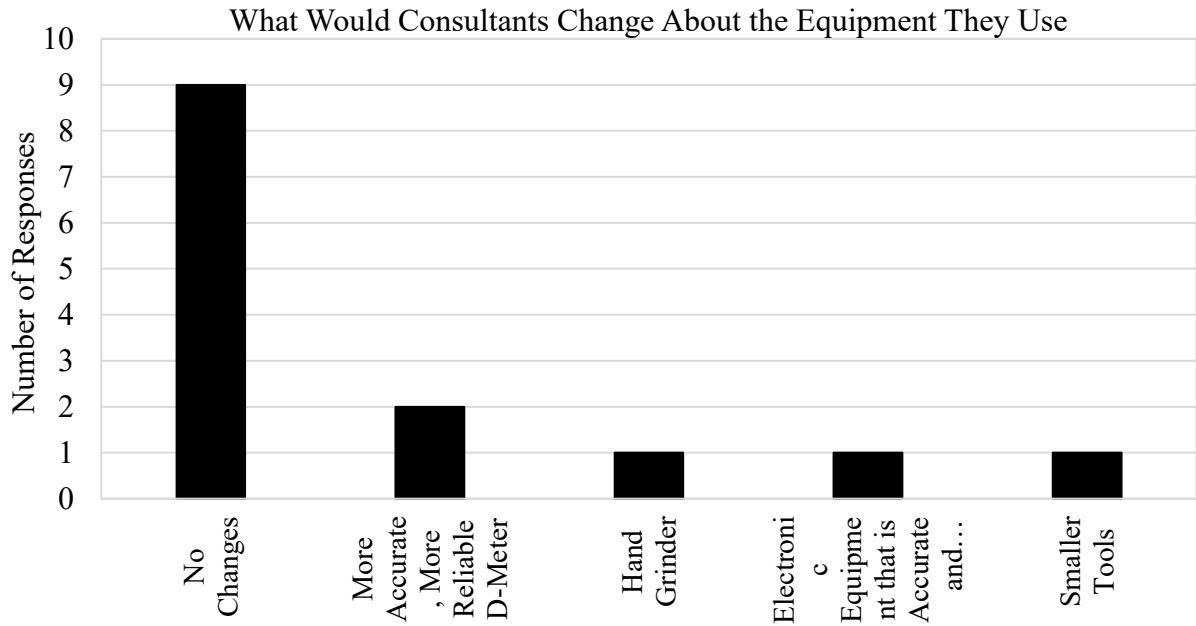
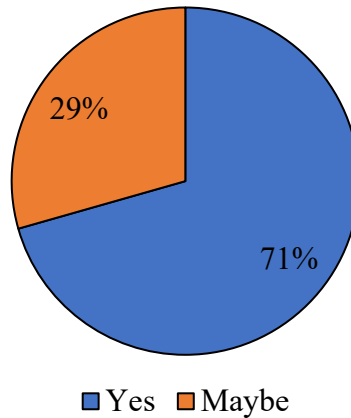


Figure 2.43: Equipment changes desired by consultants

Concerning laser scanning technology specifically, the inspectors' ability to carry a portable laser scanner and possibly a tablet or cell phone as well was questioned. It was thought that inspectors may not have two hands available to be able to carry certain equipment, which is why it was important to ask this question.

Despite this hypothesis, most inspectors (71%) felt that they could carry both, while the rest of the inspectors (29%) felt it might be possible to carry both (Figure 2.44). It was known before this questionnaire went out that laser scanning and LiDAR could be used for corrosion estimation, so it is promising to see that no one felt they could definitely *not* carry the portable laser scanner on a cell phone or tablet, making this a viable option for future corrosion assessment. It is also good to know that some inspectors are at least aware of laser scanning technology, because they stated that in the previous questions regarding technology that could be used, so it may not be a completely new technology to them.

Would You be Able to Carry a Portable Laser Scanner and Potentially a Tablet or a Cell Phone?



**Figure 2.44: Carrying a portable scanner and tablet/cell phone**

Often, corrosion causes the buildup of delamination, and that delamination may need to be removed to measure corrosion of beam ends above the support. It is important to know whether or not this could be done, and therefore inspectors were asked if it is possible to remove the delamination that has built-up over the support. Of those who responded to this questionnaire, 47% believed that they may be able to remove the delamination above the support, and the rest of those who answered said a definitive yes (Figure 2.45).

Much like the previous question, none of the inspectors said no, but in this case many more respondents said maybe. This makes sense because many expressed the difficulty they have removing rust and delamination in the previous corrosion questions, and the possibility of not being able to remove the rust above the support should be taken into consideration when formulating new corrosion mapping methods.

Is it Possible to Remove Delamination Along the Domain Above the Support?

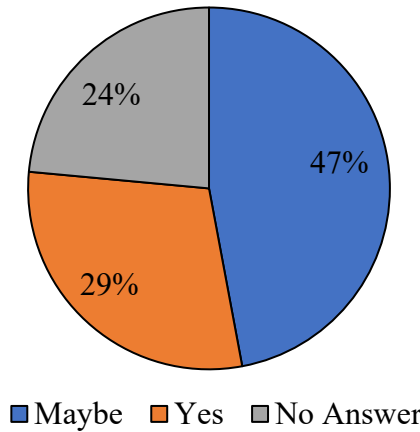


**Figure 2.45: Removing delamination above the bridge support**

To account for those maybe answers, inspectors were asked why they could not remove the delamination above the supports. According to Figure 2.46, it is apparent that delamination is hard to remove when it cannot be reached and when the design of the bridge does not allow for it. A new method for removing delamination and/or a new procedure/technology that requires little to no removal of delamination to measure corrosion would be the ideal solution to the issues presented.

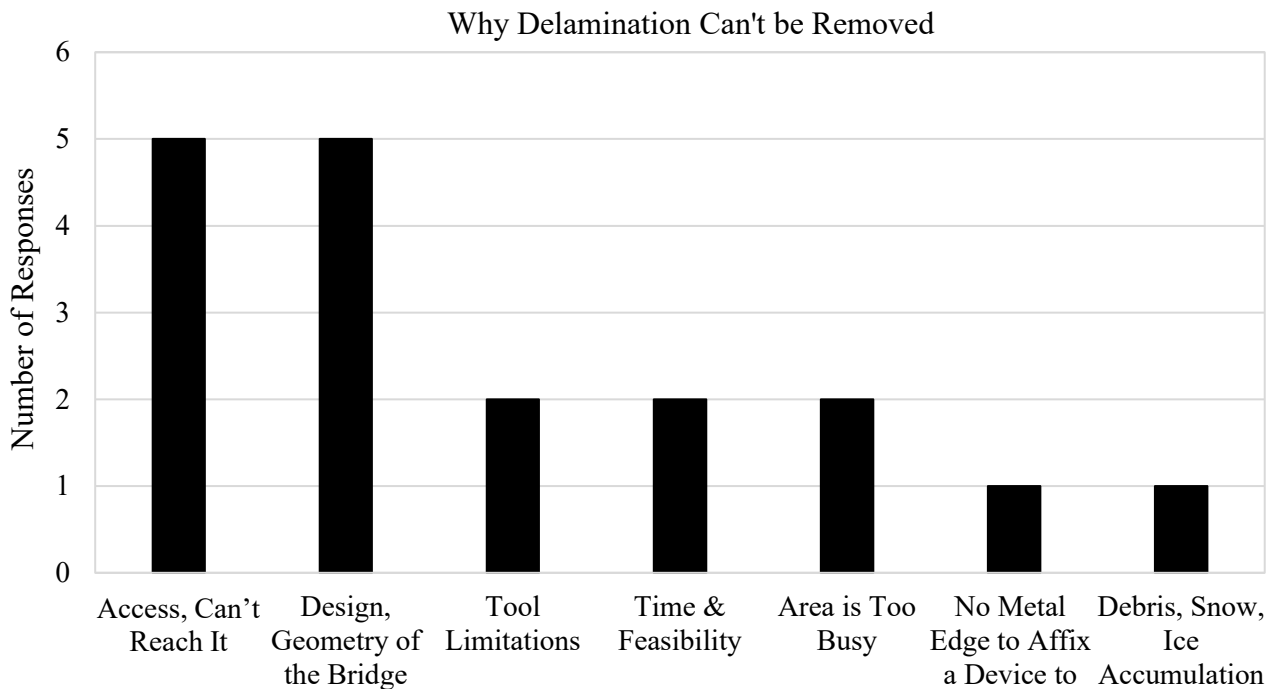


**Figure 2.46: Reasons delamination cannot be removed by inspectors**



When implementing a new procedure, it is important to keep the amount of post-processing to a reasonable amount. To gain an idea of what a reasonable amount of post-processing time is, inspectors were asked how much time is currently spent on documenting the data they collect: 9 of the 34 respondents chose one of the choices provided, and the rest provided other responses. The data showed that the actual time spent on documentation varies too much on bridge size and bridge condition, among other factors, to give a definitive amount of time (Figure 2.47). However, more often than not, more than 6 hours are typically spent on documentation, especially for a bridge that is heavily corroded. This is the time that should be considered when formulating a new corrosion method.

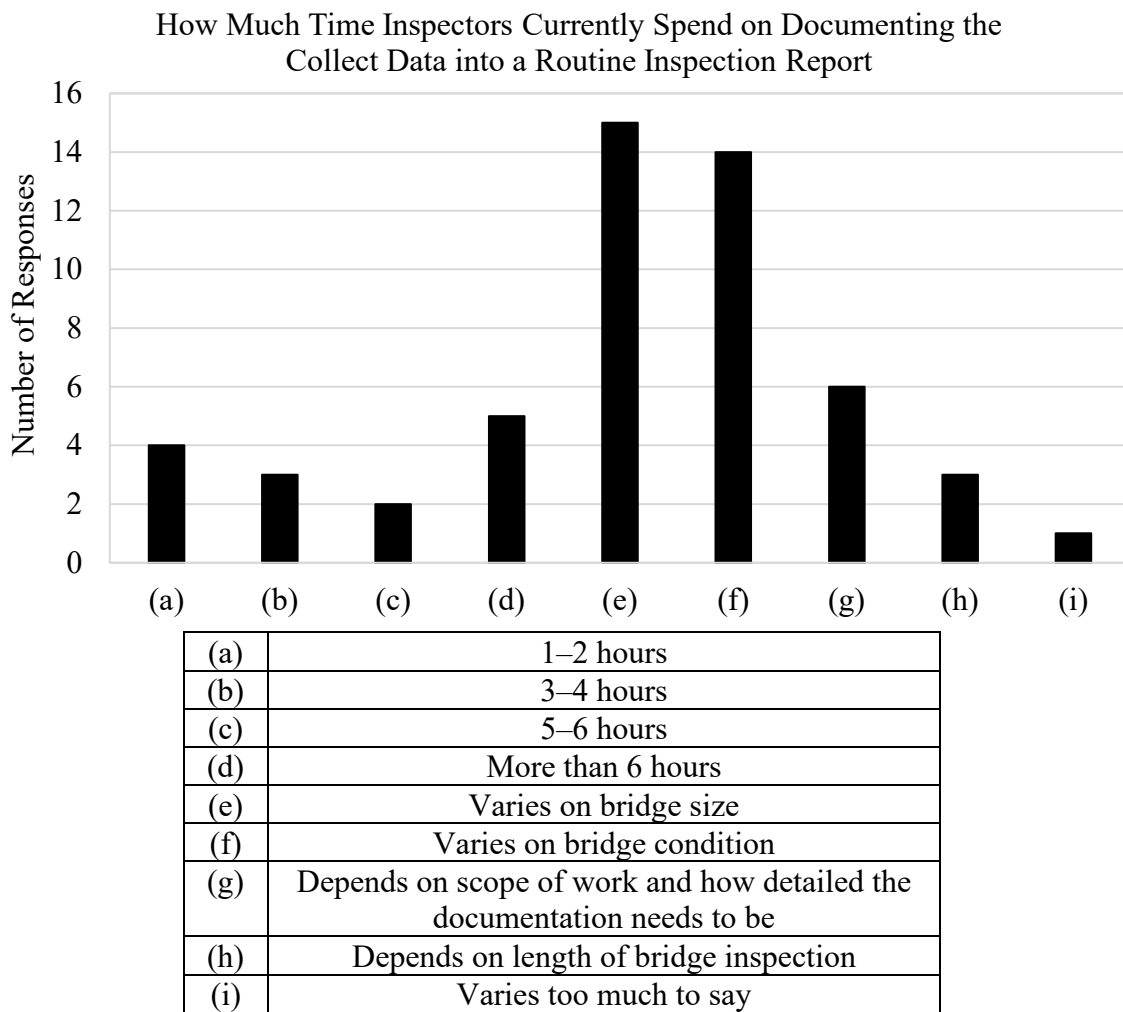


**Figure 2.47: Time spent documenting the data**

Along with how long it takes to document collected data, it is important to know if bridge inspectors spend additional time for measurements and documentation that makes them believe that a new load rating is required. Figure 2.48 shows the amount of people who responded yes, no, or sometimes. In addition to these answers, some inspectors left comments as to why they answered the way they did. These comments are recorded in Table 2.6. A common consensus among those who answered no or sometimes was that they do not need a new load rating or

they only sometimes believe they need a new load rating, because they are typically able to gather enough data during the inspection. For those who answered yes, most of the comments centered around a new load rating for section loss measurements. These comments are important to consider when providing a new way to estimate corrosion because the measurement of section loss is the measurement of corrosion.

Do You Spend Additional Time for Measurements and Documentation That a New Load Rating May be Required?

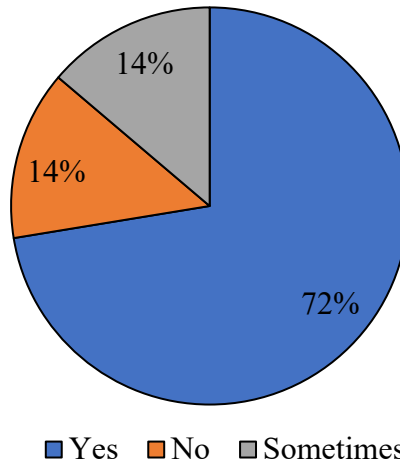


Figure 2.48: Do inspectors believe a new load rating is needed?

Table 2.6: Is a new load rating needed?

Additional comments	Number of responses for each
Typically gather enough information/data during inspection	5
No, sizes are verified regardless of losses	1
Yes, for section loss measurements	2
Yes, if required by MassDOT	1
Yes, if load rating is because of new and/or widespread section loss has been discovered	1
Yes, locations that could affect load rating	1
Yes, and a higher level of measurement will be taken for subsequent load rating	1
Depends on section loss	1
Depends on bridge complexity	1

The last couple of questions of this questionnaire were focused on the use of unmanned aerial vehicles (UAVs), or drones. Prior to the creation of this questionnaire, it was known that UAVs have been used for bridge inspections by many different state DOTs, so it was decided to include these questions to see if inspectors were familiar with this technology.

The first of the UAV questions simply asked inspectors if they had ever used a drone or witnessed a drone being used for any MassDOT related activities. Of those who responded, 25 of 34 (73.5%) said that they had not used a UAV or witnessed a UAV being used, but 26.5% said they had. Of those who said they had used a UAV or witnessed one being used, only one person was a MassDOT employee and the other eight were consultants (Figure 2.49).

Those who answered yes were asked what activities they had witnessed a drone being used for. One consultant said for both a bridge inspection and an ancillary structure inspection, another said for both a bridge inspection and a MassDOT communication tower load rating analysis, two said for high mast light tower inspections, another for automated and manual flights to gather inspection photos, another for cell tower measurements, and the last said for a tunnel air supply plenum fly through (Figure 2.50).

The last question focused on drones asked if the inspectors had ever considered using drones for bridge inspections. Most people (58.8%) responded that they had considered using drones for bridge inspections, but 32.4% said they had not considered it but think it could be useful in the future (Figure 2.51). Although a majority of respondents believed that drones could be used in some way for bridge inspections, three of 34 had not considered using drones for bridge inspections and they did not think it would be useful to implement in bridge inspections in the future.

Overall, although many inspectors had not witnessed a drone being used, many of those that had, witnessed them being used for inspections. This highlights that UAVs may be a viable option for the inspection of bridges if they can address the challenges mentioned in the responses recorded above. It is also promising that many have considered or would consider using drones in the future for bridge inspections, which means that many inspectors are aware of the possibility of using UAVs, and they are open to using this technology in the future. This awareness and willingness to use drones will help ease into a transition to drone use if that is deemed by MassDOT to be the new way for bridge inspection.

Have You Ever Used a Drone or Witnessed a Drone Being Used for Any MassDOT Related Activities?

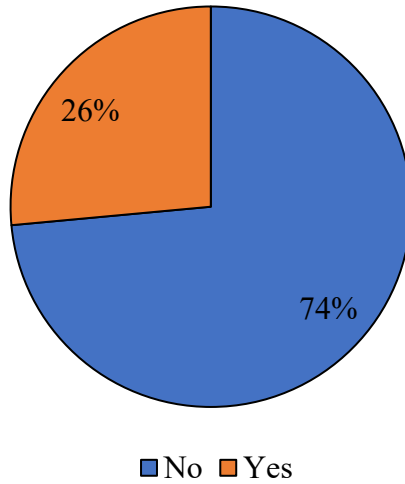
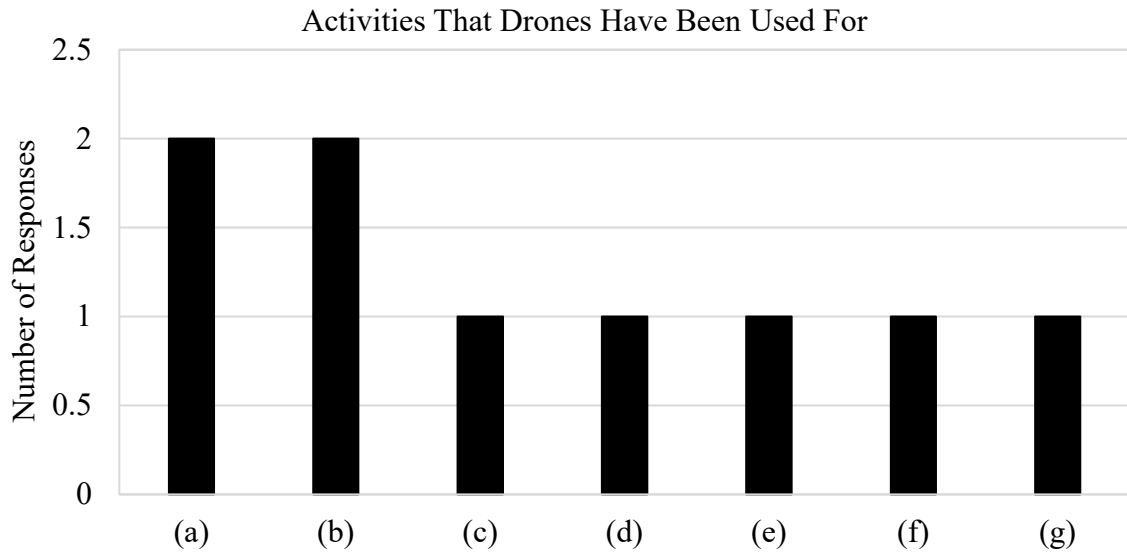


Figure 2.49: Using drones for MassDOT activities



(a)	Bridge inspections
(b)	High mast light tower inspections
(c)	Ancillary structure inspection
(d)	Automated and manual flights to gather inspection photos
(e)	Cell tower measurements
(f)	Tunnel air supply plenum fly through
(g)	MassDOT communication tower load rating analysis

Figure 2.50: Activities of the drones

Have You Ever Considered Using Drones for Bridge Inspections?

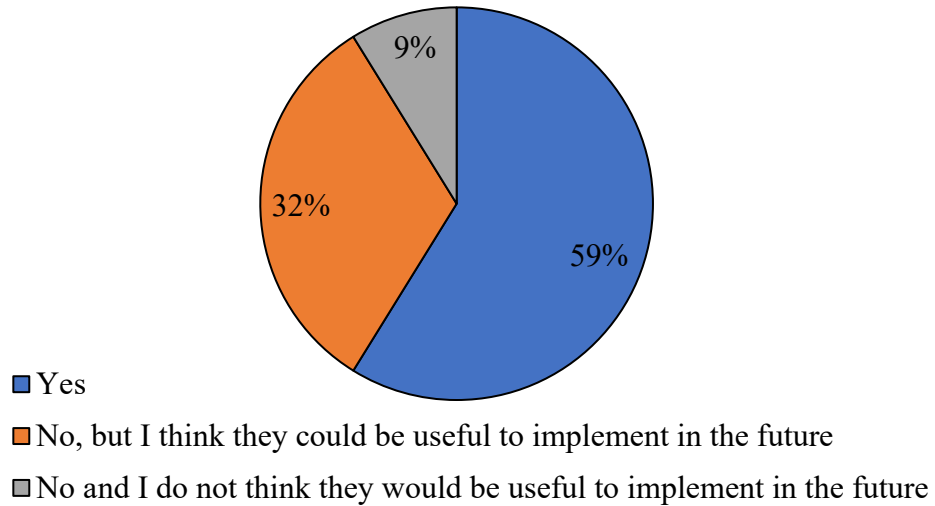


**Figure 2.51: Bridge inspectors who considered using drones**

The final question of this survey asked for any additional comments and/or suggestions that they thought should be known for this research project. Of these, 13 respondents gave additional comments, six of which pertained to the use of D-meters and drones; five of the other responses offered additional information on how they collect data, how they document the data, and how they deal with delamination. The respondents for the last two comments said to reach out to them if there are any further questions to aid this research. Overall, these additional comments, along with the other responses of the questionnaire, were kept in mind for the duration of this project to help guide the research and aid in the decision process.

## 2.4 Conclusions

---

The questionnaire presented in this report was sent out to the individuals that participate in MassDOT bridge inspections to gather and summarize information on

- general inspection practices,
- corrosion assessment practices, and
- the equipment used for bridge inspections.

Based on the data collected from the questionnaire responses, the following conclusions were made about the existing bridge inspection procedure:

- There is a consistency issue among inspectors that can affect the ability to monitor the condition of a bridge over time.
- Inspectors struggle with accessibility and visibility of corroded areas due to the bridge configuration and equipment limitations. This means that inspectors are not always able to remove the rust and delamination, and they may not be able to measure all the points necessary to get an accurate representation of the corroded area.
- Inspectors often cannot get accurate measurements due to tool limitations, particularly when measuring in harsh weather and/or measuring on uneven surfaces.
- Documentation becomes time consuming as the bridge ages because older bridges are typically more corroded, which means more measurements need to be taken, documented, and analyzed for them.
- MassDOT inspectors may typically be responsible for many bridges, which means they may not have as much time to carry out each inspection per month.
- It is concerning that most of the inspectors that responded to the questionnaire have seen webs that deviate from straightness because this can cause significant loss in beam capacity and can be very unsafe.
- Compared to the consultants, MassDOT inspectors felt that their equipment is in need of more changes.

There is a lot of room for improvement regarding the existing bridge inspection procedures, and those improvements could greatly increase the safety and efficiency of bridge inspections while also decreasing inspection costs. Suggestions for any potential procedures to be proposed in the future are as follows:

- Any new procedure should be designed to yield consistent results in order to ensure that the condition of all bridges is thoroughly assessed and monitored over time to prevent any catastrophic structural failures in the future.
- Based on the number of bridges and poor condition of bridges in Massachusetts, any increase in inspection and/or documentation time can lead to added stress for inspectors given their workload. Therefore, any new procedure, especially for corrosion assessment, should not take too much time to carry out and document to be implemented successfully.

- Given how often web deviation is observed along with it being an important parameter for estimating the remaining capacity of a corroded beam, any new procedure should address how to estimate the condition and safety of the bridge based on how much web deviation there is.
- It would be beneficial to address what a bridge inspector should do when they cannot access certain areas and/or they cannot remove delamination. This will help improve the consistency, accuracy, and efficiency of inspections.
- To address the limitations of the equipment currently used by inspectors, any new equipment should
  - Be safe to use,
  - Be easy to use,
  - Be able to access most areas of a bridge/bridge girder,
  - Be accurate,
  - Be reliable in most field conditions, specifically in harsh weather,
  - Be able to get accurate readings on uneven surfaces,
  - Not take too much time to set up and use in the field, and
  - Not take a lot of post-processing time.
- Laser scanning, or LiDAR, and UAVs are known by some inspectors and are advanced technologies that can be used to estimate corrosion
- Further research should be done on using UAVs for the inspection and corrosion assessment of steel bridge girders because
  - UAVs can help address and correct the challenges that inspectors are experiencing, and
  - The additional technology add-ons can be added to UAVs, including LiDAR, in order to measure and assess steel beam end corrosion.

## **3.0 LiDAR-Based Inspection Methods for Efficient Data Collection for Beam End Inspections**

In Massachusetts, MassDOT is responsible for assessing the condition of steel bridges. In its efforts to ensure safety and maintain the infrastructure of the state, MassDOT engineers perform periodic bridge inspections that conform to the requirements of the *Code of Federal Regulations* [3]. MassDOT has introduced and is currently using a variety of standard inspection report forms [4] that fulfill the requirements of the National Bridge Inspection Standards. These reports provide extensive information for the overall condition of the structure (e.g., deck, superstructure, substructure, culvert) in the form of figures, text, photos, and/or sketches gathered by inspection engineers.

### **3.1 Developed Tools**

---

The implementation of LiDAR technology to the substructure's condition assessment for steel bridges as well as the results documentation within the inspection report is discussed in this subsection.

In this framework, a field corroded beam obtained from a decommissioned bridge is scanned, and a methodology for estimating the remaining web thickness is developed and evaluated based on measurements taken by using a thickness gauge.

#### **3.1.1 Specimen Collection**

A corroded beam was acquired from the decommissioned bridge C-05-030 built in 1939 in the town of Charlemont. This bridge consisted of a simple span integral abutment bridge. The superstructure consisted of six rolled 21WF beams spanning approximately 20 ft. All the beams were sent to the Brack Structural Testing Laboratory at the University of Massachusetts Amherst (UMass). Of the six girders, three were tested as part of a previous research effort [5] for the development of load rating procedures for deteriorated unstiffened beam ends. Consequently, the inventory of beams in untested condition was reduced to three, and ultimately the beam that was at the best condition for potential experimental testing was chosen (Figure 3.1).





**Figure 3.1: Field corroded girder used for the study**

### **3.1.2 Corrosion Topology**

In integral abutment bridges, beam ends are embedded into the reinforced concrete abutments at each end (Figure 3.2a, b). After concrete was removed during bridge deconstruction, three holes made in the beam webs to pass diaphragm reinforcement were revealed. The end region of the web that during the in-service period was concrete embedded did not undergo significant section loss. The top flange of the beams was not encased in the deck, exposing the entire beam to weather and environmental conditions. Considering that the maximum clearance between the lower face of the deck and the stream bed did not exceed 8 ft, high moisture conditions existed at the bridge site. The extensive flange section loss observed throughout the length of beams in bridge C-05-030 could be attributed to stream flooding combined with moisture exposure. Localized areas with section loss were observed along the web (Figure 3.2c).



**Figure 3.2: (a) In-service configuration, (b) construction details for the support, and (c) web condition at midspan**

### 3.1.3 Methodologies for Thickness Estimation

To explore the capabilities of LiDAR technology, the web region selected for thickness measurements should

- contain mixed areas having intact and corroded regions,
- contain mixed areas with and without coating,
- have areas with steel delamination, and
- exhibit different levels of section loss.

A rectangular web area with dimensions 18 by 14 in. is selected close to midspan (Figure 3.3). First, the beam is scanned at the condition that was initially retrieved from the construction site (Figure 3.4). Then, deposits, coating, and rust are removed before a thickness gauge is used to obtain thickness measurements that constitute the benchmark for LiDAR data evaluation.

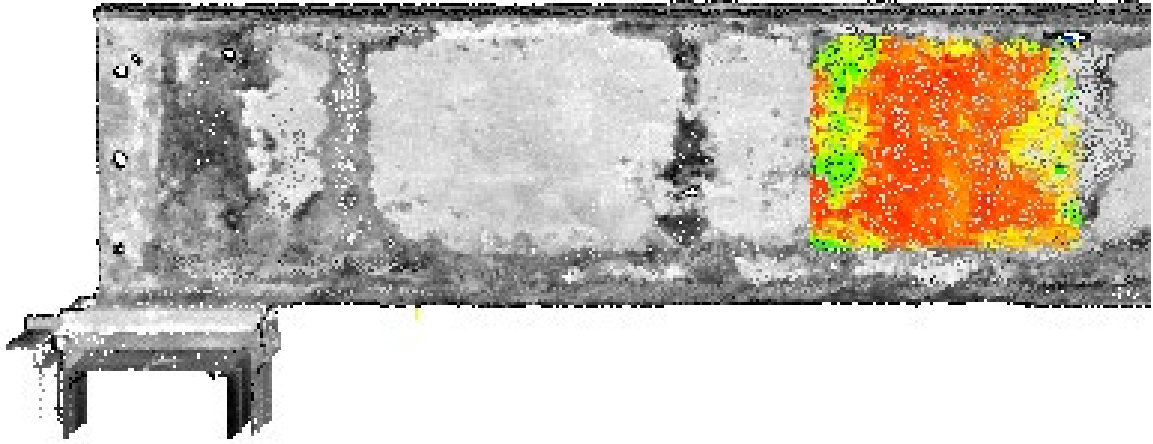


**Figure 3.3: Scanned beam and the area of interest**

### **3.1.3.1 Thickness Estimation with Gauge**

Detailed thickness measurements are performed in the selected region to determine the section loss using a thickness gauge with a resolution of 0.001 in. (0.025 mm) by GE Inspection Technologies [6]. This equipment is widely used by MassDOT inspectors, and its operation is based on measuring the speed of an ultrasonic sound pulse that travels through the material. To ensure reliable readings, a coupling layer is applied at the measurement location.

Even though the thickness gauge is placed on a clean surface, a challenge of this method is varying instrument readings. A common aftermath of the uneven section loss is bumpy steel surfaces that result in a significant variation of the measured thickness. To eliminate problems with local surface imperfections, and for reference to the thickness loss data, a grid with 1 in. spacing was drawn on both web faces (Figure 3.4), and combined measurements from both faces were obtained from 283 locations. Figure 3.4a shows the right face, and Figure 3.4b shows the left face.

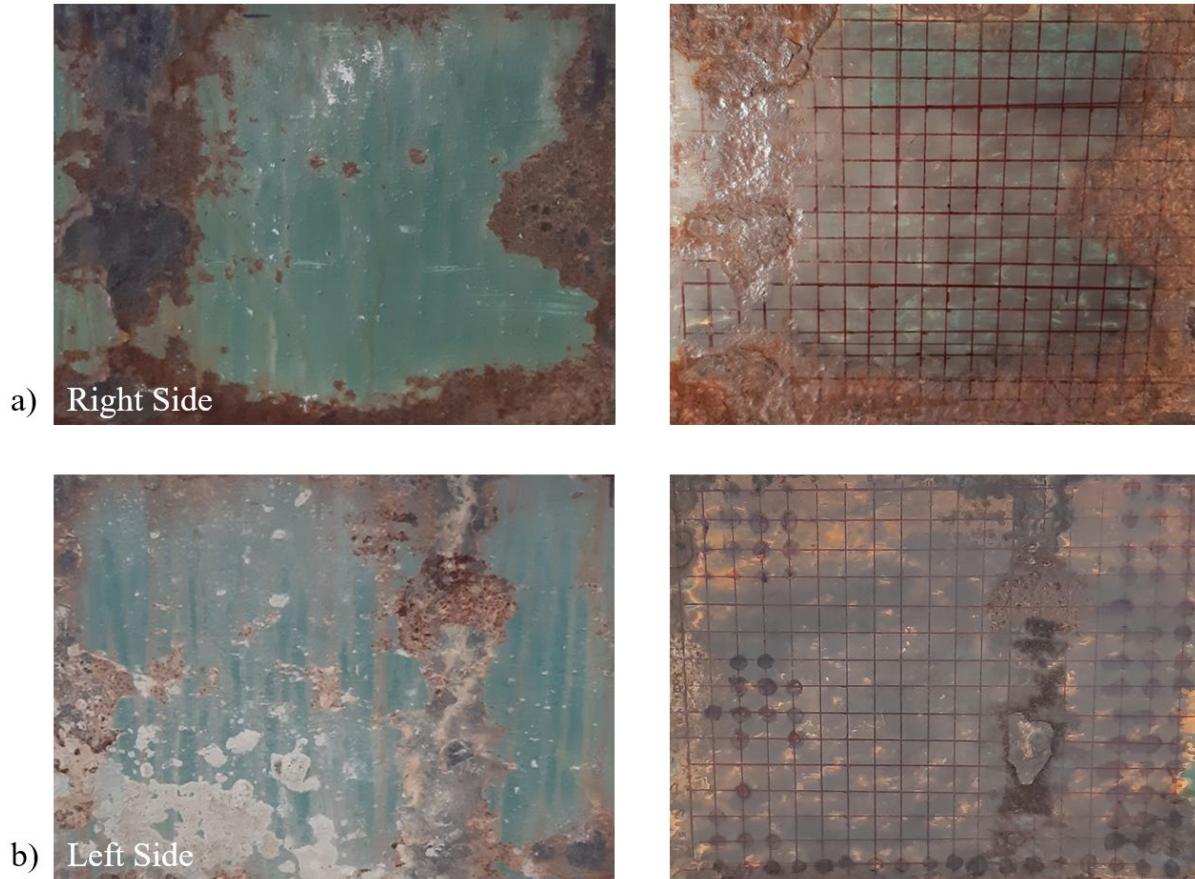


**Figure 3.4: Condition of the web before and after coating and rust were removed**

### **3.1.3.2 Thickness Estimation with LiDAR**

The Department of Civil and Environmental Engineering at UMass owns a mobile LiDAR, RIEGL VMZ-2000, that integrates three primary components: the LiDAR sensor, the precise positioning system, and the camera system. The LiDAR sensor is used to acquire the point cloud that generates up to 400,000 points/sec. The integrated precise positioning system (GPS/IMU) is used to acquire accurate coordinates from a global positioning system (GPS) and an inertial measurement unit (IMU). The camera system is used to capture video log images that are calibrated and integrated with the LiDAR sensor that captures high-resolution imagery.

Precision and accuracy are the set of specifications that significantly defines the quality of measurements. Accuracy is the degree of conformity of a measured quantity to its actual (true) value, and precision is the degree to which repeated measurements under unchanged conditions result in the same value. The available equipment provides 0.2 and 0.12 in. accuracy and precision, respectively.

Figure 3.5b presents the point distribution around the flat surface of a steel plate (Figure 3.5a) scanned by the previously described equipment. The difference between the measured and an estimation of the actual location of the scanned surface are also included. One challenge of using LiDAR technology to visualize a corroded surface lies in the ability of capturing section loss that lies in the range less than the provided precision.

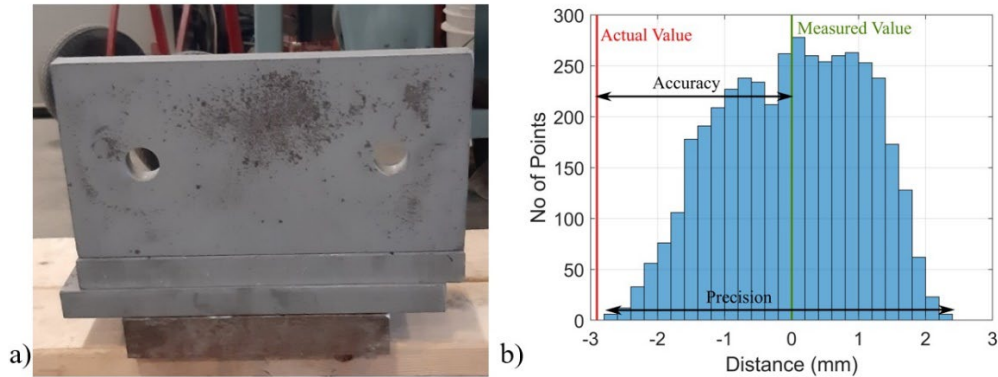


**Figure 3.5: Flat steel plate and the corresponding point distribution with removed noise**

### 3.1.3.3 Scan and Post-Processing

The beam is digitized by performing two measurement ground-based stations to capture both web sides. In the acquired point clouds, large volume interference data are manually deleted to increase the workability of the files. The two entities are aligned by picking four equivalent point pairs in both point clouds. From each web face, the points that correspond to the domain presented in Figure 3.4 are isolated and extracted in a common coordinate system. To improve the quality of the data, noise and outliers are removed.

The number of points along the web surface is determined based on two parameters: the angular resolution of the LiDAR (horizontal and vertical) and the distance from the measured surface. For each web surface, around 7,000 points are ultimately utilized for section loss estimation within the area of interest. A mesh is built and smoothed for each web face based on Delaunay triangulation [7]. One side acts as the reference and the other as the compared mesh. The distances between the vertices of the compared mesh with respect to the reference mesh are computed. The obtained values are extracted as a scalar field associated to points. These distances correspond to the thickness of the section (Figure 3.6). The procedure up to this point is carried out using the free software Cloud Compare.

In order to scale down the problem by reducing the number of the involved parameters from four ( $x$  coordinate,  $y$  coordinate,  $z$  coordinate, thickness) to three ( $x$  coordinate,  $y$  coordinate, thickness), a plane was fitted to the reference side. To avoid manually selecting points that may not reflect the best fitting plane the least squares solution was preferred. The mesh is rotated in space to position the newly introduced plane in parallel to the  $xy$  plane originally set by the laser scanner orientation, and the  $z$  coordinate of each point was replaced by the previously

calculated corresponding thickness. The resulting  $x, y, z$  data were used to create contour maps depicting the remaining material along the examined domain. This approach serves the needs of rating engineers who are interested in the remaining thickness magnitude instead of the condition of each web face separately.

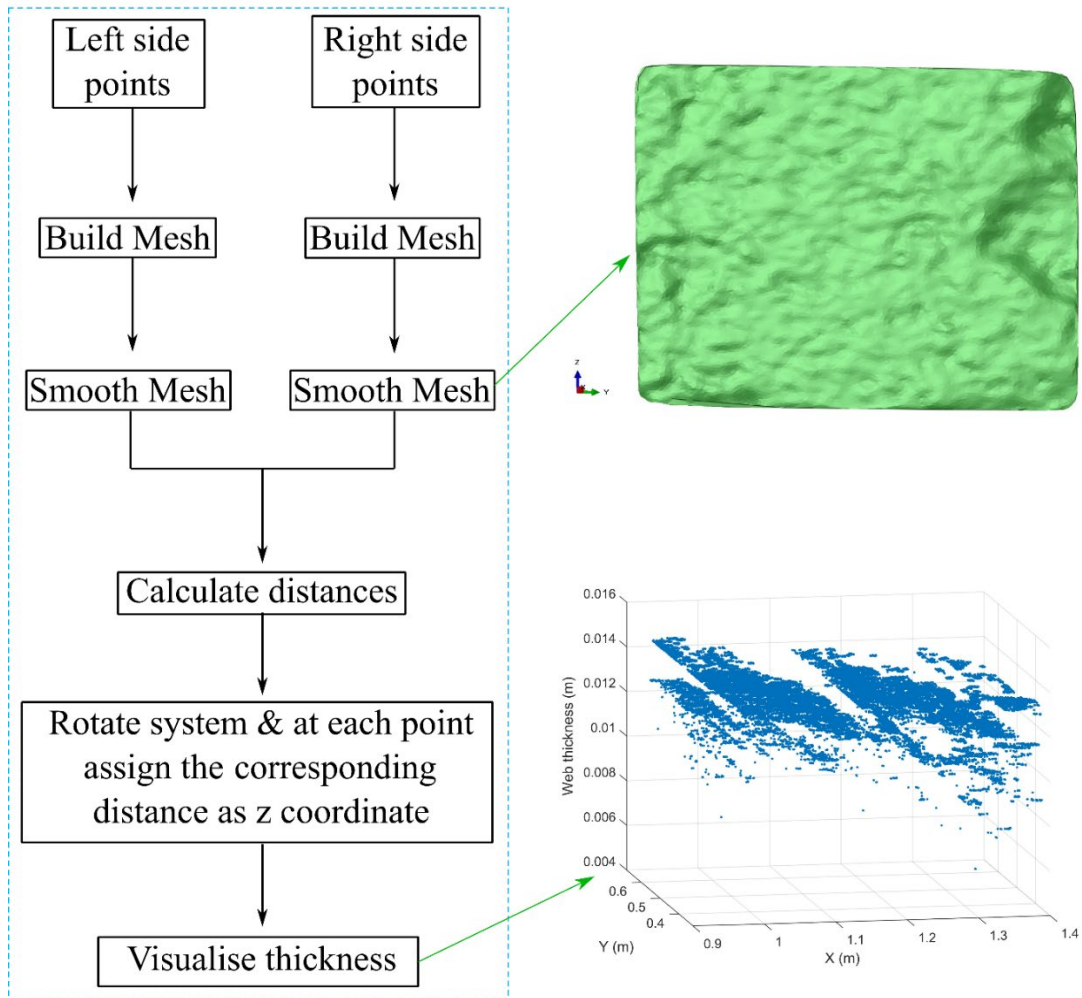


**Figure 3.6: Developed method for capacity estimation**

## 3.2 Methodology Application

To explore whether the proposed methodology can be used for capacity estimation of damaged girders, a naturally corroded specimen will be scanned and subsequently subjected to full-scale experimental testing. The derived thickness contour maps will be combined with finite-element modeling (FEM) to simulate the conducted experiment.

### 3.2.1 Experimental Work

#### 3.2.1.1 Specimen Selection

Preliminary finite-element analysis revealed that the previously described and scanned specimen from Charlemont would most likely result in a flexural failure due to the extensive flange section loss. Therefore, a girder from a second bridge is utilized to experimentally explore the validity of the proposed methodology. At the time this research began, a bridge rehabilitation project was in progress in the state of Massachusetts. Specifically, a three-span bridge (O-03-009) in Orange, MA, was under demolition. The structure, which carried Holtshire Road over Millers River, was built in 1937, and its design contained continuous 24CB120 unstiffened rolled girders. The two piers divided the total length into three equal spans of 60 ft 8 in. long each. The bridge was eventually deconstructed due to the critical condition of the deck, which contained a number of large holes throughout its surface (Figure 3.7a). According to the inspection reports, the deck underside had widespread leakages, which potentially led to widespread surface rust in the girders (Figure 3.7b).



**Figure 3.7: a) Hole through the deck, and b) map cracking with heavy efflorescence at the O-03-009 bridge**

\*Adopted from O03009-0TW-MUN-NBI.

Before transporting the beams, it was decided the best practice would be to cut the beams in half. The advantage of this was two-fold: First, it provided ease of transport, and second, it would allow both segments to be in compliance with laboratory length restrictions. In total 11 segments were shipped to the Brack Structural Testing Laboratory at the University of Massachusetts, Amherst.

For testing, the selected girder has localized areas of moderate to severe section loss above the support. While in service, the beam ends were connected transversely with 12 in. deep C beams diaphragms attached to riveted plates located at the upper half of the webs. After the bridge demolition, the steel diaphragms were removed but the plates at both web faces remained on the girder (Figure 3.8). The girders were delivered with the sole plate welded to the bottom flange, which was later removed in the lab.



**Figure 3.8: The tested specimen**

### **3.2.1.2 Remaining Thickness**

In contrast to the previously studied girder from the Claremont Bridge, no extensive delamination or deposits like mud are observed at the web faces of the girder from the Orange Bridge. To estimate the remaining web thickness at the corroded web end, the previously presented equipment and methodology were used, and the obtained thickness representation is given in Figure 3.9. Two main areas with increased section loss are observed. The first one is approximately 3.5 in. long by 1.0 in. high located below the remaining riveted plates. The second area of distinct section loss extends longitudinally directly above the bottom flange with dimensions 19.0 in. long up to 4.0 in. high. Reduced thickness is also observed toward the top flange and along the inner edge of the remaining plates.

### **3.2.1.3 Experimental Configuration**

The laboratory setup was designed to generate high shear near the corroded end. The girder is tested under a simply supported condition (Figure 3.10). An expansion bridge bearing obtained from another demolished bridge, provided by Gill Engineering, was placed below the corroded end. This 7 in. long bearing consists of two curved plates accommodating rotational and translational displacements. The far end of the beam was supported on a 12 in. long rectangular steel plate. The top flange was laterally supported to prevent lateral-torsional buckling from becoming the governing failure mode; in total, four pairs of lateral braces were placed along the length of the specimen.



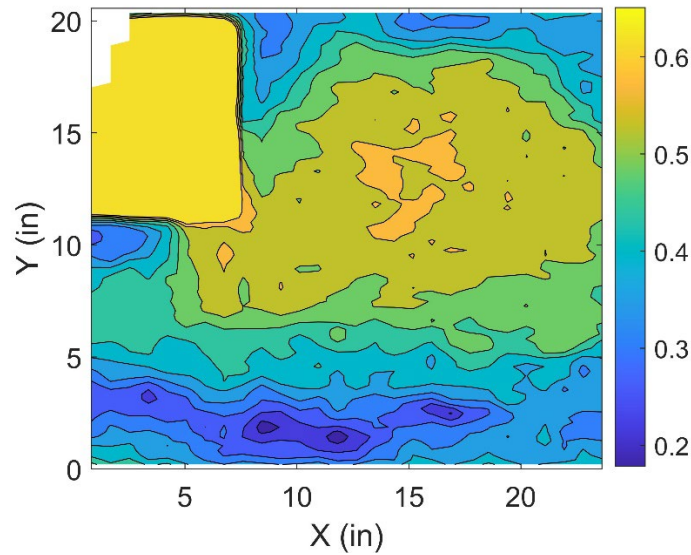


**Figure 3.9: Remaining thickness contours for the tested end**

Loading was applied using two 200-kip hydraulic jacks with top cups able to accommodate rotations along 360 degrees, located under the bearing of the tested end of the specimen. The jacks applied an upward vertical force simulating the reaction at the tested end. The force from each jack acted on a spreader beam that supported the bridge bearing on its top flange. A cross beam anchored to the laboratory strong floor by means of 1.8 in. threaded rods was used to hold the specimen down on a section located approximately 4 ft from the loaded end. The hold-down beam was fabricated using two separate W sections welded together to allow passage of a threaded rod that is anchored to the strong floor. The beam end closer to the applied load is referred to as the tested end, and the other end is referred to as the far end.

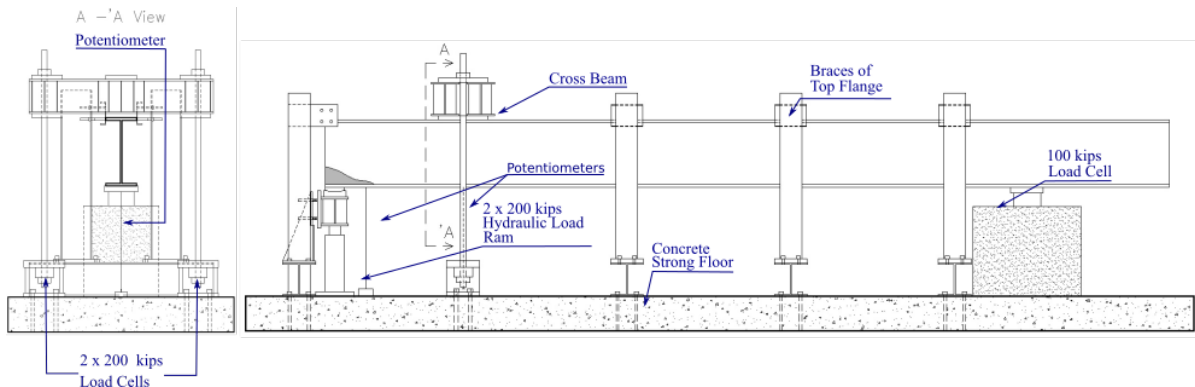


**Figure 3.10: Experimental and instrumentation configuration**

### 3.2.1.4 Instrumentation Configuration

All specimens were instrumented to record loads and deformations. To measure the applied load, two 200-kip load cells manufactured by Omega were placed at the anchorage point of the

threaded rods. A third compression load cell, with 100-kip capacity, was installed beneath the intact end to record the bearing reaction force. A TJE pressure transducer by Honeywell was installed to monitor pressure of the hydraulic fluid in the hose downstream of the hydraulic pump.

Ten displacement potentiometers were implemented to record vertical deflections. Two spring-type potentiometers by Celesco were used to measure the maximum vertical beam deflection close to the load application area, as well as below the cross beam. These potentiometers have a 10 in. measuring capacity and were attached on hooks installed at the bottom flange.

The following instrumentation equipment was used in the experiment:

- Vertical potentiometer: 2 x PT-101-10A by Celesco
- Load cells: 2 x LC8400 by Omega Engineering Inc.
- Pressure transducer: TJE by Honeywell

### 3.2.2 Computational Capacity Evaluation

#### 3.2.2.1 Section Loss Simulation

In this subsection, we develop a methodology to enable the integration of point cloud data into a three-dimensional (3D) geometrical model discretized with finite elements (Figure 3.11). We utilized the thickness determined using 3D laser scanning to capture the corrosion characteristics of the specimen in the finite-elements model. Ten levels of remaining material thickness between the minimum and the maximum recordings were derived, and a Matlab script is used to extract the coordinates of the points that constitute the contour lines. Subsequently, a script in Python, was used to partition the web face of the simulated geometry by connecting the points on these lines. Having defined the deterioration boundaries, each one of the ten thickness values determined using 3D laser scanning was assigned to the corresponding areas.

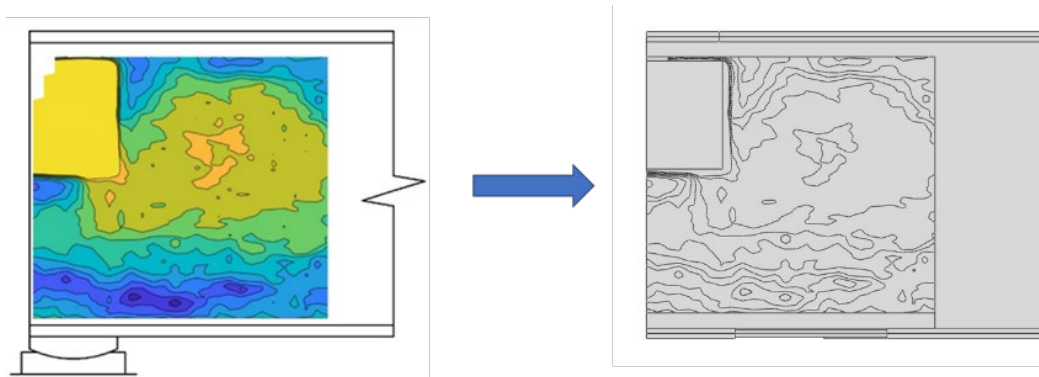


**Figure 3.11: Section loss simulation at the finite-element model**

### 3.2.3 Material Properties

The material properties for the specimen were derived through tensile testing performed in a previous work of the researchers [5]. Stress-strain curves (Figure 3.12) were obtained for coupons extracted from the web and the flanges. The discrepancy observed in yield and ultimate stress of the steel at web and flange can be attributed to the residual stresses of these sections at the time of manufacturing. However, the curves for the top and bottom flange are similar, thus the results are considered satisfactory.

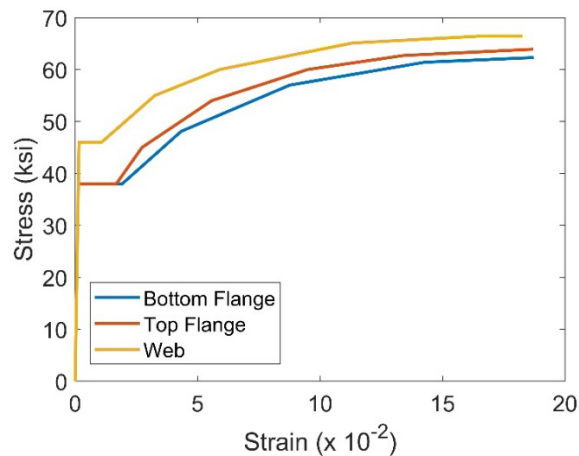


Figure 3.12: Material properties

### 3.2.4 Boundary and Loading Conditions

Both boundary and loading conditions simulate the exact experimental configuration. The bottom flange of the girder is resting on two steel bearing plates, which are considered hinges. Similar to the experimental configuration, the load is applied to the plate below the tested end. The out-of-plane displacement is not allowed at the locations of the lateral torsional buckling (LTB) restrictions.

A particular aspect of the mechanical model that was studied is the effect of the beam-rod assembly flexibility at the cross beam location. Because of the reaction force magnitude developed at the anchor rods, the cross beam is essentially a nonfixed boundary support for the corroded girder. The experimentally captured stiffness of the area (Figure 3.13) was used to resemble this behavior. The constraints derived by the anchor rods–cross beam system were taken into account by introducing a spring, with its bottom end tied to the specimen’s top flange and its top end clamped.

### 3.2.5 Geometric Imperfection

Having described the exact dimensions, thickness reduction, material properties, and boundary as well as loading conditions, the last aspect of the mechanical problem formulation is the applied geometric imperfection.

For any plate or shell buckling problem, it is well known that the structure will suffer from geometric imperfections. Overlooking imperfections can be catastrophic when predicting the capacity of a structure. For the mechanical problem of the deteriorated steel beam ends, initial geometric imperfections are needed for the proper formulation of the problem. In any similar problems, scaled eigenmode shapes are commonly used as the initial geometric shapes of the shell or plate.

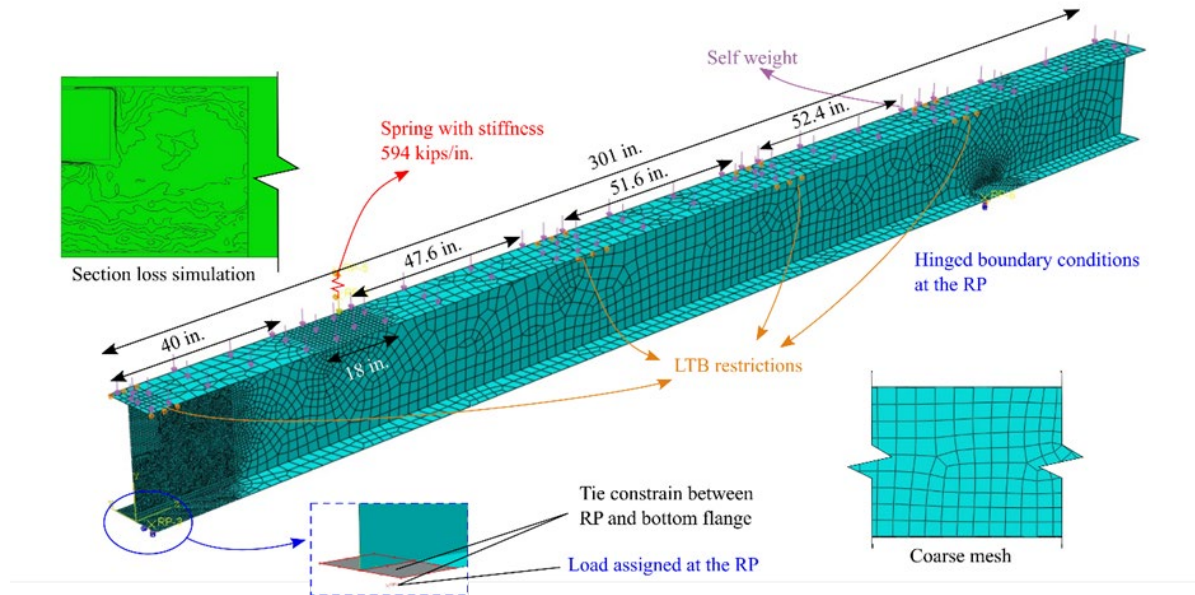


**Figure 3.13: The developed finite-element model**

For intact beams, initial imperfections obtained during the rolled steel manufacturing process are negligible. However, corrosion does not symmetrically reduce the thickness along web sides, resulting in geometric nonlinearities that are able to “trigger” an instability. Thus, extreme thickness reduction usually results in instability phenomena, making deteriorated webs slender buckling-prone members. Since no deviation from straightness was observed at the pretesting condition of the web, the amplitude of the first eigenmode was scaled to 10% of the intact web thickness.

### 3.2.6 Finite-Element Model

The girder is simulated with a mid-surface shell model. Both the web and flange thicknesses are assigned to the corresponding shell elements. The remaining thickness is simulated by assigning a uniform reduced thickness at the elements located in the deteriorated area.

The computational model was developed by using the general purpose finite-element software ABAQUS [8]. Based on sensitivity studies presented in Tzortzinis et al. [9], the S4R element type was preferred, and two element sizes were selected. A dense mesh (0.5 in.) was used to discretize the corroded end. Moreover, to ensure computational efficiency, the element size was progressively increased up to 3 in. far from the bearings. Both bearings were simulated as hinges by applying the tie constraint between the simulated bearing plates and with reference

points introduced to the centers of rotation of each bearing. The interaction between the bottom flange and the bearing plates was idealized by introducing contact. The applied load was simulated as a concentrated force applied to the reference point below the tested end.

### 3.2.7 Analytical Capacity Evaluation

In an effort to improve the reliability and efficiency of the load rating procedures that are currently contained in the MassDOT LRFD Bridge Manual, the researchers have developed closed form equations for the capacity assessment of corroded girder ends based on the results of comprehensive finite-element simulations [2]. The closed form expression is dependent on the geometric characteristics of the girder. By taking into account the negligible web deviation from straightness, which in general does not exceed 10% of the intact web thickness, as well as the  $N/d$  ratio, where  $N$  denotes the bearing length and  $d$  is the beam depth, the bearing capacity estimation is calculated by Eq. (1):

$$R_n = [0.6 \sqrt{EF_y t_f} t_{ave}^{1.5} + 0.24 \left(\frac{0.33d}{N}\right) \left(\frac{4N}{d} - 0.2\right) \frac{\sqrt{EF_y t_f}}{t_f^{1.5}} t_{ave}^3] \left(\frac{CL}{N + 0.1d}\right)^{0.15} \quad (1)$$

where  $E$  is the Young's Modulus,  $F_y$  is the steel yield stress, and  $CL$  is the length of the corroded region within the bottom part of the web bound by a rectangle with a base equal to  $N + 0.1d$  and a 4 in. height (Figure 3.14). Finally,  $t_{ave}$  denotes the average remaining web thickness calculated according to Eq. (2) as

$$t_{ave} = \frac{(N + 0.1d - H) * t_w}{N + 0.1d} \quad (2)$$

where  $H$  is the length of holes within the control rectangular area, and  $t_w$  the remaining web thickness. Given the absence of holes  $t_{ave} = t_w$ , however, the question raised regards the selection of the remaining thickness input  $t_w$ . Following the conversional data gathering techniques, inspectors use an ultrasonic thickness gauge to collect usually one or two measurements along the area of interest. The exact location of these points depends on their judgment. On the other hand, the use of 3D laser scanning technology provides more than 6,000 thickness values within the region. An investigation to conclude on a procedure for corrosion input selection follows in Section 3.4.

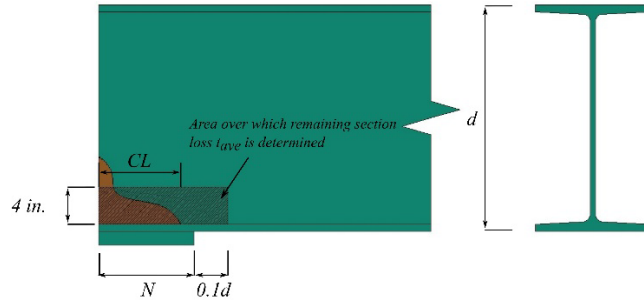


**Figure 3.14: Area of interest for residual capacity estimation**

### 3.3 Results

---

This section includes the thickness estimation of a deteriorated web section based on data taken with a thickness gauge and a LiDAR. The remaining web thickness representation determined by the gauge measurements is considered the benchmark for LiDAR output evaluation. Because the two approaches study the same area of the web, the acquired data points were used to create contours depicting the remaining web thickness. Advantages and limitations of the developed methodology are identified.

#### 3.3.1 Thickness Gauge

Figure 3.15a and b show the right and left sides, respectively, of the web domain, and Figure 3.15c shows the thickness contours produced based on 283 measurement points taken with a thickness gauge after the web surfaces had been cleaned. Visual observation indicates that corroded areas from both sides have been captured.

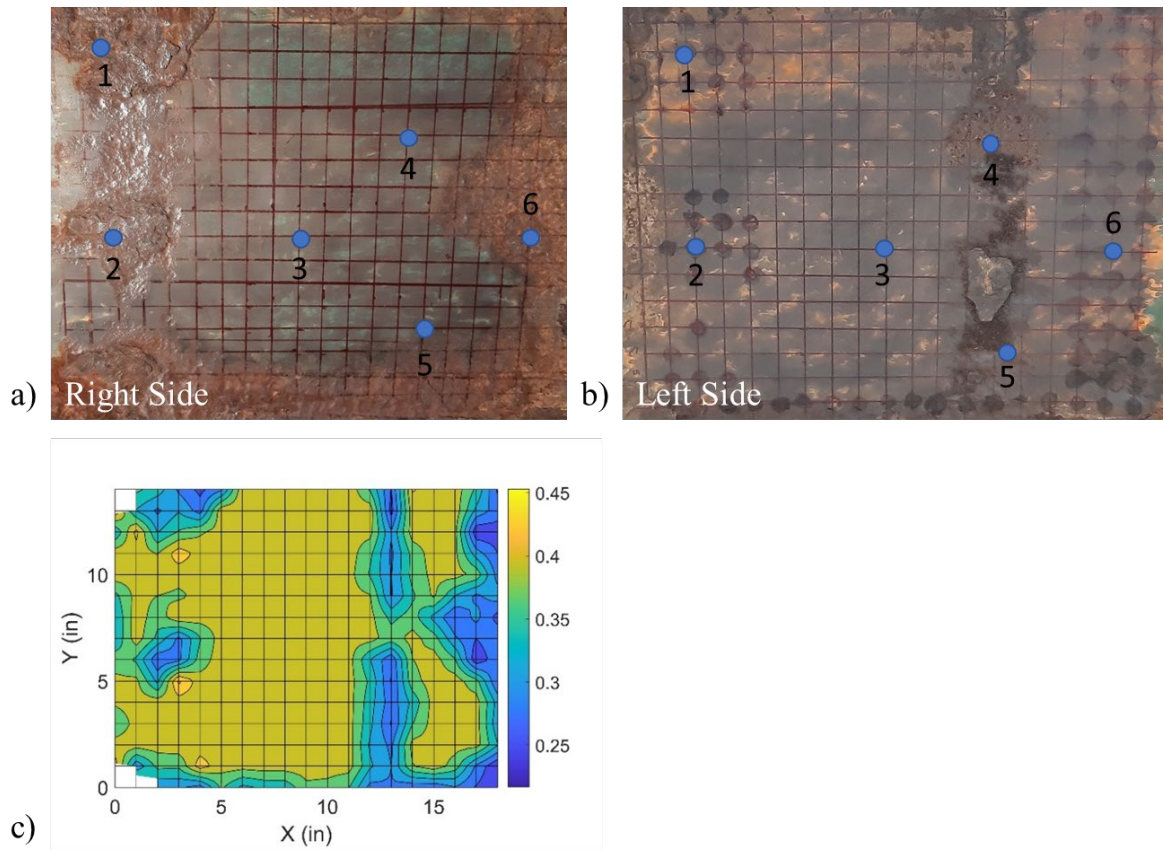


**Figure 3.15: Web domain and remaining thickness estimation (in.)**

### 3.3.2 LiDAR

Remaining thickness estimation, making use of LiDAR technology, requires the assessment of section loss along both web faces. Initially, the condition of each face is evaluated separately. Figure 3.16a and b (right and left faces, respectively) illustrates the actual web faces and their condition based on post-processing of data acquired by scanning the beam before surface cleaning.

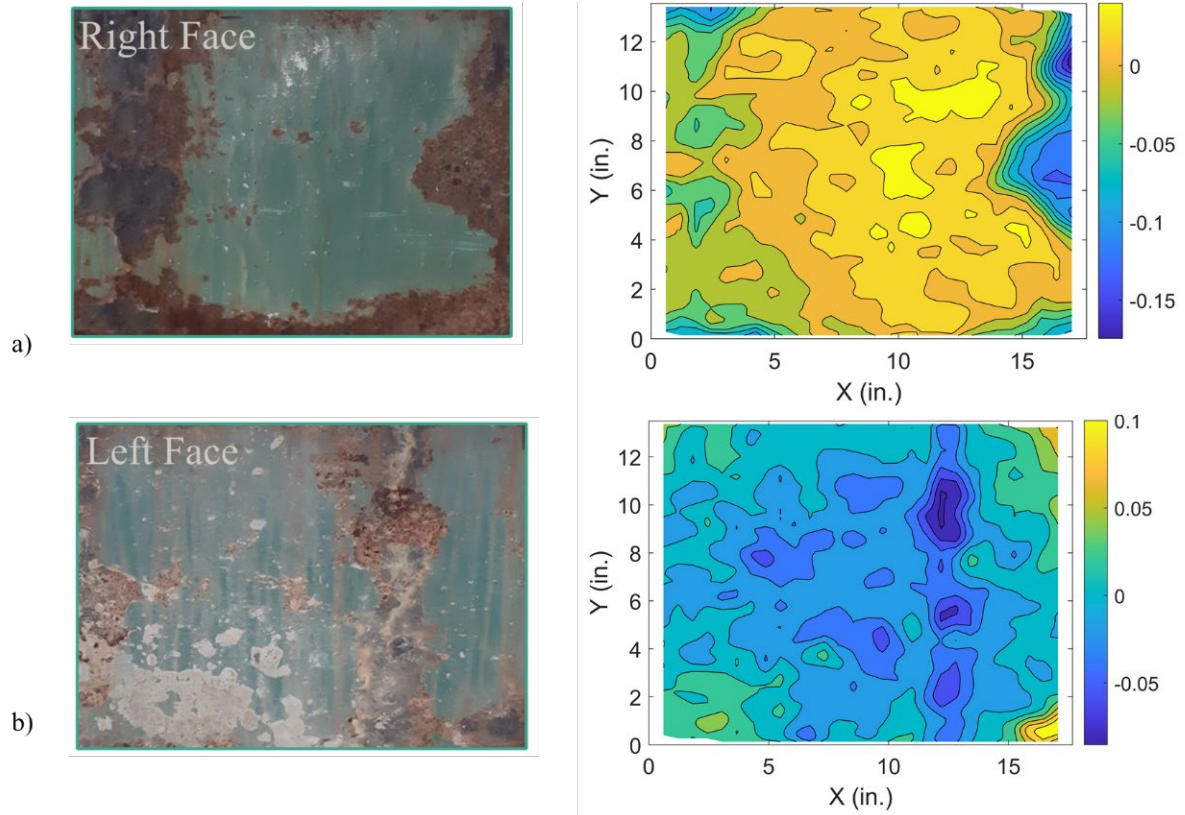


**Figure 3.16: Representation of web right and left faces (in.)**

Regarding the right face, visual observation indicates that by implementing laser scanning technology we are able to accurately capture the corroded area's boundaries located at the right part of the domain. Regarding the deteriorated area at the left part, delamination does not allow the same level of efficiency. However, localized areas with section loss are captured.

The corrosion characteristics of the left face of the web are mainly described by an area that crosses vertically the domain for  $x = 12$  in., while the rest of the web is in relatively good condition. In Figure 3.16b, different shades of light blue color dominate the contours that denote thickness reduction less than 0.01 in. from the perfect surface.

By combining the condition representations of the two faces according to the methodology previously described, Figure 3.17 illustrates the final remaining thickness based on post-processing of point cloud data (in.) for the examined domain.



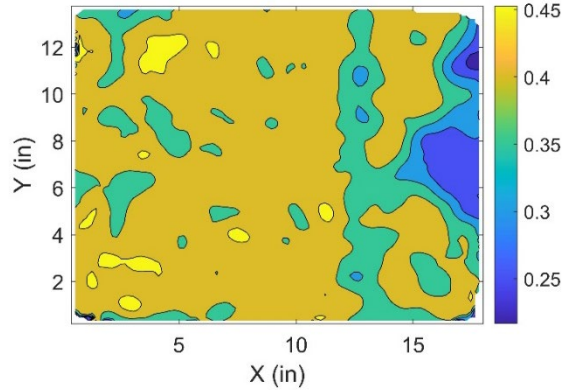


**Figure 3.17: Representation of web thickness**

### 3.3.3 Comparison

To better evaluate the differences between the two methodologies, thickness estimations are presented in Table 3.1 at six locations (Figure 3.15), representing different web conditions. Point 3 lies on the intact web part and has been captured with just 2% discrepancy, depicting an excellent agreement between the two methodologies. Point 6 is in a region with thickness reduction detected only along the right web face (Figure 3.15).

The residual thickness estimation between the two methodologies varies only by 6%. Points 4 and 5 are on the corroded stripe that crosses vertically the left web face. At Point 4, where the beam surface is similar to Point 6, the thickness estimations by the two instruments vary only by 5%. On the other hand, it can be seen that Points 1, 2, and 5 are in areas where deposits and extensive delamination were covering the web faces when the specimen was scanned. With respect to the measurements obtained by the gauge over the exposed steel, the discrepancy along these locations rises to 39%.

**Table 3.1: Comparison between thickness gauge and LiDAR estimations**

Point ID	Thickness gauge (mm)	LiDAR (mm)	Difference (%)
1	7.6	9.1	+20
2	7.1	9.9	+39
3	10.4	10.6	+2
4	10.0	9.5	-5
5	7.6	8.9	+17
6	6.4	6.8	+6

Considering that the beam was scanned in the as-received condition to meet challenges inspectors face in the field, the obtained results highlight the importance of a clean surface to avoid thickness overestimation due to delaminated steel. Delamination destroys steel's integrity and leads to thin layers that gradually detach from the web surface, reducing the beam cross section, while at the same time resulting in overestimating thickness estimations.

### 3.3.4 Implementation

Nowadays, a typical bridge inspection report includes a text description of the corrosion-induced damages. This description is usually supplemented with sketches (Figure 3.18a) and occasionally with photographs (Figure 3.18b). Pictures may provide an excellent overview of the extent of damage, while sketches of varying levels of detail include the locations of usually a unique or two-point measurement. On the other hand, the development of thickness contours based on 3D laser scanning techniques allows for capturing the remaining thickness field efficiently and accurately.

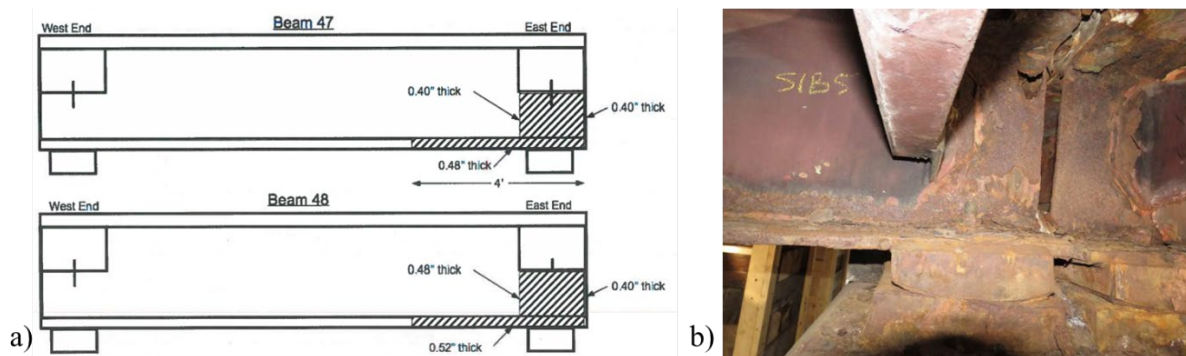


**Figure 3.18: Typical sketch and photograph in MassDOT inspection reports**

Furthermore, the provided methodology not only captures the corrosion characteristics with remarkable accuracy, but it also enables the quantification of section loss evolution in time if measurements from different periodic time intervals are compared.

The proposed methodology can be applied to any type of point cloud regardless of the instrument or method by which it was created. During the last years, many DOTs in the country have explored or even introduced UAVs for visual inspection of bridges. Using UAVs decreases the number of inspectors, speeds up the process, and increases the accessibility to bridge components, while at the same time it prevents the inspector's exposure to danger. Given the rapidly improved accuracy and precision specification of portable LiDARs, data could be also collected in the near future by aerial scanners mounted on drones, combining the advantages of both technologies.

To conclude, the proposed documentation technique can be easily processed from inspectors and engineers, it provides an overall description of the examined area, and it can be integrated in the inspection reports to upgrade the corrosion mapping.

### 3.4 Application Results

This section includes the results obtained from the experimental testing of a naturally corroded girder. The derived failure load and mode are used as a benchmark to evaluate the use of 3D scanning technology for capacity estimations, both computationally and analytically.

#### 3.4.1 Experimental Results

The selected specimen was successfully tested on December 12, 2020. Given the experimental and instrumentation configuration, the applied load is estimated as the difference between the loads measured at the cross beam and the intact end. As an intermediate step, the total reaction force developed at the cross beam is calculated from the summation of the recordings in the two load cells (east and west) installed at the bottom end of each rod (Figure 3.19b).

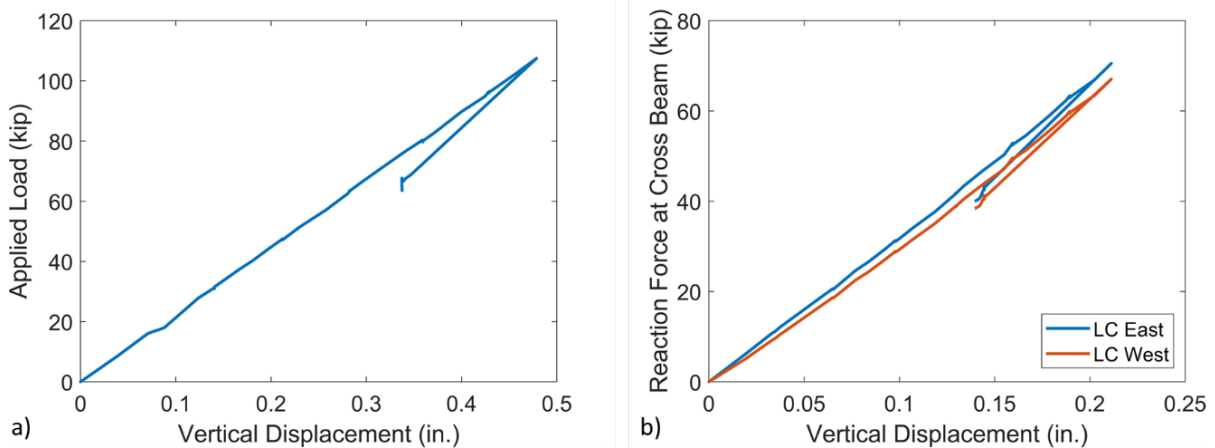


**Figure 3.19: Applied load–vertical displacement plot and reaction force developed at the cross-beam area**

From Figure 3.19, a discrepancy is seen between the recording of the east and west load cells that equals up to 5% at maximum load. This behavior might be attributed to a slight eccentricity of the beam longitudinal axis compared to the anchor rod’s location or to a nonsymmetrical shape of the beam that originates from the demolition process.

Figure 3.19a depicts the applied load versus the vertical displacement at the tested end and captures the failure load at 107.5 kips for 0.48 in. of displacement. A relatively linear response of the specimen is observed until a sudden failure occurs, captured as instant capacity drop. This behavior is consistent with the macroscopic specimen’s behavior, where no large deformations were noticed prior to the sudden failure. The whole experimental process was captured by two cameras. The first camera was recording the plane of the web (side view of the beam), while the second camera was recording the beam profile. Figure 3.20 shows the girder’s deformation at the initial condition before loading, followed by deformations observed at failure. A buckling wave was formed at the bottom part of the web with maximum magnitude

at the outer web edge just above the bearing. The maximum lateral displacements profile is developed diagonally along the longitudinal axis of the beam, aligned to the region of the extensive section loss presented in Figure 3.20.

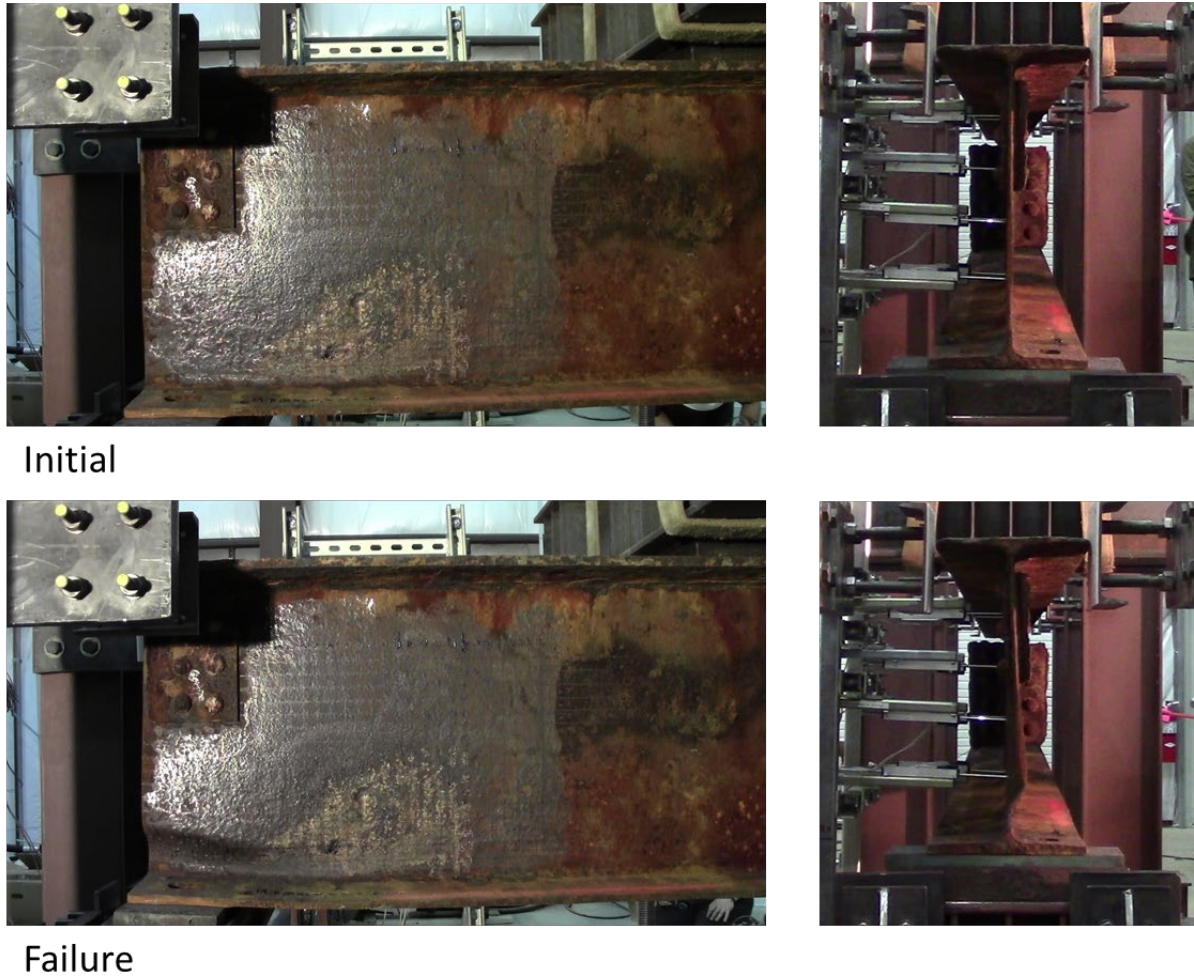


**Figure 3.20: Side and profile views of the specimen**

### 3.4.2 Computational Results

Following the procedure described previously, the applied load–vertical displacement curve is plotted to compare the finite-element output with the experimental results for the tested specimen. Quasi-static analysis was performed up to failure as post-buckling is currently out of the scope of this study. Comparison of load–vertical displacement curves for numerical and experimental models is presented in Figures 3.21a indicating that the computational model satisfactorily captures the failure load as well as the stiffness of the specimen. In detail the difference between the numerically acquired peak load and the experimental value is 4.1% (experimental: 107.5 kip, FEM: 111.9 kip). In Figure 3.21b, the reaction force developed at the cross-beam area is also included.

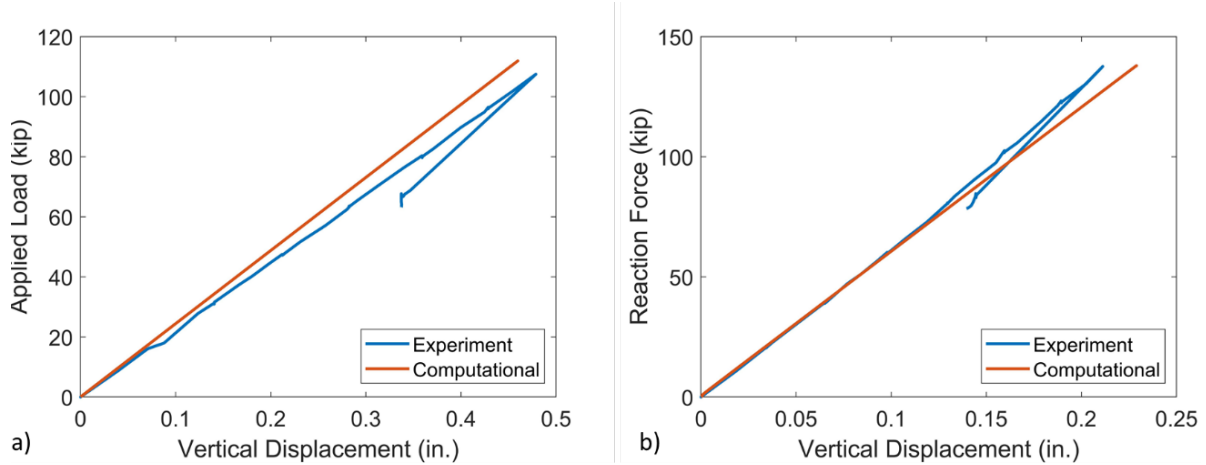


**Figure 3.21: Load-displacement curves.**

Figure 3.22 presents side by side the experimental (Figure 3.22a) and the computational (Figure 3.22b) failure modes, highlighting the buckling wave captured at the same location by both approaches. It is also worth noting that the section loss topology defined the developed displacements at failure. An important first finding from this analysis is that the 3D laser scanning procedure provides an accurate framework for the estimation of the capacity of corroded girders.

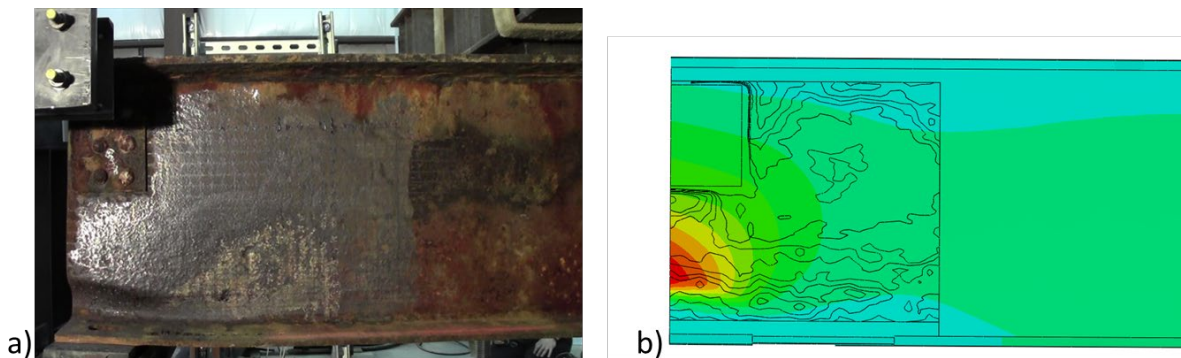


**Figure 3.22: Experimentally and computationally obtained deformations at failure**

\*Lateral displacements contours have been projected on the computational representation.

### 3.4.3 Analytical Results

For the tested specimen and by averaging the scanned cloud data on the area of interest as defined by the examined specifications (Figure 3.23a),  $t_w$  equals 0.33 in. Using this thickness value in Eq. (2) would result in a capacity of 132.2 kips, showing a clear discrepancy between the capacity prediction and a measured capacity of 107.2 kips during the test.

The source of this difference between the predicted value and the experimentally obtained capacity is attributed to the simplistic definition of the parameter  $t_w$ .

One could expect that by scanning a corroded area and by averaging the measured values within this area would lead to a more accurate prediction of the capacity of the beam, but in reality, the nonuniformity of the corrosion must be taken into account for a correct prediction. For the specimen under study, the average thickness of 0.33 mm is the source for a significant overestimation of the predicted capacity, because the nonuniformity of corrosion is dictating the capacity. The capacity is governed by buckling of a region within the 4 in. by  $N+0.1d$  area of interest in which the remaining thickness is less than the average of the area of interest. This would mean that if a laser scanner is to be used to obtain measurements for predicting the capacity of corroded ends, a calculation of the remaining thickness in the 4 in. by  $N+0.1d$  area by averaging the measurements is a faulty calculation.

In reality, this calculation needs to account for the nonuniformity of the corroded area and depending on the level of nonuniformity, perform a weighted average calculation. In this case, if only the lower 76% of the measurements is used (Figure 3.23b), the predicted capacity is 107.5 KN, which corresponds to the experimental value. The failure load is analytically captured by calculating the average thickness of points (red dots) located mainly along the diagonal domain that governed the failure mode.

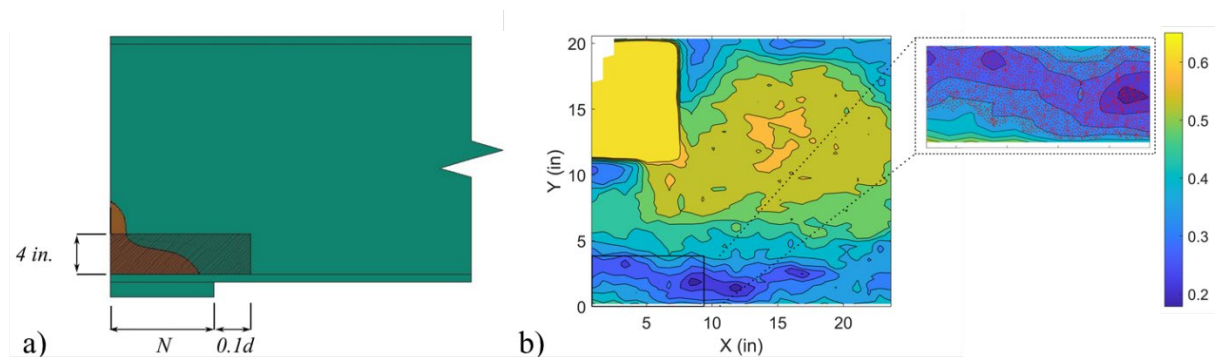


**Figure 3.23: Area of interest for residual capacity estimation and failure load**

### 3.4.4 Implementation

The main finding from using laser scanning measurements with analytical calculations is that there should be significant attention and more research on the calculation of  $tw$ . A weighted average method should be developed that would account for the nonuniformity of the corrosion. In terms of today's practice of obtaining limited values of the remaining material, the strategy of most inspectors to obtain values at the worst locations (lowest values of remaining materials) is very important and should continue to be followed.

Regarding the computational implementation of 3D laser scanning data, the proposed automated procedure can enable engineers to create finite-element models that encapsulate the exact corrosion condition of damaged girders. This methodology provides a game-changing tool for dealing with the uncertainty that usually comes along with the analytical evaluation of beams presenting varying levels of corrosion-induced thickness losses, which currently results in conservative estimates of remaining capacity.

### 3.5 Conclusions

---

The efficiency of 3D laser scanning as a potential technology for bridge inspection has been explored and validated. LiDARs can address the shortcomings of conventional data acquisition techniques and at the same time abolish the sensitivity of ultrasonic thickness gauges along bumpy surfaces. Thickness estimations resulting from 3D laser scanning post-processing were verified and subsequently used for capacity estimations. More details for these conclusions are as follows:

1. Data acquisition
  - The need for cleaning the steel surfaces prior to scanning was highlighted. The existence of delaminated parts can result to overestimating thickness estimation.
2. Documentation
  - Thickness contour maps were proposed as a two-dimensional representation of the remaining thickness profile along the deteriorated area. This approach provides an overall description of the examined area, and they can be integrated in the inspection reports to upgrade the corrosion mapping.
3. Capacity evaluation
  - A numerical study included the creation of computational meshes that integrate the exact condition of corroded girders. This approach was validated with full-scale experimental testing of a naturally corroded girder. Comparison of numerically and experimentally obtained results provided credibility to the proposed automated methodology, because the failure load of the simulated specimen was captured with an error of 4.1%.
  - The post-processed data was used to inform analytical tools for capacity evaluation. The obtained results provide evidence that a generalized average of the web thickness as corrosion input should be avoided, because it may result in overestimating predictions.

## **4.0 Technological Solutions for Efficient Data Collection for Beam End Inspections: Unmanned Aircraft Systems (Drones)**

This research section focuses on how unmanned aerial vehicles can be used during bridge inspections to monitor and estimate the amount of corrosion of steel bridge beams.

This section is broken into reviews of three phases:

1. How UAVs have been used for general transportation activities.
2. How UAVs have been used for bridge inspections.
3. Different corrosion technologies that could be used on UAVs to monitor and estimate corrosion in the future.

In detail, this section presents the results of a literature review of reports from Caltrans, Illinois DOT, Iowa DOT, Indiana DOT, Ohio DOT, Kansas DOT, Kentucky DOT, New Hampshire DOT, Missouri DOT, Vermont DOT, and the American Association of State Highway and Transportation Officials (AASHTO). These reports focused on how they have each used UAVs to perform general transportation activities. Furthermore, this research specifically records what each DOT used UAVs for, why they found it beneficial, and any research they conducted using drones. In addition, this section presents the results of a literature review of reports from Idaho DOT, Michigan DOT, Minnesota DOT, Nebraska DOT, North Carolina DOT, Oregon DOT, Carnegie Mellon University, Colorado State University, Florida Institute of Technology, Mid-American Transportation Center, Union Pacific Railroad, and Norfolk Southern Railway. These reports contained information on bridge inspections that each research team had performed using UAVs. This report specifically records the research efforts of each entity, along with which drones were used, what technology was used, and what conclusions were reached.

Last, this section presents the results of a literature review focused on different corrosion technologies and how they are or can be used with drones in order to estimate corrosion. The reports for this chapter were broken into two sections: contact nondestructive testing methods and noncontact nondestructive testing methods. Reports for some methods described how researchers attached the technology to a drone, whereas other reports detailed technology that could be used to measure steel thickness for corrosion estimation. The reports only dealing with corrosion measurement technology were included because the research had promising results and could potentially be used on drones as technology advances.

### **4.1.1 UAV Usage for Transportation Purposes**

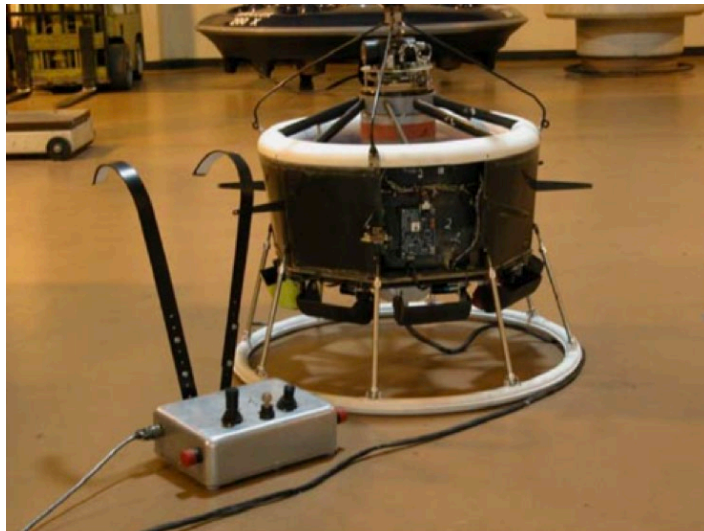
Many states, universities, and other organizations have begun to research and use unmanned aerial vehicles for various purposes. For the first part of this research project, a review of technical reports and presentations that are geared toward using UAVs for transportation



purposes was conducted. The studies herein come from California, Illinois, Iowa, Indiana, Ohio, Kansas, Kentucky, New Hampshire, Missouri, Vermont, and AASTHO.

In California, the DOT, known as Caltrans, has created a Division of Aeronautics, which oversees its UAV operations [10, 11]. As of 2016, Caltrans had received a number of questions from various offices asking if drones could be used in order to cut costs, improve safety, and increase efficiency. Such query led to an increase in research on UAVs in general.

After concluding that drones can be beneficial to their operations, Caltrans began to explore how to improve AVs operations more effectively. Part of the research conducted by Caltrans looked into either owning in-house drones or outsourcing to inspection companies. As part of this research, the University of California at Davis built their own drone for the California DOT [11]. Creating the custom drone shown in Figure 4.1 [10] allowed them to facilitate the data acquisition of interest by insuring it could collect the data they needed and could fit into the spaces they need it to. Besides drone outsourcing, Caltrans also considered other operations for which they could use drones. They focused on the possibility of using drones for terrain investigations, vegetation and soil investigations, disaster response surveys, confined space inspections, roadway inspections, and bridge inspections [11].



**Aerobot with Roving-Cockpit**

**Figure 4.1: Drone built by the University of California at Davis research team**

In Illinois, IDOT took on a “phased implementation” to determine if and how drones should be implemented into their transportation operations [12]. After initial research was done, IDOT found that using drones is very promising as long as there is good communication, adaptation to changing environments and needs, and use of the proper equipment. They also concluded that there are three main categories of UAV use: surveying, inspections, and visuals. Examples of how IDOT used drone collected images and data can be seen in Figure 4.2 [13]. There was such high interest throughout the different transportation departments within IDOT, that there

is a plan to do further testing into how they can use it for other general transportation services such as construction documentation, asset management, corridor planning, material estimation, traffic flow observation, resource identification, and land acquisition. These tests fall into future research plans which also include looking into more sophisticated methods of making data deliverables for post processing and collaborating with other agencies.

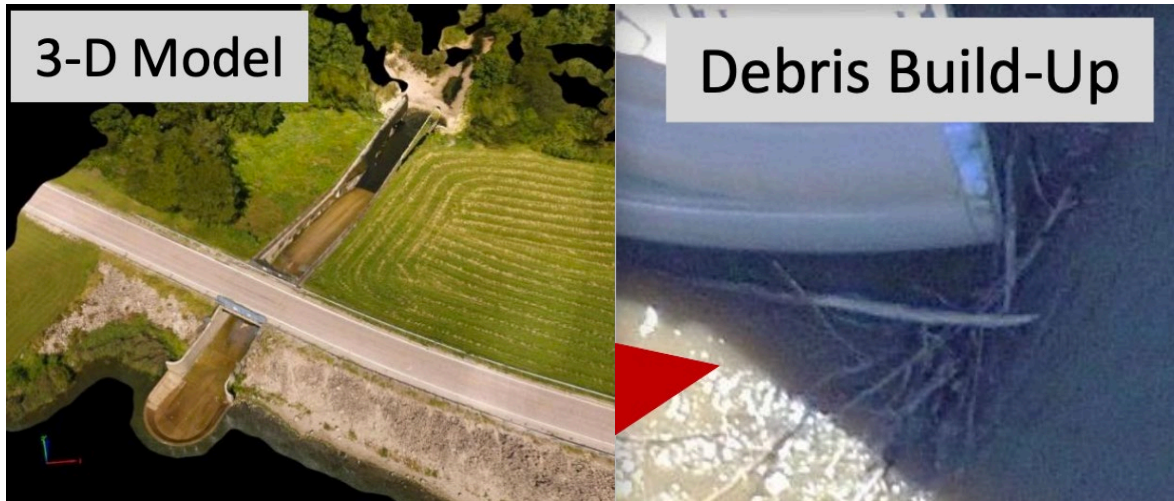


**Figure 4.2: How IDOT used drone collected images and data**

For Iowa DOT, the Office of Aviation is in charge of their unmanned aircraft systems (UAS). Iowa is the first state in the United States to fly a UAV and get a waiver to fly in all airspaces [13]. So far, they have been testing and using the commercially available DJI Phantom 4 drone (Figure 4.3) for many different purposes such as airport/heliport directories, flood monitoring, railroad inspections, wetland mitigation, and highway surveys. A highway survey image taken by the Iowa DOT DJI Phantom 4 can be seen in Figure 4.4 [13]. Due to the promising results, Iowa DOT considers expanding UAS use on crash investigations and bridge inspections.



**Figure 4.3: Iowa DOT's DJI Phantom 4**



**Figure 4.4: Highway survey photo taken with DJI Phantom 4**

In Ohio, the DOT has joined forces with the Indiana DOT to create the UAS center [14]. After getting the proper approval and waivers, the Ohio/Indiana UAS Center has been able to successfully perform various general transportation activities. Those activities included environmental mapping and assessment, modeling and simulations, and precision agriculture. This center has helped a number of different agencies across Ohio and Indiana that use drones to perform data procession and valuable analysis for future decision making.

The Kansas DOT, along with Kansas State University, conducted a broad survey centered around drone usage [15]. Their goal was to see what activities are suitable for drones. After sending a survey to all state DOTs, the Kansas DOT conducted a strength, weakness, opportunities, and threats/challenges (SWOT) analysis. From this analysis, they concluded that there are significant benefits that come from drone usage. The benefits are mainly related to cost, efficiency, and safety. They also summarized how UAVs have been successfully used for surveying, mapping, stockpile measurement, inventories, traffic data collection, and inspections of different structures.

In Kentucky, the DOT created a UAS program [16]. So far that program has done extensive research on using drones for surveying to prove that drones can be useful tools for their transportation activities. The contour map shown in Figure 4.5 [16] shows one of the many products of the research done by the KDOT program. Since their proof of concept was so successful, they are now looking into using drones for digital terrain modeling, construction monitoring, as-built plans, stockpile measuring, crash management, GIS, and inspections.



**Figure 4.5: Contour map using data collected by a UAV**

The New Hampshire DOT, in collaboration with the University of Vermont, has undertaken a research project to explore UAV uses, limitations, and cost-benefits [17]. The project is going to be testing possible activities: accident reconstruction, traffic monitoring, aeronautics, construction monitoring, rock slope inspection, traffic, and bridge and rail inspections. The researchers involved in this project plan to compare the UAV results to the results produced by their current methodologies to come up with advantages and disadvantages.

The Missouri DOT (MoDOT) is very keen on implementing drones [18]. They started the process by first sending out a survey to several state DOTs, as well as several different agencies, such as police and fire departments. Using the collected information, the MoDOT has recommended using UAVs as soon as possible, developing a UAV policy, education program, and partnerships with different stakeholders. They also recommend using UAVs for various construction, agriculture, and manufacturing purposes associated with the DOTs' activities.

The Vermont DOT, along with the University of Vermont, published a presentation of pictures taken by their UAVs and images constructed using the data taken from their UAVs. From these images they have been able to use drones to analyze roadway conditions, capture pictures of traffic collisions, survey and map different sites, monitor floods, assess damage, and perform inspections [19]. One such image used by the Vermont DOT for flood monitoring is shown in Figure 4.6 [19].



**Figure 4.6: Flood monitoring conducted using UAVs in Vermont**

Along with different state DOTs, AASHTO has put out several reports detailing what states are doing with their UAVs. The reports that were reviewed summarized the results of the survey that AASHTO sent out regarding using drones to be more efficient, safe, and cost effective. Their survey was performed in March 2016, and it found that 17 state DOTs had used UAVs for accident clearance, surveying, monitoring and mitigating risks, and inspections [20–22].

Table 4.1 presents a list of the possible transportation activities that UAVs could be used for.

**Table 4.1: Transportation activities for UAVs**

Traffic monitoring
Crash response and reconstruction
Stockpile measurement
Land mapping and surveying
Construction site monitoring
Disaster response
Flood monitoring
Soil and vegetation investigation
Bridge, rail, and road inspections

#### 4.1.2 UAV Usage for Bridge Inspections

Over the last decade, there has been an increase in the amount of research done to determine whether UAV technology is suitable for roadway and railroad bridge inspections. Many of the reports published by various state DOTs and universities start by exploring previous use of drones for bridge inspections to determine if it is feasible to launch a UAV bridge inspection program. Most of the references that explored previous drone usage reached the same conclusion: using UAVs for bridge inspections has the potential to be very beneficial. Such a resolution is a common consensus among those who have considered utilizing UAVs for bridge inspection because it is both cost effective and safer.

Cost efficiency of using UAVs is attributed to the fact that there is no need to halt all traffic to perform inspections, there is no need to spend as much time at each bridge to conduct inspections, and fewer people are needed on site during the inspections. In terms of safety, using UAVs would mean that there is much less need to send inspectors into situations where they could sustain injuries, specifically when they need to be dangled over the side of a bridge using a special truck.

After verifying how promising UAV use is, many states have gone on to perform laboratory tests and test inspections on actual bridges to determine which drones to use, which equipment to use, what can be detected, and if in fact drones can detect what inspectors are expected to detect. Some states have decided to focus on specific detection areas and equipment, whereas others have conducted a general study on all detection areas and available equipment. For this research, reports from six states (Idaho, Michigan, Minnesota, Nebraska, North Carolina, and Oregon), three universities (Carnegie Mellon University, Colorado State University, and the Florida Institute of Technology), a transportation agency (Mid-American Transportation Center), and two railroad companies (Union Pacific and Norfolk Southern) who have launched extensive research projects geared toward bridge inspections were analyzed.

A 2017 report by Idaho DOT and Utah State University details their efforts on utilizing UASs to detect fatigue cracks during under bridge inspections [23]. Their research project was broken into four parts. The first was a literature review in which they looked at how other state DOTs have used UASs. The second part was a small bridge experiment in which a 3DR Iris was flown with a GoPro Hero 4 and FLIR E8 Thermal Camera around a mock bridge constructed at a Utah State University laboratory. During this small bridge experiment, it was evident that it is possible to map a bridge in 3D and detect concrete cracks and delamination visually using the UAV and the different cameras.

The third part of the Idaho DOT's research involved determining the requirements for fatigue crack detection. During this part, three different drones were tried out, the 3DR Iris, the DJI Mavic, and a handmade drone called "The Goose," along with a GoPro Hero 4, the DJI Camera onboard the Mavic, a Nikon COOLPIX L830, a FLIR E8, and a FLIR SC640. After picking the proper equipment, an attempt was made to detect the fatigue cracks in a test specimen both inside and outside the laboratory; and by creating different lighting conditions, to determine the proper technology, lighting, and conditions that would capture an image clear enough to get an accurate fatigue crack mapping from the automatic fatigue crack software Utah State created. From these experiments, it was concluded that the DJI Mavic and its onboard camera

could detect fatigue cracks in any lighting condition, particularly those with an illumination of 200 lx or more, and the FLIR cameras could detect the cracks only through active thermography. Active thermography is a process in which the specimen is heated up using lights and then taking photos using the thermal camera.

The last part of the project was performing an actual bridge inspection on the Fall River Bridge in Ashton, Idaho, using a UAV. This bridge is on a 12-month inspection cycle because of the fatigue cracks present in the steel members underneath the bridge, which is the main reason it was chosen. The research team chose to use the DJI Mavic (Figure 4.7) [24], to capture images of the bridge, specifically where there are known fatigue cracks. Overall, the conclusions from this part of the experiment were that the UAV was able to capture concrete cracks and delamination, but it was unsuccessful in capturing fatigue cracks due to visibility and the drones ability to get close to the crack location. After analyzing all the findings from the four parts of this research project, the research team concluded that a UAS could not detect fatigue cracks using only images, therefore, their future research will focus on thermal imaging for fatigue cracks along with research into other uses for UAVs for bridge inspections.



**Figure 4.7: DJI Mavic inspecting the Fall River Bridge in Idaho**

Michigan DOT, in collaboration with the Michigan Technical Research Institute (MTRI), has been very involved with using drones for transportation-related activities, especially bridge inspections [24–27]. MDOT launched a multiphase project to test the viability of using drones for bridge inspections.

The first phase of this project focused on the feasibility of using UAVs for transportation projects, which ultimately led the state and MTRI to conclude that it was worth continuing their UAV research, given the promising cost, safety, and efficiency benefits that was shown in this phase [24]. The report from the second phase, published in 2018, delved deeper into the actual testing and use of UAVs [25]. This project started with analyzing five different UAV platforms: the Bergen Hexacopter and Bergen Quad 8 Octocopter (both made in Michigan),

the DJI Phantom 3 Advanced quadcopter, the DJI Mavic Pro quadcopter, and the Mariner 2 Splash quadcopter, which is waterproof. They also tested the Nikon D810, the FLIR Vue Pro and Vue Pro R, the FLIR Duo, and a Velodyne LiDAR Puck-16. Several images of the drones and drone equipment are displayed in Figures 4.8 through 4.11 [25].



**Figure 4.8: MDOT's Bergen Hexacopter with dual FLIR cameras**



**Figure 4.9: FLIR Vue Pro onboard the Bergen Hexacopter**



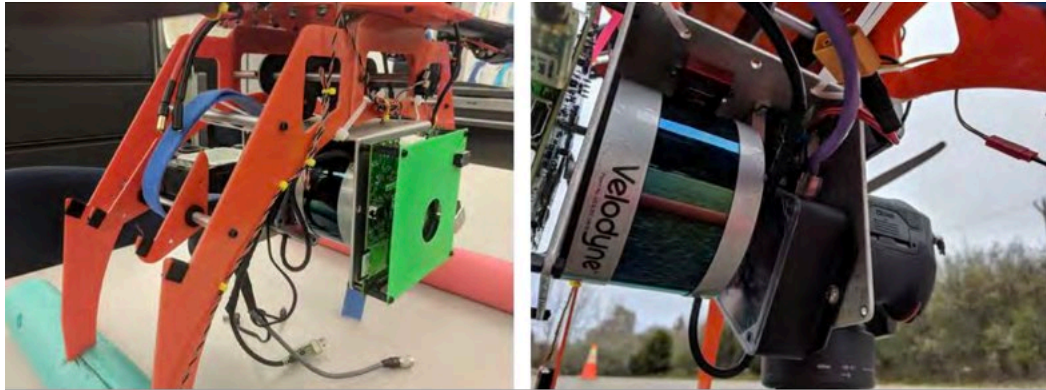


**Figure 4.10: Velodyne LP-16 LiDAR attached to the Bergen Quad-8 UAV**



**Figure 4.11: Mariner 2 Splash with GoPro cameras**

From this first experiment, the research team concluded that the Bergen Hexacopter equipped with a FLIR thermal camera and the Bergen Quad-8 with a digital camera or LiDAR sensor are the best platforms for infrastructure inspections. Along with that, the team also felt the Phantom 3 was best for quick overview shots for roads and bridges, the Mavic Pro was best for quick traffic monitoring video, and the Mariner 2 worked best for capturing images underneath a bridge. After determining which drone/technology combo worked best for each task, the state decided to perform field tests on five bridges, three road corridors, one construction site, and one test near MTRI's office building. Using the images and data collected by the drones and their attachments, the team was able to construct digital elevation models (DEMs), Hillshade models, orthophotos, thermal images, and point clouds for each field test, while also being able to test their automatic spall and delamination algorithms for them as well.

The DEMs are created using Agisoft Photoscan Pro, which utilizes optical images to create a 3D model that has accurate elevation data. These models worked best for spall detection because the algorithm could compare the elevation change between pixels to determine if there

is spall. The Hillshade models (grayscale 3D representations of a surface) were derived from the DEMs using ESRI's ArcGIS software to better display distress features without the inclusion of elevation data. The orthophotos were also created by Agisoft Photoscan, but instead of a 3D model, the software produced an orthorectified image using the optical images, which were then used for comparing potential delamination to visible deck features. The thermal images captured by the FLIR camera also aided in delamination detection, while the point clouds allowed for accurate production of 3D models. Python, MATLAB, and ArcPy were used to create the spall and delamination algorithms that proved to work reasonably well during testing.

After successfully performing field testing and post-processing of the photos and data, the research team determined that UAV technology could meet the needs of MDOT concerning both data and decision support. The conclusion was based on the improved bridge inspection, road assessment, and traffic monitoring they were able to conduct. Also, to further prove that UAVs should be implemented into MDOT operations, a cost-benefit analysis was done at the end of the report, which demonstrated the savings that would come with using UAVs. Last, the phase two report includes the next steps for implementing UAV in day-to-day DOT operations.

The Michigan DOT findings [26–27] and public presentations aim to inform the public about the promising results UAV research has been producing in the hopes of gaining support for their efforts. A “3D Bridge App” has also been developed that allows MDOT inspectors to interact with a 3D bridge model on an element-level to increase the department's efficiency and decrease paper usage [26]. Overall, the Michigan DOT has decided that UAVs can and should be used in day-to-day operations, especially for bridge inspections.

Similar to Michigan, the Minnesota DOT (MnDOT) has also launched a multiphase project focused on using drones for bridge inspections [28–30]. The first phase of this research was a demonstration project in which four bridges were inspected using drones to determine their effectiveness compared to traditional inspection methods. The four bridges selected for this phase varied in both type and size. The drone used for these inspections was the Aeyron Skyranger.

From the first phase results, MnDOT pointed out that UAVs are more useful for large bridges. They concluded that developing technology is very cost effective and presents the potential to improve their overall effectiveness. However, more research is needed to create a program manual for using drones for inspections.

Phase two of the MnDOT research project involved inspecting four more bridges, performing a cost-benefit analysis, and creating a summary of best practice and safety guidelines. For this phase, the Sensefly Albris was used instead because it is able to fly under bridge decks and look straight up, unlike the Aeyron Skyranger.

The research conducted in this phase proved further that UAVs will be a useful and cost-effective tool for inspectors to use for bridge inspections [29]. The last report included a summary of phase one and phase two along with a description of the UAVs used, the post-

processing and deliverables, a cost analysis, and the safety improvements. This report not only highlighted the Sensefly Albris (Figure 4.12) [30], but also introduced the Flyability Elios UAS (Figure 4.13) [30], which is collision tolerant and shows promise for bridge inspections.

In terms of deliverables, this report detailed 3D models, photo logs, and orthophotos that can be made using the drone data, all of which can be stored in an interactive map that can be updated over time to show the evolution of a bridge and its specific elements. The cost and safety analysis showed that drones can significantly reduce spending, protect inspectors, and increase efficiency [30]. Overall, the research project conducted by MnDOT has brought them closer to implementing UAVs in daily bridge inspections.



**Figure 4.12: SenseFly Albris UAV**



**Figure 4.13: Flyability Elios UAV**

In *The Roadrunner*, published in 2018, the Nebraska DOT detailed how they conducted UAV field tests on 11 bridges [31]. To test a variety of conditions, NDOT chose to do UAV

inspections on three bridges in downtown Omaha (an urban area), two bridges over the Platte River (to test under-bridge inspections), one culvert, one long bridge over the Mississippi River, two arch bridges, and two fracture-critical bridges.

After performing all the inspections, NDOT concluded there were far more advantages than disadvantages to implementing drones for bridge inspections. NDOT reported that drones were faster and safer than using the typical snooper truck and boats that are usually used for bridge inspections. Because drones can get closer to the structure than inspectors, UAVs would be able to replace “within arm’s reach” inspections. The document also reported disadvantages, which are mainly related to the training and education needed for drone operation, and FAA regulations, which interfere with the operation of drones.

The North Carolina DOT (NCDOT) partnered with North Carolina State University (NCSU) to analyze the potential of using UAVs for various transportation activities, including bridge inspections [32]. In a research report from 2016, there are details of six field tests performed with drones: (1) a small survey on Lake Wheeler; (2) a high-resolution survey of Kinston Jetport; (3) a construction site survey in Waynesville; (4) geotechnical monitoring of I-40 in Haywood County; (5) traffic monitoring at Diverging Diamond Interchange; and (6) a bridge inspection of Gallants Channel Bridge.

The bridge inspection was performed using the DJI Inspire drone (Figure 4.14) [32]. According to researchers of this report, the inspection confirmed that UAVs would be helpful to reach new locations on every bridge, especially the underside of bridge decks. Using the FLIR E4 and FLIR Tau 640 X 480, the research team was able to detect delamination on the bridge deck. Using the other images captured by the drone, a 3D model and a DEM was constructed for this bridge using Agisoft Photoscan. Overall, after the research finished, NCDOT found that the use of UAV was promising; and as technology improves, it will be an even better tool to use for their transportation activities, especially bridge inspections.



**Figure 4.14: DJI Inspire UAV used by NCDOT**

A 2018 research report published by the Oregon DOT (ODOT) shows that this state is also interested in implementing drones for bridge inspections as well as radio tower inspections [33]. This report details the six bridge test inspections and four radio tower test inspections

conducted by the DOT. A Sensefly Albris, which has a regular and thermal camera, a custom DJI S900 hexacopter with a Sony a5000 camera, and a DJI Phantom Pro 3 (Figure 4.15) [37] were used to perform the bridge inspections.

After inspecting all six bridges of varying sizes, ODOT was able to draw several conclusions. First, the report states that all inspection types can use drones in some way. They also conclude UAVs can capture several details, although a high resolution is required. The ODOT study has also analyzed flight modes, concluding that the two optimal flight modes are the manual mode with sensor assistance and the waypoint-assistance mode. Concerning the flight, the wind is the most impactful condition. Finally, the report points out that it is critical to plan post-processing before the flight. Overall, ODOT concluded that UAS is an important tool that they would like to use for inspections in the near future.



**Figure 4.15: DJI Phantom 3 Pro with a pilot**

Carnegie Mellon University launched the Aerial Robot Infrastructure Analyst (ARIA) project [34]. This project aims to utilize small, low flying drones equipped with 3D imaging technology for infrastructure inspection, particularly bridges. Their micro air vehicles (MAVs) are octo-rotor and equipped with a single-line laser scanner, three video cameras, an inertial measurement unit, GPS, and wireless communication technology. Such features make them superior when flying over water and other hazards compared to drones with ground-based sensors. One such MAV is included in Figure 4.16 [34] along with an image of a bridge model created using MAV captured data.

The ARIA program involves a quick process that starts by completing a flight route over the bridge, while using the onboard technology to capture valuable data and images. Using what the MAV has captured, researchers and inspectors then create a 3D point cloud that is developed into a semantic component-based model used for visual detection of defects. That component model is then converted into a finite-element model for simulation and further structural assessment. This process allows inspectors to have an immersive experience to better analyze the infrastructure over time. Overall, the inspections performed by these drones are safer and more efficient than typical inspection practices, and the university is working closely with the Pennsylvania DOT inspectors to make this project useful for everyone.

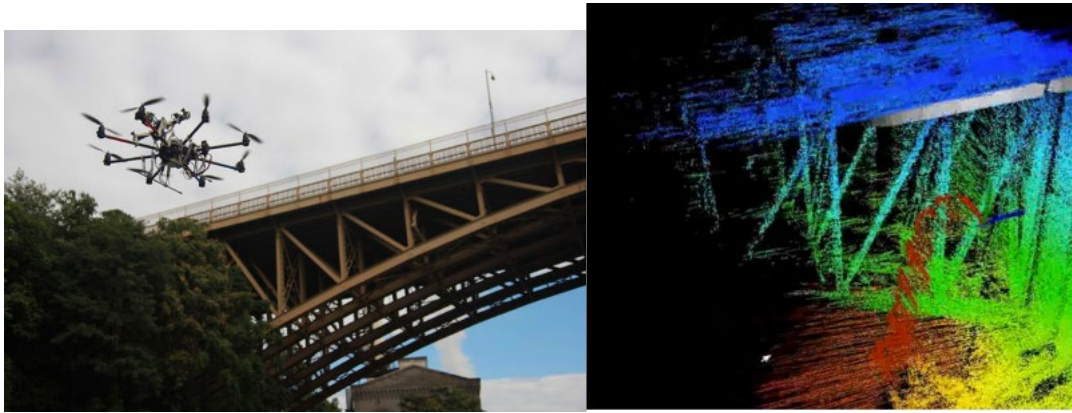


**Figure 4.16: ARIA MAV and a bridge model produced using the MAV collected data**

In a 2019 project, Colorado State University detailed their plans for phase two of their research project [35]. In the search for better inspection methods, the university's research team launched a project focused on feasibility of drone use and post-processing techniques. The first phase was a feasibility study, which has already been completed. For this phase, the team conducted live bridge tests for which optical and thermal images were collected. These images were used to make 3D models that allowed researchers to identify damage and assess the bridge conditions, which proved the feasibility of using drones for inspecting bridges. Phase two being proposed is about research that is centered around developing a way to automatically detect damage and quantify that damage using the data and images captured by the drone. There are four tasks outlined for this project, which are estimated to take about 12–24 months each from the project start date.

The Florida Institute of Technology prepared a research report for the Rail Safety IDEA Program that centered around the inspection of railroad bridges [36]. In particular, they dealt with imaging sensors and mobile LiDARs for remote sensing of concrete cracks and bridge element displacement. Along with the sensors, the research team developed an algorithm to detect and classify concrete cracks. To test both the sensing technologies and algorithms they chose, researchers conducted three experiments.

The first experiment consisted of an in-lab experiment. The researchers built a bridge out of PVC pipe and scanned it using a stationary Velodyne HDL-32E LiDAR. Afterward, they put several wood blocks under one end one-by-one. Each time they added a block of wood they took another scan to see if they could detect movement using the LiDAR. They also moved the LiDAR closer to the bridge, aiming to see if distance affected the scans. From this experiment, with only a few scans, they were able to accurately measure the displacement of the bridge, as well as observe that the closer the LiDAR was, the denser the point cloud became.

The second experiment again involved keeping the LiDAR a set horizontal distance from the bridge, but this time they scanned a concrete bridge in Melbourne, Florida. This bridge had battered piles that deviated from 90 degrees. They raised and lowered the LiDAR vertically to get a complete scan, and they were able to get enough scans to get a point cloud that accurately

displayed the angled piles. The last experiment utilized a UAV that Florida Tech built, known as the MAV-F8 (Figure 4.17) [40]. They then strapped the LiDAR to this drone and flew it around the PVC bridge to collect scans. They found that they got the same quality of scans as a stationary LiDAR; therefore, a drone could be used. They also did a successful railroad bridge inspection on a bridge in Palatka, Florida, using the UAV/LiDAR combo. The successful experiment conducted for this IDEA program has led to support from the Florida DOT and a push toward further research into the use and implementation of drones for railroad bridge inspections.

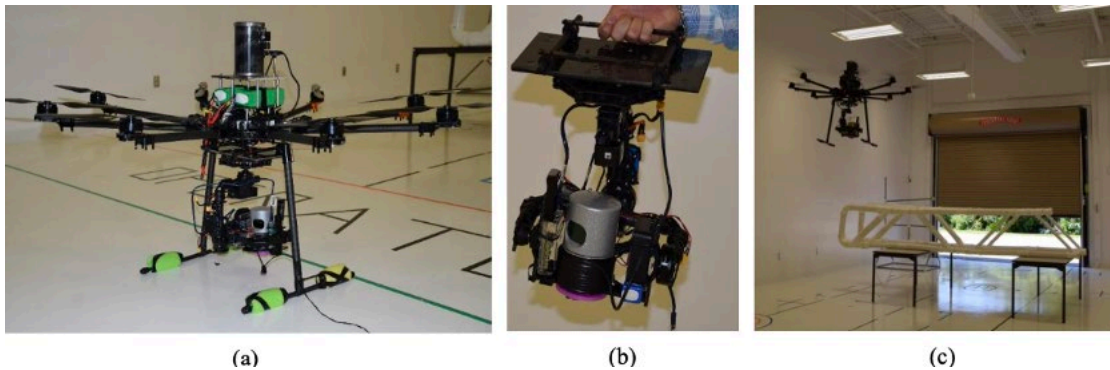


**Figure 4.17: MAV-F8 built by the Florida Tech research team**

The Mid-American Transportation Center is comprised of the University of Nebraska Lincoln, Kansas State University, the University of Kansas, Missouri University of Science and Technology, Lincoln University, the University of Missouri, Iowa State University, and the University of Iowa [37]. These universities completed a cooperative research project centered around developing a UAS to automatically conduct bridge inspections. As part of this project, the research team built their own UAVs and algorithms. They conducted several experiments to test the external sensors they put on their drones to see whether they could be used with or without GPS. Because the results were promising, they developed a prototype UAV system to inspect bridges autonomously, which one hopes to improve the sustainability of transportation infrastructure.

Two major railroad companies in the United State, Union Pacific Railroad and Norfolk Southern Railway, have already begun to implement drones for bridge inspections [38–42]. Union Pacific has been using drones since 2014, and in 2016 the use of UAVs made it possible for them to have the best safety record in their history.

Union Pacific has a program to train their inspectors, and they are continuously trying to advance the technology for railroad bridge inspection [38]. One such technology Union Pacific developed is the Perceptive Navigation Technology (PNT) that allows drone flight without a GPS signal. An image of the drones used by Union Pacific Railroad is shown in Figure 4.18 [38].



**Figure 4.18: UAVs used by Union Pacific to conduct railroad bridge inspections**

Norfolk Southern has also been progressive with their drone use, and they have partnered with HAZON Solutions in Virginia Beach, Virginia, to further their UAV program. They have seen great results so far, particularly, with the speed of inspections—they have been able to perform 64 inspections in 18 months. Besides speed, Norfolk Southern is particularly in favor of using drones to obtain angles they could not obtain before. Overall, implementing drones for railroad bridge inspections is progressing at a fast rate, and the technological advancements being made are helping to make the implementation of drones for both railroad and regular bridges easier and more efficient.

The following tables present several pieces of key information from the aforementioned reports. Table 4.2 presents the outputs that can be made using the data collected by UAVs, along with how they can be used by inspectors. Table 4.3 presents what drones are able to detect, along with how they can be detected. Table 4.4 lists the different drones along with their corresponding state and some of the specifications that are important to know before picking that drone to use for bridge inspections. Finally, Table 4.5 lists the other technology that researchers used with the drones, along with their corresponding states and key specifications.



**Table 4.2: Possible UAV outputs and uses**

<b>Output</b>	<b>Uses</b>
Images and video	Detecting visible defects
Thermal images	Detecting delamination, fatigue, and other distresses
Point clouds	Helps construct the different models
Digital elevation models	Input for automatic spall detection algorithm
Hillshade models	Helps detect possible distresses
Orthophotos	Input for automatic delamination detection algorithm
3D models	Determining bridges structural health and response Monitor changes over time

**Table 4.3: Detection possibilities of UAVs and how they are detected**

<b>Detection possibilities</b>	<b>Detected using</b>
Concrete delamination	Regular and thermal images
Concrete cracks and spall	Regular images and video
Weld, bolt, and connection health	Regular images and video
Visible stress	Regular images and video
Fatigue	Thermal images
Rust/corrosion	Regular images and video
Structural response	3D model constructed from the data collected by the drone
Overall bridge health	Everything collected during the bridge inspection

**Table 4.4: Summary of UAV features**

<b>Technology</b>	<b>Features</b>	<b>Flight Time (minutes)</b>	<b>Payload (lbs.)</b>	<b>Cost</b>	<b>Size (in.)</b>	<b>States</b>
DJI Mavic Pro	4 Blades Onboard Camera 3-Axis Gimbal	21–27	2	\$1,000-1,500	3.3×3.3×7.8	Idaho & Michigan
DJI Phantom 3 Advanced	4 Blades Onboard Camera 3-Axis Gimbal	23	3	\$800	18×13×8	Michigan
DJI Inspire	4 Blades Onboard Camera 3-Axis Gimbal	18	6.27	\$2,500	17.2×11.9×17.8	North Carolina
DJI S900 Hexacopter	6 Blades	18	3	\$3,300	18.1×17.7×14.2	Oregon
Bergen Hexacopter	6 Blades 2 Axis Gimbal	16	5	\$4,900	N/A	Michigan
Bergen Quad-8 Octocopter	8 Blades 2 Axis Gimbal	20	10	\$5,500	N/A	Michigan
Sensefly Albris	4 Blades Onboard Camera Thermal Camera Inspection Drone	22	N/A	\$35,000	22×32×7	Minnesota & Oregon
Flyability Elios 2	Onboard camera Protective Cage	8–10	N/A	\$2,500	15.8 (round cage)	Minnesota
3DR Iris	4 Blades Can be Autonomous	12–19	0.8	\$650	19.5×24.5×12	Idaho
Mariner 2 Splash	4 Blades Waterproof	12–19		\$1,200		Michigan
Aeryon Skyranger	4 Blades Military Use	30–50	1.5	N/A	40 diameter 9.3 height	Minnesota

**Table 4.5: Other technology used with the UAVs**

	<b>Technology</b>	<b>Weight (lbs.)</b>	<b>Cost</b>	<b>Size (in.)</b>	<b>States</b>
Video and photos	GoPro Hero 4	0.19	\$400	1.6×2.3×1.2	Idaho
	Nikon COOLPIX L830	1.125	\$400	4.4×3.0×3.6	Idaho
	Nikon D810	1.95	\$1,200	5.8×4.9×3.3	Michigan
	Sony a5000	0.59	\$600	4.3×2.5×1.4	Oregon
Thermal cameras	FLIR E8	1.3	\$3,000	6.3×15×12	Idaho
	FLIR SC640	4.2	\$3,250	11.1×5.7×5.8	Idaho
	FLIR E4	1.3	\$1,000	6.3×15×12	North Carolina
	FLIR Tau 640X480	0.15	\$10,000	1.8×1.8×1.2	North Carolina
	FLIR Vue Pro	0.25	\$3,850	2.26×1.75	Michigan
	FLIR Vue Pro R	0.25	\$4,850	2.26×1.75	Michigan
	FLIR Duo	0.9	\$7,000	1.6×2.3×1.2	Michigan
LiDAR	Velodyne LiDAR Puck-16 (VLP-16)	1.9	\$4,000	4 diameter 2.8 height	Michigan
	Velodyne HDL-32E	2.9	>\$4,000	3.4 diameter 5.7 height	Florida Tech
Software	Agisoft Photoscan Pro	N/A	\$3,500	N/A	Michigan & North Carolina
	ESRI ArcGIS	N/A	\$3,500/yr.	N/A	Michigan

#### 4.1.3 UAV Usage for Corrosion Estimation

This subsection focuses on techniques for corrosion detection and estimation for steel girder bridges, which is very common in the state of Massachusetts (Figure 4.19). Section loss due to corrosion is observed at the boundaries between the web and the concrete diaphragms or along the bottom flange where the steel is repeatedly splashed with water from the roadway below. However, the locations that are most vulnerable to corrosion are the beam ends.



**Figure 4.19: Typical condition of aged bridges**

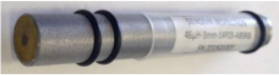



The previously presented research efforts demonstrated that drones can be utilized for various transportation activities, specifically bridge inspections. The purpose of this subsection is to determine if and how corrosion detection and section loss quantification can be improved using available technology and UAVs. In detail, we conduct a literature review to identify compact solutions that could be attached to drones. Although these technologies may not be ready for use immediately, they should be considered for use in the future as technology improves and inspection needs change.

In general, the reports that were collected for the corrosion estimation portion of this research project can be separated into two categories of nondestructive testing (NDT) methods. Nondestructive testing methods are testing techniques that analyze a material, element, or structure without damaging the component under test. The two categories that the reports have been split into are contact (C-) and noncontact (NC-) NDT methods. Contact NDT methods consist of pressing a probe or instrument directly to the bridge element itself. In this case, the drone will carry the instrument/probe and hold it against the corroded area. This experiment outputs the thickness of the corroded area directly under the contact point. On the other hand, NC-NDT methods do not require any instrument to be pressed against the bridge element. Instead, these methods require the drone to hover at a certain distance from the corroded area aiming to read the thickness of the area.

#### **4.1.3.1 Contact Nondestructive Testing Methods**

There are three main C-NDT methods that have been proposed to measure the thickness of a corroded area. The first is through the use of eddy currents, which use electromagnetic induction to capture flaws by measuring changes in flow or magnitude of the current. There is a research study detailing how researchers built their own eddy current probe to detect and

measure corrosion of steel rebar embedded in concrete [40]. This equipment has not been used yet to measure section loss along steel girders, whether as part of a drone or not. However, recent progress in the field has resulted in the creation of an ultralight and compact tester that could potentially be combined with UAV technology. According to the published specifications, the probes included with the tester can be used for crack detection, weld inspection, metal sorting, material properties, coating thickness assessment, and corrosion detection [41]. A chart from those specifications is included in Figure 4.20 [41]. Therefore, using eddy currents is very promising for the purpose of detecting and measuring corrosion of steel girders.

Probe Type	Surface Inspection Applications					
	Crack detection	Weld inspection	Corrosion detection	Coating thickness assessment	Metal sorting	Material properties
 Flat Absolute (with reference coil in bridge)			✓	✓	✓	✓ (3)
 Conical Absolute (with reference coil in bridge)	✓	✓ (2)	✓	✓		✓ (3)
 Smart-PlusProbe (Anisotropic)	✓	✓ (2)				
 Pencil-Probe Absolute 0.9mm	✓ (1)		✓			✓ (4)

- (1) For crack detection in constrained access applications
- (2) Suited to accomplish standard BS 1711:2000
- (3) For conductivity, heat treatment and porosity assessment
- (4) For fine resolution conductivity and porosity measurements

**Figure 4.20: Different eddy current probes that can be used on a drone**

The second contact method that has been researched is the impedance-based nondestructive testing method, which uses vibrations to identify and measure damage. The researchers tested the accuracy of a piezometer and the ability to use it on a drone [42]. A diagram created to show how this process would work with drones and the equipment that is needed is shown in Figure 4.21 [42]. The piezometer measures electrical admittance and converts that to an impedance value. In the same research work, the authors tested the piezometers’ ability to measure progressive damage and thickness loss of a material. Both tests proved the usefulness of piezometers and impedance testing to detect and quantify corrosion. It is also proposed to attach the piezometer to a magnet and then fly the drone up and stick it to the corroded area [43]. The readings would then be transmitted to a laptop to be recorded for post-processing. The piezometers or nodes similar to it can also be placed there permanently to record readings over time [43]. Both papers support the fact that impedance testing can measure thickness losses caused by corrosion, and piezometers can be strapped to a drone to measure that loss during a bridge inspection.

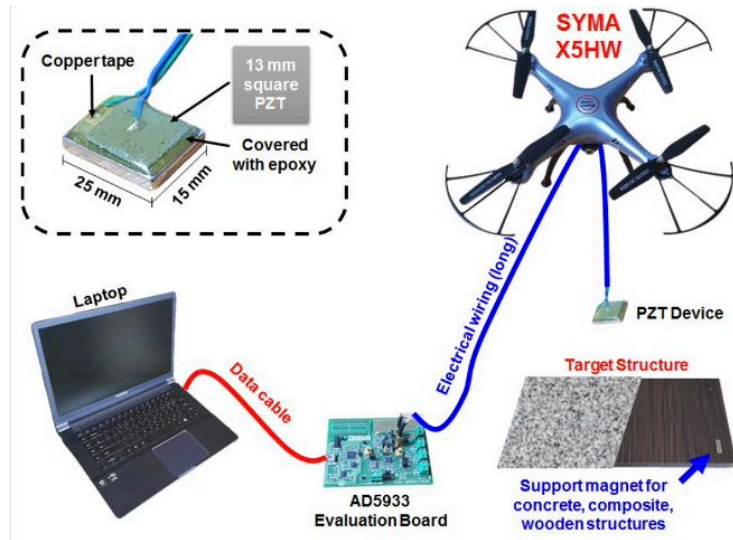


**Figure 4.21: How impedance-based nondestructive testing works and the equipment needed**

Ultrasonic testing is the last C-NDT method that can be used for corrosion estimation. Ultrasonic testing is when a probe sends an ultrasound pulse through a material and uses the returning echo to determine the material's thickness [44]. Researchers in the R&D department at Amerapex Corporation in Houston, Texas, created a testing rig by attaching two electromagnets to an ultrasonic probe, similar to the Tritex Multigauge 6000 Drone Thickness Gauge. Subsequently, this rig was attached to an arm that extended from the researchers' drone (Figure 4.22) [44]. The drone was then driven up to a metal storage tank and the probe was held up to the side so that the electromagnets could stick to the metal and the probe could get a reading (Figure 4.23) [44]. They took many readings around the tank, with each reading taking about 3–5 sec, and the drone/probe combo was successful in reading the thickness of the metal walls of the tank. Overall, this shows the great promise in using ultrasonic testing technology on drones to measure corrosion. All three C-NDT methods have proven to be promising for use in detection and measurement of corrosion, and with more research they could be used on drones for bridge inspections in the near future.



**Figure 4.22: Amerapex drone with UT equipment**



**Figure 4.23: Amerapex drone measuring wall thickness**

#### **4.1.3.2 Noncontact Nondestructive Testing Methods**

In addition to the C-NDT methods, there are three main NC-NDT methods proposed to be used for corrosion detection and measurement. All three methods are spectroscopic, which means that they observe how electromagnetic radiation interacts with the corroded area to determine and measure the corrosion of metal. The first spectroscopic method involves using microwave signals to detect corrosion in steel rebars that are embedded in cement and steel corrosion under paint [45–46]. Using microwave technology for both purposes would be helpful for both steel beam end corrosion estimation, as well as doing general inspections on other steel elements of

a bridge. After making several samples, researchers used microwave 3D imaging to capture images that could be used to make observations about the embedded steel rebar and the steel specimens. The setup for the experiments is shown in Figure 4.24 [45]. The resulting images led researchers in both studies to conclude that using microwave 3D imaging is a promising NC-NDT method for corrosion detection, but there is a lot of research that needs to be done to fully utilize this technology for this purpose.

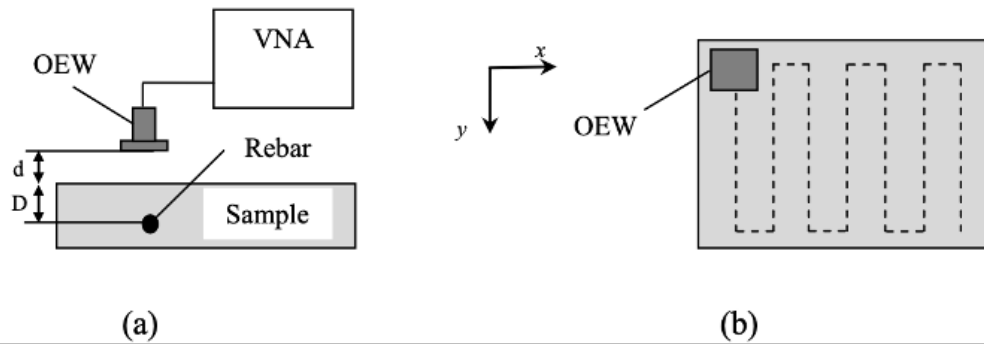


**Figure 4.24: Experimental setup for the microwave 3D imaging**

The second spectroscopic method is terahertz (THz) radiation, which is utilized to detect corrosion under paint [47]. Produced by Picometrix, Inc., the THz system used for this experiment sends the THz frequency from the transmitter through a focusing lens and then the receiver picks up the THz response amplitude from each scan point (Figure 4.25) [47]. Those points are plotted on a graph and on an image to determine paint layer thickness, surface roughness, and ultimately corrosion. After conducting experiments on several corroded pieces of metal, thicker paint and a rougher surface indicated corrosion of the metal. From the results of the experiments, researchers also concluded that using terahertz radiation and imagery is a promising method to detect corrosion, but more research needs to be conducted before using this method in the field.

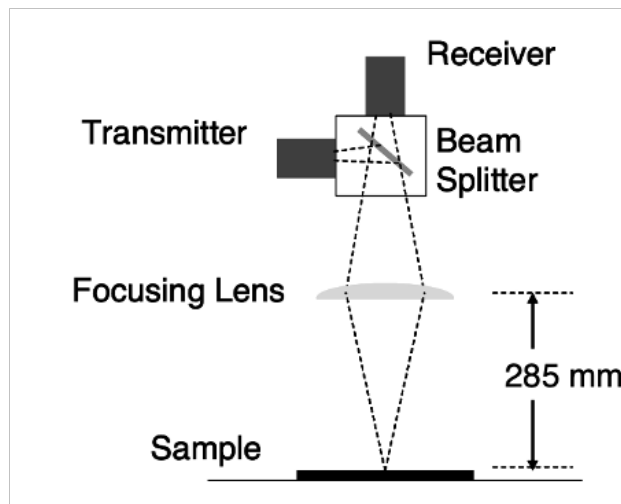


**Figure 4.25: Experimental setup for the terahertz radiation and imagery**



The last noncontact spectroscopic method that has been researched for use in corrosion detection is infrared (IR) thermography. Passive infrared thermography uses infrared cameras to capture the IR admitted from a material and compares it with the IR radiation from its surroundings. Active infrared thermography, which is more commonly used for NDT, uses an external stimulus (such as lasers or lights) to heat up a material to achieve a temperature gradient. Pulse thermography is the most common of the active thermography methods, and it utilizes flash lamps and infrared cameras to observe where the heat accumulates, which indicates a defect. The experimental setup for the active pulsed thermography can be seen in Figure 4.26 [48].

Two research efforts utilize this technology to detect and measure corrosion [48–49]. The first is a study in which they utilize pulse thermography to determine if they can detect blisters and filiform corrosion. These researchers captured IR images of carbon steel and magnesium specimens with these defects and used them to measure the height and area of both types of corrosion. The second study was done at the University of Firenze in Firenze, Italy. These researchers utilized pulse thermography to map corrosion of two aluminum plates; one plate was machined on one side to simulate corrosion. Heat was applied to one side of both plates, and IR images were captured on the other side at a set interval. After performing extensive data analysis, researchers were able to map the corrosion pretty accurately, but they would like to try mapping it in 3D in the future. Both studies concluded that infrared thermography is a promising method of corrosion detection, measurement, and mapping, but more research needs to be done to perfect this method for use in the field.

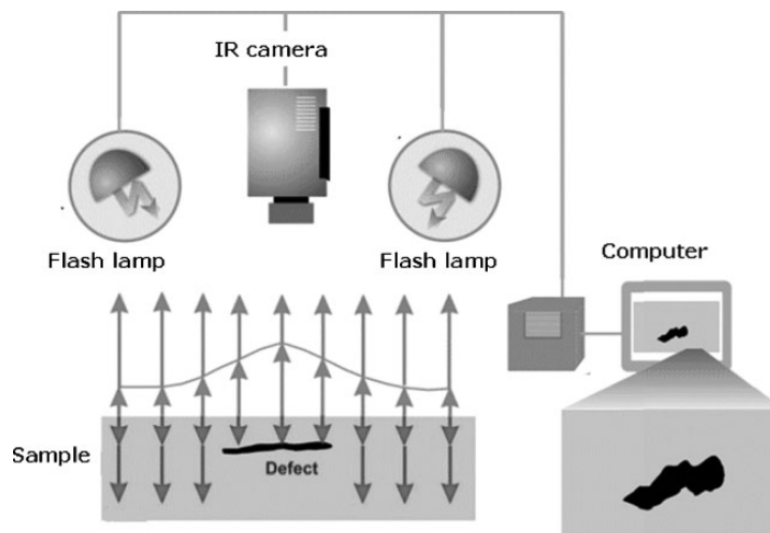


**Figure 4.26: Experimental setup for the infrared pulsed (active) thermography**

All three NC-NDT methods proved to be promising for detecting and measuring corrosion, but all of them are far from being ready to use in the field in the near future. Also, the equipment being used is too large and heavy to be attached to a drone. Perhaps as technology improves and these spectroscopic methods are perfected, they can be used on drones for bridge inspections in the future.

Overall, the researchers of each of the six NDT methods found that they were able to detect and measure corrosion of metal surfaces to some extent. The technology for the contact methods is more available, ready to use, and small enough to be attached to a drone, which means that the contact methods have the potential to be utilized for drone bridge inspections in the near future (Table 4.6). The noncontact methods, however, need much more research before they are ready to use in the field, because they need to be small and light enough to fit on a drone. Therefore, the noncontact methods could not be used for drone bridge inspections in the near future, but the promising results from these methods should not be ignored for there is great potential for their use in corrosion monitoring (Table 4.6).

**Table 4.6: Methods for corrosion assessment**

	<b>Method</b>	<b>Use</b>	<b>Equipment</b>	<b>Advantages</b>	<b>Disadvantages</b>
	Current	Steel bridges	Thickness gauge Hammer	Low cost equipment	Single point measurement Accessibility Required labor
C-NDT	Eddy current	Steel bridges	Thickness gauge Hammer	Low cost Lightweight	Single point measurement Accessibility Required labor
	Impedance-based	Steel bridges	Piezometer Magnet	Small Low cost	Single point measurement Accessibility Hard to attach and detach
	Ultrasonic	Steel bridges	Ultrasonic probe Electromagnets	Small Low cost Easy to use Excludes paint layer	Single point measurement Accessibility Required labor
NC-NDT	Microwave	Steel rebar	Vector network analyzer Open-ended waveguide probe	Large scan Penetrates through concrete No contact needed	High cost Large setup Heavy equipment Required labor
	Terahertz	Metal	Transmitter Receiver Beam splitter Focusing lens	Large scan No contact needed Detect corrosion under paint	High cost Large setup Heavy equipment Required labor
	Infrared thermography	Metal	Infrared camera Flash lamp(s)	Large scan No contact needed Blistering and filiform corrosion can be measured	High cost Large setup Heavy equipment Required labor

## 4.2 Conclusions

---

This report summarized a review of the use of unmanned aerial vehicles in typical transportation activities, a review of the use of UAV for bridge inspections, and a review of methods for the detection and estimation of corrosion along steel girders. This was done to properly research the viability of using UAVs for MassDOT bridge inspections.

The literature presented in Section 4.1 of this report identified the transportation activities, detection possibilities, drone types, drone attachments, and common conclusions that have been researched and presented by the many state DOTs and university papers that were analyzed. This review led to the following conclusions:

- UAVs are a technologically advanced tool that can cut costs for DOTs by helping DOT employees quickly and safely carry out daily transportation activities.
- State DOTs want to start using UAVs for several different transportation activities, which are presented in Table 4.1.
- UAVs and their respective attachments are able to capture what a bridge inspector can, but much quicker, much safer, and at a much lower cost.
- A proper procedure and training program is needed to successfully implement drones.
- Manual mode with sensor assistance and the waypoint-assistance mode are the best flight modes.
- The weather condition that has the biggest effect on drone performance is wind.
- States want to start using UAVs for bridge inspections as soon as possible.
- Many different outputs, uses, detection possibilities, drones, and drone equipment are mentioned in the literature, all of which are presented in Tables 4.2, 4.3, 4.4, and 4.5.

The literature review presented in Section 4.1.3 was focused on several nondestructive testing techniques that can be used to detect and measure corrosion. The conclusions from that review are as follows:

- Each of the six NDT methods were able to detect and measure corrosion of metal surfaces to some extent.
- The technology for the C-NDT methods is more available, ready to use, and small enough to be attached to a drone.
- C-NDT methods have the potential to be utilized for drone bridge inspections in the near future.
- Skilled pilots would be needed to make proper contact with the steel bridge girders.
- NC-NDT methods need a lot more research to be ready to use in the field.
- NC-NDT technology needs to be made small and light enough to fit on a drone.

- NC-NDT methods could not be used for drone bridge inspections in the near future, but the promising results from these methods should not be ignored for there is great potential for their use in corrosion monitoring.
- Noncontact technology will not need as skilled of a pilot because they do not need to touch the girders and will be able to capture a larger area.
- For both C-NDT and NC-NDT, weather could greatly affect the thickness readings obtained, especially wind. Wind tends to make drones unstable and susceptible to movements that can cause inaccuracies in the thickness readings.
- The methods, uses, equipment, advantages, and disadvantages for C-NDT and NC-NDT are summarized in Table 4.6.

Overall, drones and their respective attachments are promising technologies to use for bridge inspections and the estimation of corrosion of a steel bridge girder. Based on this review, UAVs have the potential to replace traditional bridge inspections to make the process easier, safer, and less costly, but more research and testing are needed before that replacement can happen.

## 5.0 Bridge System Behavior

In previous research works [2, 50], we proposed load rating procedures based on experimental and computational evaluation of individual corroded beams. Although the findings of these efforts are important and provide very good insight into the capacity of beam ends, they are currently considered to be conservative because testing did not incorporate system behavior. With that work, we aim to computationally explore the system behavior of bridge systems with deteriorated beam ends.

### 5.1 Research Goals

---

Recent studies completed by our group [2, 7, 9, 50, 53, 54, 55, 56, 57] have classified the commonly found corrosion patterns in the State of Massachusetts, done experimental testing, analyzed computationally, and proposed analytical formulation and rating procedures for the remaining capacity assessment of girders. Moreover, a comprehensive protocol for inspection and assessment of aging steel bridges is proposed using 3D laser scanning of field-corroded girders for deteriorated steel beam ends. Those studies provide insight into the behavior of naturally deteriorated steel girders; however, these studies are not sufficient for the full understanding of the system behavior of bridges in which some of the beams are deteriorated due to complex interaction among the elements of bridge systems.

Capitalizing on our knowledge from building the high-fidelity computational model for individual beams containing deteriorated ends [2, 51], we aimed to perform exploratory computational work on a representative bridge by assembling models containing multiple beams and simulating diaphragms and concrete deck. The goal of this work was to explore the benefit that comes from system behavior and assess the increased capacity of the system compared to the individual beam capacity. It is expected that the benefit resulting from the system behavior can be substantial and could alter load rating procedures. Laboratory tests incorporating system behavior are rare and have only been conducted in very few instances in the United States. We believe that MassDOT would therefore be at the forefront of knowledge in this topic should they decide to pursue it.

The findings presented in this report constitute the exploratory work (Task 5) toward understanding the behavior of a bridge system with corroded beam ends. Within this task, a bridge system, whose one beam is corroded in a naturally corroded shape at its one end, is selected for the analysis.

### 5.2 Methodology for Computational Work

---

This section includes the description of a representative bridge, which is used for the exploratory computational analysis to understand bridge system behavior when one of its beams is corroded.

### 5.2.1 Geometry of the Representative Bridge

For the computational analysis, we choose a bridge of span 634 in. and width 336 in. that is supported by four girders and four diaphragms (Figure 5.1). For the beams, the length is 634 in., the web depth is 32.245 in., the flange width  $b_f$  is 11.51 in., depth  $d$  is 43.75 in., the intact web thickness  $t_{web}$  is 0.58 in., and the intact flange thickness  $t_f$  is 0.855 in.

For the diaphragms,  $d$  is 18 in.,  $b_f$  is 3.95 in.,  $t_{web}$  is 0.58 in., and  $t_f$  is 0.625 in. The diaphragms distance from the edge is 4 in. and from the top is 2.5 in. The diaphragm spacing is 208.67 in., the diaphragm length is 252.00 in., the beam spacing is 84.00 in., and the beam length is 634 in. The plan of the bridge is shown in Figure 5.1, where C1, C2, C3, and C4 represent the beams, and B1, B2, B3, and B4 represent the diaphragms. One of the middle beams C2 is corroded at one of its ends (Figure 5.1). The details about the corrosion pattern will be discussed in next.

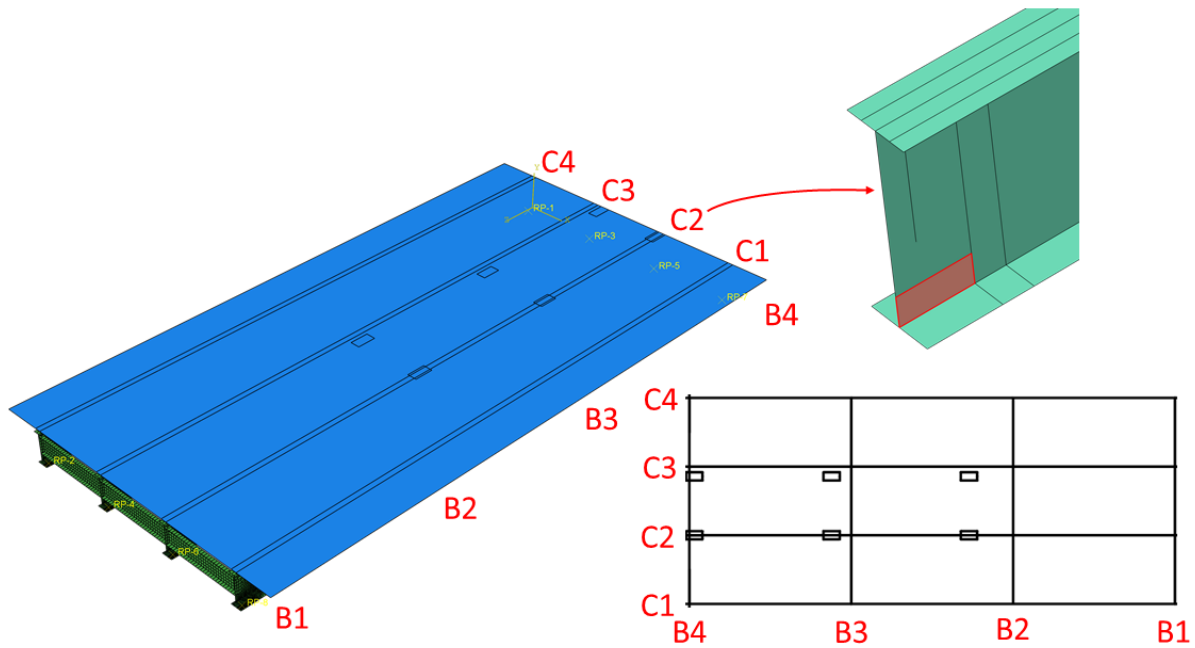


Figure 5.1: Representative bridge system used in this study

### 5.2.2 Corrosion Pattern

To understand the bridge response when some of its beams are corroded, we assigned corrosion at one beam of the representative bridge. Beam ends can be corroded in diverse shapes, and the thickness loss varies significantly depending on several parameters. In our previous study [2], the commonly found corrosion patterns were studied and classified.

In the current study, we chose pattern type 1 from the listed class [2] of the corrosion patterns. This corrosion pattern is shown in Figure 2.2 and is fully characterized by three parameters: CH, CL, and  $t_w$  loss. The nomenclature of these parameters is described in Figure 5.2. We choose the values of CH, CL, and  $t_w$  loss as 5 in., 12 in., and 0.29, respectively, for the current analysis.

### 5.2.3 Material Properties

The material is modeled as a bilinear model with hardening, isotropic with Young's Modulus equal to 29.000 ksi, Poisson's ratio equal to 0.27 and the Von Mises yield condition is applied. The yield stress is 46 ksi and 38 ksi at 0.2% of strain for the web and the flanges, respectively.

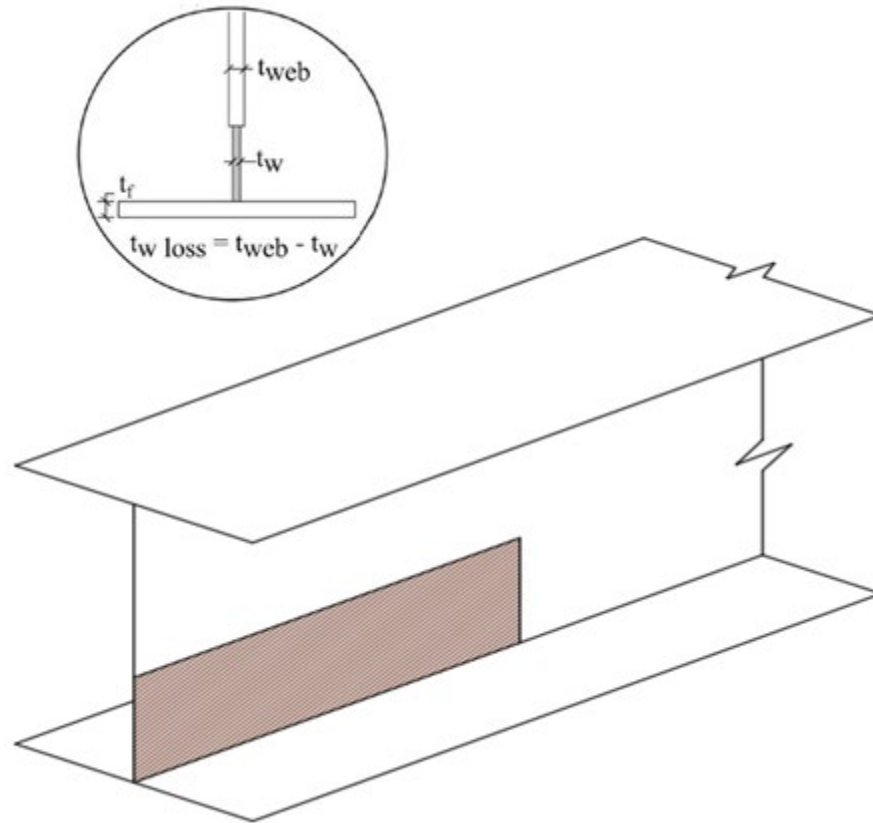
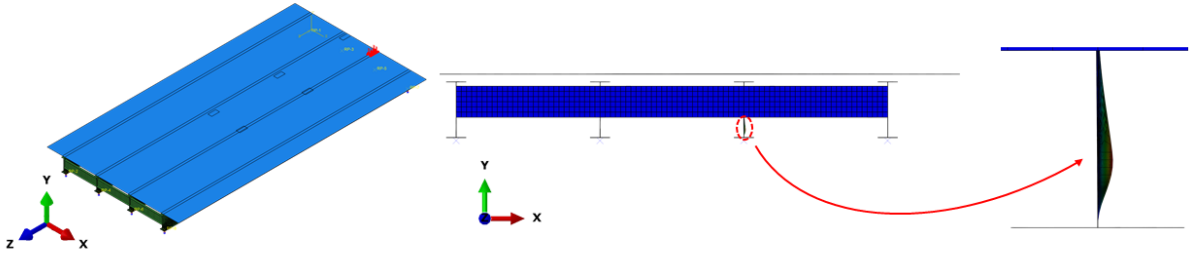


Figure 5.2: Type 1 corrosion pattern used in this study

### 5.3 Geometric Imperfections

To account for the imperfect geometry of the corroded ends, we induce geometric imperfection in the deteriorated beam end (C2). The shape of the imperfection is chosen such that it is present only at the deteriorated beam end (C2). To do that, the first eigenmode is taken as the imperfection when the load is present only on the deteriorated beam end (C2) (Figure 5.3). The shape of the first eigenmode is also shown in Figure 5.3, and it can be seen that deformation is only at the deteriorated beam end. This imperfection is scaled up to 0.058 in. and induced in the bridge as initial imperfection. The scaling value 0.058 in. is based on the real observation of the deteriorated bridges during our previous study.





**Figure 5.3: First eigenmode of the bridge solved using an eigenvalue buckling analysis algorithm and when the load is only on the top of the deteriorated end**

\*This is done to get an imperfection shape in form of lateral deviation of the web. This shape is introduced in the bridges with scaling factor 0.057 in.

## 5.4 Finite-Element Modeling

The simulation of the representative bridge is done in the commercial finite-element software ABAQUS [8] using shell elements (*S4R*) to approximate a three-dimensional continuous body with a surface at the middle of the section. The thicknesses of the elements of the bridge are assigned to the corresponding shell elements. Using shell elements for representing the three-dimensional bridges is a reasonable assumption considering the smaller thickness of the beam's components compared to the other two dimensions. At the beam ends, where stress concentration and failure are expected to occur, a dense mesh is utilized.

Following our previous experimental and computational study, a hard contact constraint is used for the normal contact behavior between the web edge nodes and flange surface in case of a hole keeping the other simulation parameters the same.

Four types of loading are applied on the bridge:

1. uniformly distributed deal load with value 255.63 kips,
2. uniformly distributed lane load with value 283.75 kips,
3. two rear axle loads with value 192.00 kips, and
4. front axle load with value 24 kips.

The axle loads are uniformly distributed in a small area (Figure 5.4), and the values of the loads are based on the guidelines of AASHTO [52] and the density of the concrete deck. The axle loads are located in the middle of the bridge such that one rear axle load is in the middle of the deteriorated beam end. This is done to create a worst-case scenario for the deteriorated end beam.

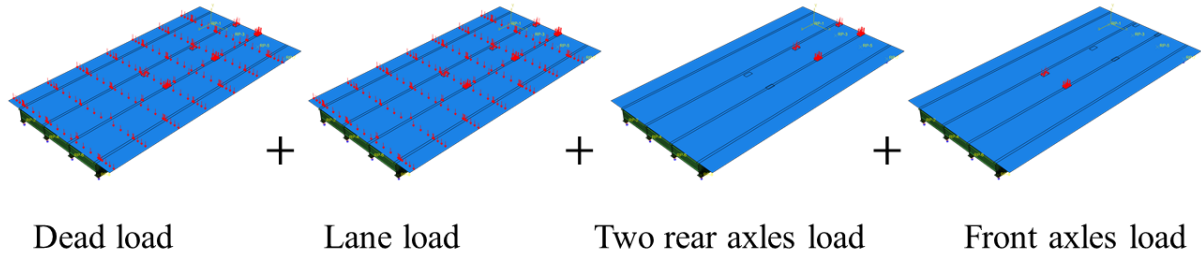


**Figure 5.4: Applied loads on the bridges**

The analysis is performed in two steps. In step 1, the dead load is applied quasi-statically considering nonlinearity. After all the dead load is fully applied in step 1, all the other loads are applied proportionally in step 2 using the arch-length-based Riks method. Here, proportionally means the loads are increased by increasing  $x$  where loads are defined as  $x$  (*lane load + two rear axles load + front axles load*), and Riks method is a numerical scheme to analyze the post-failure regions. Further, using the Riks method, the value of  $x$  could be more than one that helps to get the capacity of the bridge, even if that is more than the applied load.

## 5.5 Results

This section includes the key findings of the response of the bridge having deteriorated beam end, and the behavior of the deteriorated beam individually and when it is in the bridge system.

### 5.5.1 Capacity of the Bridge

To find the capacity of the bridge, first, all the dead loads are applied, and then the other loads (lane load + two real axles load + front axles load) are increased proportionally until the value of the applied loads starts reducing.

We found that the bridge can bear dead load (255.63 kips) +  $1.57 \times$  lane load (283.75 kips) +  $1.57168 \times$  two real axles load (192.00 kips) +  $1.57168 \times$  front axles load (24 kips). In total, the bridge can bear 1,040.40 kips in this particular arrangement of the loads. To understand the behavior of the bridge in more detail, the applied load is drawn against the time in Figure 5.5. Here, the time does not represent any physical quantity, but an applied load multiplier.

In Figure 5.5, the first straight line shows the application of dead load. Once the dead load is applied fully (283.75 kips), the other loads are applied using the Riks method, which is shown by the second line in Figure 5.5. At point A1, the failure occurs as the unique deteriorated end buckles; however, the bridge is still able to bear more load. As the load increases further, at point A2 global failure occurs as the adjacent beam end also buckles and the bridge cannot take any more load.

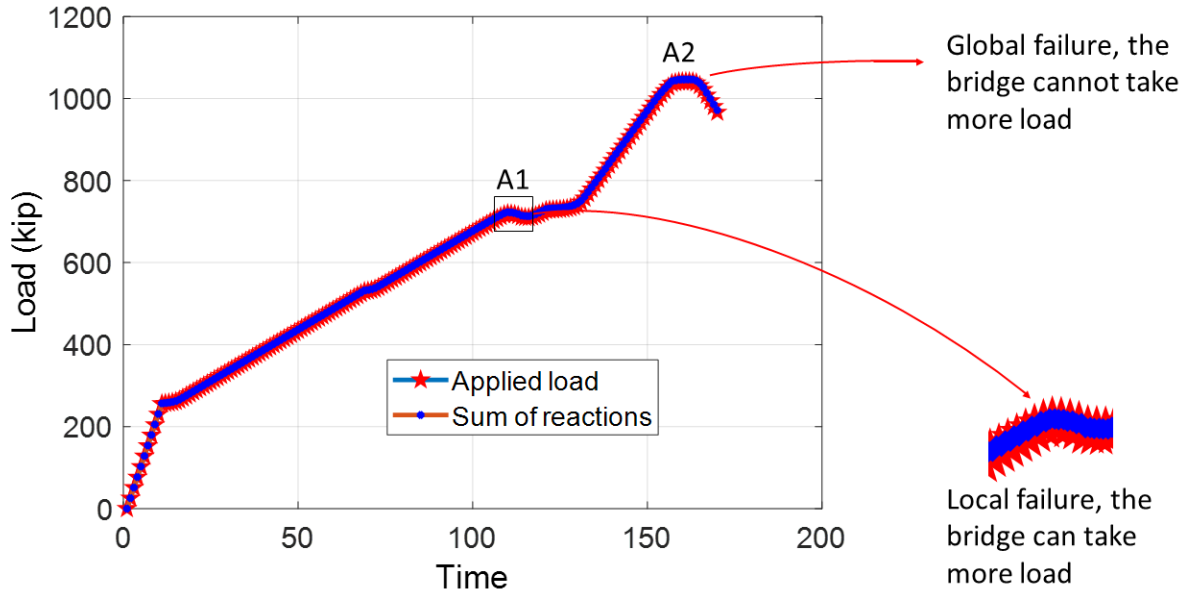


**Figure 5.5: Applied load against the time**

### 5.5.2 Reaction Forces

The reaction forces at bearings will give details about the local and global failure of the bridge. For that purpose, the reactions are plotted against the time in Figure 5.6. R5 represents the beam end that is deteriorated, and R3 represents the beam that is the middle adjacent to R5. In Figure 3.2, it can be seen that initially the reaction forces are more on R5 and R3 and they are almost identical. This is expected because the axles loads are on top of joints R5 and R3, and these joints are identical mechanically. As the loads are increasing, joint R5 buckles as shown by the reduction in reaction at R5 (point A1) in Figure 5.6. This is also expected because the beam deteriorates at that joint. However, the bridge can carry more load due to the load transfer that is taking place from the deteriorated joint to its adjacent joints: at the middle span and the edge.

The load distribution mechanics can be seen in Figure 5.6. After the buckling of the deteriorated end, the reduction in the reaction force at joint R5 is accompanied by a sharp increase in reaction forces at joints R3 and R7. As the load increases, the deteriorated beam end enters into its post-buckling region as shown by the deformation of the deteriorated end beam in Figure 3.3. As the load increases further, the bridge reaches its full capacity at point A2. At point A2, buckling takes place also in the intact girder at joint R5 as shown by the deformation profile of the adjacent intact beam in Figure 5.6. At point A2, two beams are buckled, and the bridges cannot bear any more load.

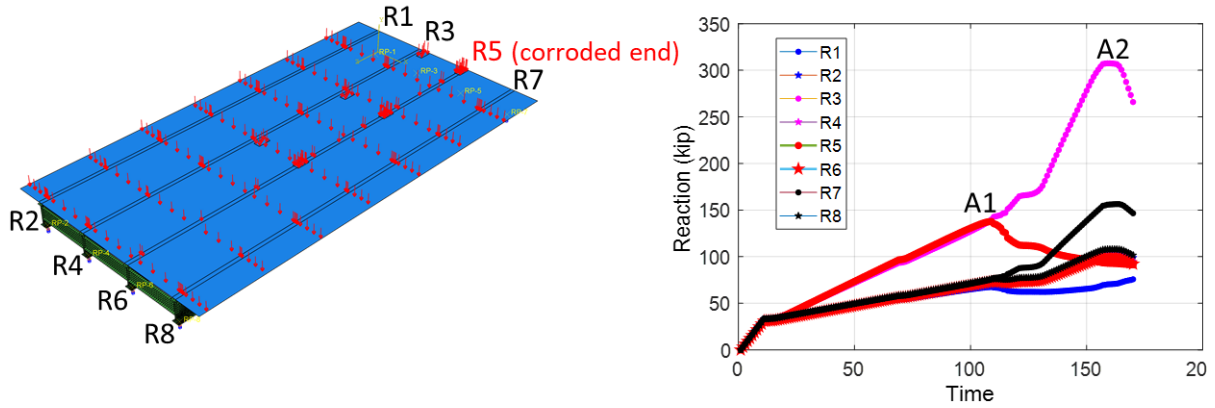


**Figure 5.6: Reaction forces at the beam ends**

## 5.6 Conclusions

Many key observations can be made from the results. First, the failure of the one beam end does not mean that the whole bridge will fail. The bridge has remaining capacity even if the deteriorating beam end fails due to the load redistribution at the adjacent beams. In the current example, the load on the bridge is 1,040.00 kips when the deteriorated end C2 fails, but the bridge fails at an almost 30% higher load. This is an important finding and shows that the bridge fails when the intact beam adjacent to the deteriorated beam also fails (Figure 5.7). This means the load rating procedures should account for the system behavior of the bridges, and the capacity of a bridge should not be reduced based only on the deterioration of one or some beams without considering the whole bridge system behavior.

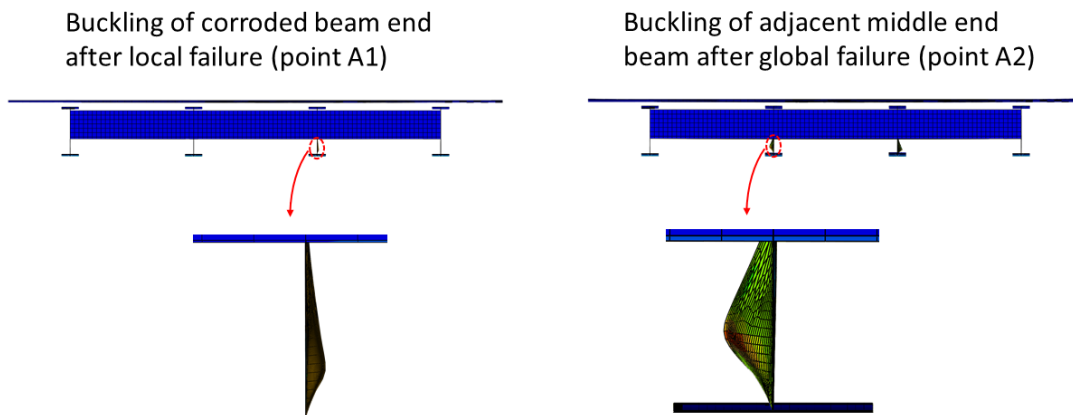


**Figure 5.7: Failure of deteriorated beam ends and the middle adjacent beam end**

## 5.7 Limitations and Future Work

---

This work is exploratory, but the results are very promising and encouraging and thus justifiably demands rigorous study on the system behavior of bridges. In this section, we list and discuss the several limitations of this study along with the plan for future work.

- The first limitation is the selection of the representative bridge that is used in this study. We choose a very simple system for the analysis as it simplifies the work; however, it is not sufficient for the field application because there are several other complexities. It will be extremely useful to work on an actual deteriorated bridge, including all its complexities in the analysis. The results of that study will certainly be a treasure for the development of road rating procedures.
- The second limitation is that in this study only one beam end is corroded, which is far from reality. In reality, many beam ends of a bridge are deteriorated, and it is worthy to understand their interplay and influence on the bridges. Especially, it is of interest to find the capacity of bridges in a worst-case scenario when all the end beams are deteriorated.
- The third and perhaps the most important limitation is the experimental investigation of the bridges by doing experiments on the existing deteriorated bridge. This will refine and validate our computational model. Further, it will help to develop a rating procedure that reflects reality.

## 6.0 Conclusions

Drawing on the recent findings made while developing new load rating procedures for deteriorated steel beam ends, the project at hand documents the current state of practice of beam end inspections, then explores new technological solutions for improvement of these inspection techniques, and finally performs preliminary analysis of a bridge system. Several useful conclusions have been reached and are presented here for each of the distinct research aspects.

### 6.1 Phase I: Evaluation of Current Inspection Procedures

---

A detailed questionnaire was prepared and sent out to the individuals that participate in MassDOT bridge inspections to gather and summarize information on general inspection practices, corrosion assessment practices, and the equipment used for bridge inspections. Based on the data collected from the questionnaire responses, the following major conclusions were reached about the existing bridge inspection procedure:

- The main issues with the current inspection procedures are accessibility and visibility of corroded areas due to the bridge configuration and equipment limitations.
- Documentation becomes time consuming as the bridge ages because older bridges are typically more corroded, which means more measurements need to be taken, documented, and analyzed for them.
- MassDOT inspectors may typically be responsible for many bridges, which means they may not have as much time to carry out each inspection per month.
- It is concerning that most of the inspectors who responded to the questionnaire have seen webs that deviate from straightness because this can cause significant loss in beam capacity and can be very unsafe.
- MassDOT inspectors believed that their equipment was in need of more changes compared to the consultants.

There is a lot of room for improvement regarding the existing bridge inspection procedures, and those improvements could greatly increase the safety and efficiency of bridge inspections while also decreasing inspection costs. Suggestions for any potential procedures to be proposed in the future are as follows:

- Any new procedure should be designed to yield consistent results to ensure that the condition of all bridges is thoroughly assessed and monitored over time to prevent any catastrophic structural failures in the future.

- Given how often web deviation is observed along with it being an important parameter for estimating the remaining capacity of a corroded beam, any new procedure should address how to estimate the condition and safety of the bridge based on how much web deviation there is.
- Laser scanning, or LiDAR, and UAVs are known by some inspectors and are advanced technologies that can be used to estimate corrosion
- Further research should be done on using unmanned aerial vehicles for the inspection and corrosion assessment of steel bridge girders because
  - UAVs can help address and correct the challenges that inspectors are experiencing; and
  - The additional technology add-ons can be added to UAVs, including LiDAR, to measure and assess steel beam end corrosion.

## **6.2 Phase II: New LiDAR-Based Inspection Methods for More Efficient Data Collection for Beam End Inspections**

---

The efficiency of 3D laser scanning as a potential technology for bridge inspection has been explored and validated. LiDARs can address the shortcomings of conventional data acquisition techniques and at the same time abolish the sensitivity of ultrasonic thickness gauges along bumpy surfaces. Thickness estimations resulting from 3D laser scanning post-processing were verified and subsequently used for capacity estimations. More details for these conclusions are as follows:

4. Data acquisition
  - The need for cleaning the steel surfaces prior to scanning was highlighted. The existence of delaminated parts can result to overestimating thickness estimation.
5. Documentation
  - Thickness contour maps were proposed as a two-dimensional representation of the remaining thickness profile along the deteriorated area. This approach provides an overall description of the examined area, and they can be integrated in the inspection reports to upgrade the corrosion mapping.
6. Capacity evaluation
  - A numerical study included the creation of computational meshes that integrate the exact condition of corroded girders. This approach was validated with full-scale experimental testing of a naturally corroded girder. Comparison of numerically and experimentally obtained results provided credibility to the proposed automated methodology, because the failure load of the simulated specimen was captured with an error of 4.1%.
  - The post-processed data was used to inform analytical tools for capacity evaluation. The obtained results provide evidence that a generalized average of the web thickness as corrosion input should be avoided, because it may result in overestimating predictions.

### **6.3 Phase III: New Technological Solutions for More Efficient Data Collection for Beam End Inspections—Unmanned Aircraft Systems (Drones)**

---

This report summarized a review of the use of unmanned aerial vehicles (UAV) in typical transportation activities, a review of the use of UAV for bridge inspections, and a review of methods for the detection and estimation of corrosion along steel girders. This was done to properly research the viability of using UAVs for MassDOT bridge inspections. This review led to the following conclusions:

- UAVs are a technologically advanced tool that can cut costs for DOTs by helping DOT employees quickly and safely carry out daily transportation activities.
- UAVs and their respective attachments are able to capture what a bridge inspector can, but more quickly, more safely, and at a much lower cost.
- The technology for the contact nondestructive technique methods is more available, ready to use, and small enough to be attached to a drone.

Overall, drones and their respective attachments are promising technologies to use for bridge inspections and the estimation of corrosion of a steel bridge girder. This review has found that UAVs have the potential to replace traditional bridge inspections to make the process easier, safer, and less costly, but more research and testing is needed before that replacement can happen.

### **6.4 Phase IV: Bridge System Behavior**

---

Many key observations can be made from the preliminary results presented in the report. First, the failure of the one beam end does not mean that the whole bridge will fail. The bridge has remaining capacity even if the deteriorating beam end fails owing to the load redistribution at the adjacent beams. This is an important finding that shows that the load rating procedures should account for the system behavior of the bridges, and the capacity of a bridge should not be reduced based only on the deterioration of one or some beams without considering the whole bridge system behavior.



This page left blank intentionally.

## **7.0 Limitations and Future Work**

The methodology of this work emerges from real corrosion data and acts complementary to a previous work by the authors; the aim is to address the remaining capacity of rolled girders with corroded ends. Because of complications with the lockdown from COVID, we did not have the opportunity to fly drones ourselves and experiment with the collection of data in this way. This is an area of future work, combining LiDAR technology with drones.

Future studies should examine the behavior of the corroded beams as part of the whole bridge and the potential redistribution of forces after the failure (or even the loading) of one beam end. The first analyses of the bridges as a system are very promising, and a new research effort in that area is deemed as significantly important. This future work is expected to provide more room for less strict load rating procedures.

This page left blank intentionally.

## 8.0 References

1. American Society of Civil Engineers. 2021 Report Card for America's Infrastructure. <https://www.infrastructurereportcard.org/>. Accessed January 20, 2021.
2. Tzortzinis, G., S. Gerasimidis, S. F. Breña, and B. T. Knickle. *Development of Load Rating Procedures for Deteriorated Steel Beam Ends*. MassDOT Research Rep. 19-008, Massachusetts Department of Transportation Office of Transportation Planning, Boston, 2019.
3. 23 C.F.R. <https://www.govinfo.gov/content/pkg/CFR-2021-title23-vol1/pdf/CFR-2021-title23-vol1.pdf>. Accessed January 20, 2022.
4. Massachusetts Dept. of Transportation. *MassDOT Bridge Inspection Handbook*. Massachusetts Dept. of Transportation Highway Division Bridge Section, Boston, 2015.
5. Tzortzinis, G., B. T. Knickle, A. Bardow, S. F. Breña, and S. Gerasimidis. Strength Evaluation of Deteriorated Girder Ends. I: Experimental Study on Naturally Corroded I-Beams. *Thin-Walled Structures*, Vol. 159, 2021, 107220.
6. *PocketMIKE, Operating Manual*. GE Inspection Technologies, Lewistown, PA, 2004.
7. Delaunay, B. Sur la sphère vide. *Bulletin de l'Académie des Sciences de l'URSS, Classe des Sciences Mathématiques et Naturelles*, Vol. 6, 1934, pp. 793–800.
8. *ABAQUS User's Guide*. Dassault Systems Simulia Corporation, Providence, RI, 2014.
9. Tzortzinis, G., B. T. Knickle, A. Bardow, S. F. Breña, and S. Gerasimidis. Strength Evaluation of Deteriorated Girder Ends. II: Numerical Study on Corroded I-Beams. *Thin-Walled Structures*, Vol. 159, 2021, 107216.
10. Moller, Paul S. *CALTRANS Bridge Inspection Aerial Robot Final Report*. TRID, Sept. 2008. <https://trid.trb.org/view/917744>. Accessed May 7, 2020.
11. Cathey, G. California Dept. of Transportation UAS Operations. *Unmanned Aircraft Systems (Drones) | Caltrans*, Apr. 6, 2016. [www.sp.air.transportation.org/Documents/California%20UAS%20Operations%20-%20Gary%20Cathey.pdf](http://www.sp.air.transportation.org/Documents/California%20UAS%20Operations%20-%20Gary%20Cathey.pdf). Accessed May 7, 2020.
12. Illinois Dept. of Transportation. *IDOT's UAS Program*. October 3, 2017. [http://www.idot.illinois.gov/Assets/uploads/files/About-IDOT/Pamphlets-&-Brochures/Events/Multi-Modal-Planning/Fall-Planning/2017/S1B1\\_2017-10-03-UAS-IDOTFallPlanningConf.pdf](http://www.idot.illinois.gov/Assets/uploads/files/About-IDOT/Pamphlets-&-Brochures/Events/Multi-Modal-Planning/Fall-Planning/2017/S1B1_2017-10-03-UAS-IDOTFallPlanningConf.pdf). Accessed March 18, 2020.
13. McClung, T. *Unmanned Aircraft Systems*. Iowa Dept. of Transportation. October 17, 2017. [https://www.iowadot.gov/2017leadershipconference/presentations/Unmanned%20Aircraft\\_Tim%20McClung.pdf](https://www.iowadot.gov/2017leadershipconference/presentations/Unmanned%20Aircraft_Tim%20McClung.pdf).
14. Judson, F. *Ohio DOT's Ohio/Indiana UAS Center – Enabling UAS Operations*. Ohio/Indiana UAS Center. <https://aviation.transportation.org/wp-content/uploads/sites/8/2019/08/Ohio-and-Indiana-UAS-Center-Enabling-UAS-Operations-Fred-Judson.pdf>. Accessed March 17, 2020.
15. McGuire, M., M. Rhys, and A. Rhys. *A Study of How Unmanned Aircraft Systems Can Support the Kansas Department of Transportation's Efforts to Improve Efficiency, Safety, and Cost Reduction*. Kansas Dept. of Transportation. August 2016. [https://rosap.nhtl.bts.gov/view/dot/31030/dot\\_31030\\_DS1.pdf](https://rosap.nhtl.bts.gov/view/dot/31030/dot_31030_DS1.pdf).

16. Siwula, J. J. *How State DOTs Are Using Unmanned Aerial Systems Webinar*. Unmanned Aircraft Systems | KYTC, Kentucky Transportation Cabinet Unmanned Aircraft Systems (UAS) Program, Apr. 6, 2016. <https://www.fhwa.dot.gov/uas/webinars.cfm>.
17. *Update of Research: Unmanned Aircraft Systems (UAS)*. New Hampshire Dept. of Transportation. May 2018. <https://www.nh.gov/dot/org/projectdevelopment/materials/research/documents/2018-1FINAL.pdf>.
18. Lercel, D., R. Steckel, and J. Pestka. *Unmanned Aircraft Systems: An Overview of Strategies and Opportunities for Missouri*. Missouri Dept. of Transportation. June 2018. <https://rosap.ntl.bts.gov/view/dot/36248>. Accessed March 21, 2020.
19. Ni, D., and M. Plotnikov. *The State of the Practice of UAS Systems in Transportation*. The University of Vermont. November 30, 2016. <https://www.umasstransportationcenter.org/Document.asp?DocID=282>.
20. AASHTO. State DOTs Using Drones to Improve Safety, Collect Data and Cut Costs. *AASHTO News*, Mar. 28, 2016. <https://www.forconstructionpros.com/asphalt/press-release/12187251/american-association-of-state-highway-and-transportation-officials-state-dots-using-drones-to-improve-safety-collect-data-and-cut-costs>. Accessed May 5, 2020.
21. Survey Finds a Growing Number of State DOTs Are Using Drones to Improve Safety and Collect Data Faster and Better. *AASHTO Transportation TV*, <https://adobeindd.com/view/publications/12579497-56a5-4d8a-b8fe-e48c95630c99/1/publication-web-resources/pdf/Drones'18cc.pdf>. Accessed May 6, 2020.
22. AASHTO. *Scan 17-01: Successful Approaches for the Use of Unmanned Aerial Systems by Surface Transportation Agencies*. NCHRP Project 20-68A. AASHTO, Washington, DC. July 2018. <https://trid.trb.org/view/1604420>. Accessed April 21, 2020.
23. Dorafshan, S., M. Maguire, N. V. Hoffer, and C. Coopmans. *Fatigue Crack Detection Using Unmanned Aerial Systems in Under-Bridge Inspection*. Idaho Dept. of Transportation, Boise, ID. August 2017. <http://apps.itd.idaho.gov/apps/research/Completed/RP256.pdf>. Accessed April 2, 2020.
24. Brooks, C., et al. *Evaluating the Use of Unmanned Aerial Vehicles for Transportation Purposes*. Michigan Dept. of Transportation, Lansing, MI. April 7, 2015. [https://www.michigan.gov/documents/mdot/RC1616\\_Part\\_B\\_488516\\_7.pdf](https://www.michigan.gov/documents/mdot/RC1616_Part_B_488516_7.pdf). Accessed April 14, 2020.
25. Brooks, C., et al. *Implementation of Unmanned Aerial Vehicles (UAVs) for Assessment of Transportation Infrastructure—Phase II*. Michigan Technological University, May 9, 2018. [www.mtu.edu/mtri/research/project-areas/transportation/sensors-platforms/mdot-uav/](http://www.mtu.edu/mtri/research/project-areas/transportation/sensors-platforms/mdot-uav/). Accessed April 15, 2020.
26. Cook, S. J. *Evaluating the Use of Unmanned Aerial Systems (UAS) for Transportation Purposes*. Michigan Dept. of Transportation, Lansing, MI. [https://www.michigan.gov/documents/mdot/RC1616\\_Part\\_C\\_488517\\_7.pdf](https://www.michigan.gov/documents/mdot/RC1616_Part_C_488517_7.pdf). Accessed April 15, 2020.
27. Brooks, C. N. *Application of UAVs for Transportation Infrastructure Assessment*. Michigan Tech Research Institute, Ann Arbor, MI.

- <http://www.ctt.mtu.edu/sites/ctt/files/resources/bridge2016/workshop/10brooks-uav-assessment.pdf>. Accessed April 15, 2020.
28. Lovelace, B. *Unmanned Aerial Vehicle Bridge Inspection Demonstration Project*. TRID, Minnesota Dept. of Transportation Office of Transportation System Management, St. Paul, MN, June 30, 2015. <https://www.lrrb.org/pdf/201540.pdf>. Accessed April 3, 2020
  29. Lovelace, B. *Unmanned Aircraft System Bridge Inspection Demonstration Project Phase II*. Minnesota Dept. of Transportation, St. Paul, MN, June 2017. <http://dot.state.mn.us/research/reports/2017/201718.pdf>. Accessed April 3, 2020.
  30. Lovelace, B. *Improving the Quality of Bridge Inspections Using Unmanned Aircraft Systems (UAS)*. TRID, Minnesota Dept. of Transportation, St. Paul, MN, July 2018, <https://www.dot.state.mn.us/research/reports/2018/201826.pdf>. Accessed April 3, 2020.
  31. NDOT Explores Unmanned Aerial Vehicle Bridge Inspection. *The Roadrunner*. Nebraska Dept. of Transportation, Lincoln, NE. Winter 2018. <https://dot.nebraska.gov/media/10948/rr-winter-2018.pdf>. Accessed April 15, 2020.
  32. Zajkowski, T., K. Snyder, E. Arnold, and D. Divakaran. *Unmanned Aircraft Systems: A New Tool for DOT Inspections*. Final Rep 2016-2. North Carolina Dept. of Transportation, Raleigh, NC. October 2016. <https://connect.ncdot.gov/resources/Aviation%20Resources%20Documents/RP2015-16%20UAS%20Study%20Final%20Report.pdf>. Accessed April 16, 2020.
  33. Gillins, D. T., C. Parrish, M. N. Gillins, and C. Simpson. *Eyes in the Sky: Bridge Inspections with Unmanned Aerial Vehicles*, Final Report, SPR 787. Oregon Dept. of Transportation Research Section, Salem, OR. [https://www.oregon.gov/ODOT/Programs/ResearchDocuments/SPR787\\_Eyes\\_in\\_the\\_Sky.pdf](https://www.oregon.gov/ODOT/Programs/ResearchDocuments/SPR787_Eyes_in_the_Sky.pdf). Accessed April 2, 2020.
  34. Huber, D. ARIA: the Aerial Robotic Infrastructure Analyst. *SPIE Newsroom*, June 9, 2014. <https://spie.org/news/5472-aria-the-aerial-robotic-infrastructure-analyst?SSO=1>. Accessed April 25, 2020
  35. Guo, Y., R. Atadero, J. W. van de Lindt. *Development of an Autonomous Transportation Infrastructure Inspection System Based on Unmanned Aerial Vehicles*. MPC-592, 2019. Colorado State University.
  36. Otero, D. L., A. Peter, and M. Moyou. *Remote Sensing with Mobile LiDAR and Imaging Sensors for Railroad Bridge Inspections*. Final Report for Rail Safety IDEA Project 26. TRB Rail Safety IDEA Program, Washington, DC, 2016. <http://onlinepubs.trb.org/onlinepubs/IDEA/FinalReports/Safety/Safety26.pdf>. Accessed May 7, 2020.
  37. Yin, Z., Y. Mao, and C. Seto. *Develop a UAV Platform for Automated Bridge Inspection*. Mid-America Transportation Center, 2015. [http://matc.unl.edu/assets/documents/matcfinal/Yin\\_DevelopaUAVPlatformforDevelopaUAVPlatformforAut.pdf](http://matc.unl.edu/assets/documents/matcfinal/Yin_DevelopaUAVPlatformforDevelopaUAVPlatformforAut.pdf). Accessed April 30, 2020.
  38. How America's Top Railroad Learns to Fly. *Union Pacific Inside Track*. December 5, 2017. [https://www.up.com/aboutup/community/inside\\_track/railroad-learns-to-fly.htm](https://www.up.com/aboutup/community/inside_track/railroad-learns-to-fly.htm). Accessed April 18, 2020.

39. Vantuono, W. C. NS Bridge Inspection “Drones” On. *Railway Age*, August 22, 2017. <https://www.railwayage.com/news/ns-bridge-inspection-drones-on/>. Accessed April 18, 2020.
40. Mukherjee, I., J. Patil, S. Banerjee, and S. Tallur. Phase Sensitive Detection of Extent of Corrosion in Steel Reinforcing Bars Using Eddy Currents. *ArXiv.org*, Jan. 11, 2020, [arxiv.org/abs/2001.03756](https://arxiv.org/abs/2001.03756). Accessed May 12, 2020.
41. UltraPortable EC USB Tester Product Sheet. *Sensima Inspection*, [www.sensimainsp.com/product%20sheet%20UPEC-SFM26W%2020150312.pdf](http://www.sensimainsp.com/product%20sheet%20UPEC-SFM26W%2020150312.pdf). Accessed June 5, 2020.
42. Na, W. S., and J. Baek. Impedance-Based Non-Destructive Testing Method Combined with Unmanned Aerial Vehicle for Structural Health Monitoring of Civil Infrastructures. *Applied Sciences*, Vol. 7, No. 1, 2016, 15. <https://doi.org/10.3390/app7010015>.
43. Mascarenas, D. D. L., et al. Development of Capacitance-Based and Impedance-Based Wireless Sensors and Sensor Nodes for Structural Health Monitoring Applications. *Journal of Sound and Vibration*, Vol. 329, No. 12, 2010, pp. 2410–2420. <https://doi.org/10.1016/j.jsv.2009.07.021>.
44. Mattar, R. A., and R. Kalai. Development of a Wall-Sticking Drone for Non-Destructive Ultrasonic and Corrosion Testing. *Drones*, Vol. 2, No. 1, 2018, p. 8.
45. Kharkovsky, S., J.T. Case, M. T. Ghasr, R. Zoughi, S. W. Bae, and A. Belarbi. Application of Microwave 3D SAR Imaging Technique for Evaluation of Corrosion in Steel Rebars Embedded in Cement-Based Structures. AIP Conf., Proceedings, Vol. 1430, 2012, pp. 1516–1523. doi:10.1063/1.4716395.
46. H. Zhang, Y. He, B. Gao, G. Y. Tian, L. Xu, and R. Wu. Evaluation of Atmospheric Corrosion on Coated Steel Using K-Band Sweep Frequency Microwave Imaging. *IEEE Sensors Journal*, Vol. 16, No. 9, 2016, pp. 3025–3033.
47. Anastasi, R. F., and E. I. Madaras. Terahertz NDE for Under Paint Corrosion Detection and Evaluation. AIP Conf., Proceedings, Vol. 820, 2006, 515. doi:10.1063/1.2184571.
48. Jönsson, M., B. Rendahl, and I. Annergren. The Use of Infrared Thermography in the Corrosion Science Area. *Materials and Corrosion*, Vol. 61, No. 11, 2010, pp. 961–965.
49. Bison, P., M. Ceseri, and G. Inglese. Mapping Corrosion of Metallic Slab by Thermography. *Journal of Physics: Conference Series*, Vol. 214, 2010, 012073.
50. Tzortzinis, G., S. Gerasimidis, and S. F. Breña. Experimental Testing, Computational Analysis and Analytical Formulation for the Remaining Capacity Assessment of Bridge Plate Girders with Naturally Corroded Ends. *Engineering Structures*, Vol. 252, 2022, 113488.
51. Tzortzinis, G., S. F. Breña, and S. Gerasimidis. *Improved Load Rating Procedures for Deteriorated Steel Beam Ends with Deteriorated Stiffeners*. MassDOT Research Rep. 21-024. Massachusetts Dept. of Transportation, Office of Transportation Planning, Boston, 2021.
52. AASHTO. *Standard Specifications for Highway Bridges*. AASHTO, Washington, DC, 2002.

53. Tzortzinis, G., B. Knickle, S. Gerasimidis, A. Bardow, and S. Brena. *Identification of Most Common Shapes and Locations for Beam End Corrosion of Steel Girder Bridges*. Proc. 98th Annual Meeting of the Transportation Research Board, 2019.
54. Tzortzinis, G., B. Knickle, S. Gerasimidis, A. Bardow, and S. Brena. *Experiments and Computations on Steel Bridge Corroded Beam Ends*, AISC Structural Stability Research Council, 2019.
55. Provost, A., A. Pires, G. Tzortzinis, S. Gerasimidis, and S. Brena. *Improved Load Rating Procedures for Deteriorated Unstiffened Steel Beam Ends. Deliverable 1: Identification of Common Unstiffened Steel Beam-End Corrosion Topologies*. [https://25a95cd7-fdb2-4b65-a427-47d07fb89a24.filesusr.com/ugd/86e27c\\_c4feecd88638413896c450f8153fa190.pdf](https://25a95cd7-fdb2-4b65-a427-47d07fb89a24.filesusr.com/ugd/86e27c_c4feecd88638413896c450f8153fa190.pdf), 2021
56. Gerasimidis, S., and M. Ettouney. On the Definition of Resilience. In *Objective Resilience: Policies and Strategies*, ASCE, Reston, VA, 2022, pp. 1–24.
57. Hou, P., S. Mooraj, V.K. Champagne, M.J. Siopis, P.K. Liaw, S. Gerasimidis, and W. Chen. Effect of build height on temperature evolution and thermally induced residual stresses in plasma arc additively manufactured stainless steel. *Metallurgical and Materials Transactions A*, Vol. 53, No. 2, 2022, pp. 627–639.